

EFFECT OF NATURAL POLYSACCHARIDES ON THE  
INTEGRITY AND TEXTURE OF SUGAR BASED MATRICES  
IN  
THREE DIMENSIONAL PRINTING

A THESIS SUBMITTED TO  
THE GRADUATE SCHOOL OF NATURAL AND APPLIED SCIENCES  
OF  
MIDDLE EAST TECHNICAL UNIVERSITY

BY

TUNCAY BAYDEMİR

IN PARTIAL FULFILLMENT OF THE REQUIREMENTS FOR THE DEGREE OF  
MASTER OF SCIENCE

IN

THE DEPARTMENT OF POLYMER SCIENCE AND TECHNOLOGY

SEPTEMBER 2003

Approval of the Graduate School of Natural and Applied Sciences

---

Prof. Dr. Canan ÖZGEN  
Director

I certify that this thesis satisfies all the requirements as a thesis for the degree of Master of Sciences.

---

Prof. Dr. Ali USANMAZ  
Head of Department

This is to certify that we have read this thesis and that in our opinion it's fully adequate, in scope and quality, as a thesis for the degree of Master of Science in Polymer Science and Technology.

---

Prof. Dr. Erdal BAYRAMLI  
(Supervisor)

Examining Committee in Charge

Prof. Dr. Duygu KISAKÜREK (Chairman)

Prof. Dr. Erdal BAYRAMLI

Prof. Dr. Bekir PEYNİRCİOĞLU

Prof. Dr. Nesrin HASIRCI

Assist. Prof. Dr. Gök Nur BAYRAM

## **ABSTRACT**

### **EFFECT OF NATURAL POLYSACCHARIDES ON THE INTEGRITY AND TEXTURE OF SUGAR BASED MATRICES IN THREE DIMENSIONAL PRINTING**

**BAYDEMİR, Tuncay**

**M.S., Department of Polymer Science and Technology**

**Supervisor: Prof. Dr. Erdal BAYRAMLI**

**September 2003, 118 pages**

Three dimensional printing (3DP) is one of the most important solid free-form fabrication (SFF) methods that can produce any material with desired 3D shape by using suitable powder-binder formulations. It differs from the standard molding operations in that it can produce a complicated shapes by a software driven instrument in a laminated fashion and the cost is lower. This method can be applied in a very wide area including drug release operations, biomaterial production especially for bone fixation, prototype production for all purposes, wound dressing etc. It can also be used in obtaining edible objects by using natural polysaccharides with water based binders.

In this study, it is aimed to understand the gelling behaviour of some of the gelling materials, which are alginates, pectins and carrageenans, and effect of various factors on the production of confectionary objects by means of 3DP process. Effect of multivalent cations, especially  $\text{Ca}^{2+}$  ion, on the gelling behaviour of these materials are investigated. The “egg-box” structure obtained between the polymer segments increases the water holding capacity of the materials and much more chewy structures can be obtained. The molecular changes are followed by Fourier Transform infrared spectroscopy (FTIR). In 3DP applications, the composition of powder and binder, pH, temperature, relative humidity (RH) and machine parameters are important factors affecting the texture of the final object. The texture of the produced specimens is examined by using a texture analyzer and maximum force values are given as g/cm at failure. Alginate and carrageenans are found to be more effective in obtaining chewy textures with  $\text{Ca}^{2+}$  ion content in sugar based matrices and optimization of machine parameters are performed to obtain a higher resolution on the specimens.

**Keywords:** Three dimensional printing (3DP), alginate, carrageenan, pectin, multivalent cation, viscosity, gelling behaviour, rheology, egg-box structure, calcium bridging, degree of esterification, methoxyl content, packing density.

## ÖZ

### ÜÇ BOYUTLU BASKIDA DOĞAL POLİSAKKARİTLERİN ŞEKER BAZLI MATRİSLERİN BÜTÜNLÜK VE TEKSTÜRÜNE ETKİSİ

BAYDEMİR, Tuncay

Y.L., Polimer Bilimi ve Teknolojisi Bölümü

Tez Yöneticisi: Prof. Dr. Erdal BAYRAMLI

Eylül 2003, 118 sayfa

Üç boyutlu baskı (3DP), herhangi bir malzemeyi uygun toz-bağlayıcı formülasyonları ile istenilen 3-boyutlu şekilde üretebilen katı serbest-form fabrikasyonu (SFF) metodlarının en önemlilerinden biridir. Standart kalıplama uygulamalarından farkı ise karmaşık şekilleri bilgisayar yazılımı ile çalışan bir cihazla katmanlar halinde daha ucuz bir maliyetle üretebilmesidir. Bu metod, ilaç salınım uygulamaları, özellikle kemik onarımı için biomateryal üretimi, tüm amaçlar için prototip üretimi, yara kaplaması vb. gibi çok geniş bir alanda uygulanabilir. Ayrıca, doğal polisakkaritler ve su bazlı bağlayıcılar kullanılarak yenilebilir objeler eldesinde de kullanılabilir.

Bu çalışmada, aljinat, pektin ve kareggenan gibi bazı jel yapıcı maddelerin jelleşme davranışlarını ve üç boyutlu baskı yöntemiyle şekerleme üretimine çeşitli faktörlerin etkisini anlamak amaçlanmıştır. Çok değerlikli katyonların, özellikle  $Ca^{2+}$  iyonunun, bu malzemelerin jelleşme davranışları üzerine olan etkisi incelenmiştir. Polimer bölümleri arasında elde edilen “yumurta-kutusu” yapısı, bu malzemelerin su tutma kapasitesini artırır ve daha yumuşak yapılar elde edilebilir. Moleküler değişimler Fourier Transform infrared spektroskopisi (FTIR) ile izlenmiştir. Üç boyutlu baskı (3DP) uygulamalarında, toz ve bağlayıcı kompozisyonları, pH, sıcaklık, bağıl nem (RH) ve makine parametreleri final yapının tekstürünü etkileyen önemli etkenlerdendir. Üretilen numunelerin tekstürü tekstür analizörü ile incelenmiş ve kırılmadaki en yüksek kuvvet değerleri g/cm cinsinden verilmiştir. Aljinat ve kareggenanlar,  $Ca^{2+}$  ion içeren şeker bazlı matrislerde yumuşak yapıların eldesinde daha etkili olmuş ve daha yüksek çözünürlüklü numuneler elde etmek için makina parametrelerinin optimizasyonu yapılmıştır.

**Anahtar Kelimeler:** Üç boyutlu baskı (3DP), aljinat, kareggenan, pektin, çok değerlikli katyon, viskozite, jelleşme davranışı, reoloji, yumurta-kutusu yapısı, kalsiyum köprüsü, esterifikasyon derecesi, metoksil içeriği, paketleme yoğunluğu.

***TO MY FAMILY***

## **ACKNOWLEDGEMENTS**

I would like to express my deepest gratitude to my supervisor Prof. Dr. Erdal BAYRAMLI for his guidance, patience, advice, encouragement and endless support throughout this study. He is not only enlightened me with his scientific knowledge but also let me gain much from his social and managerial skills.

I would like to thank with all my heart to my love and fiancée Işıl KABAL for her endless love, and moral support during my studies.

I wish to express my sincere thanks to Yasin Ağırtopçu for his friendship, help and valuable discussion.

I am also thankful to Elif Vargün, Selahattin Erdoğan, Zeynep Duru, Yusuf Aktaş, Güralp Özkoç and all my friends in the Polymer Science and Technology and Chemistry Department for their friendship, helps and support.

I am also thankful all of the technicians in our department for their help and support during my study.

Finally, I would like to express my sincere thanks to my family for their great sacrifice, unshakeable faith and moral support during my education.

## TABLE OF CONTENTS

<b>ABSTRACT</b> .....	<b>iii</b>
<b>ÖZ</b> .....	<b>v</b>
<b>ACKNOWLEDGEMENTS</b> .....	<b>viii</b>
<b>TABLE OF CONTENTS</b> .....	<b>ix</b>
<b>LIST OF TABLES</b> .....	<b>xiii</b>
<b>LIST OF FIGURES</b> .....	<b>xiv</b>
<b>ABBREVIATIONS</b> .....	<b>xvii</b>

### CHAPTER

<b>1.INTRODUCTION</b> .....	<b>1</b>
1.1 Polysaccharides; nature, occurrence and classification.....	2
1.2 Hydrocolloids .....	6
1.2.1 Some aspects of hydrocolloid gelation.....	9
1.3 Alginates.....	12
1.3.1 Source.....	12
1.3.2 Raw materials.....	12
1.3.3 Structural unit.....	13
1.3.4 Molecular structure .....	13
1.3.5 Functionality - structuring using alginates.....	15
1.3.6 Manufacturing process .....	19
1.4 Carrageenans .....	20
1.4.1 Source.....	20

1.4.2	Raw materials.....	20
1.4.3	Structural unit.....	20
1.4.4	Molecular structure .....	21
1.4.5	Functionality - structuring using carrageenan.....	21
1.4.6	Manufacturing process for refined carrageenan.....	27
1.5	Pectins .....	29
1.5.1	Source.....	29
1.5.2	Raw materials.....	29
1.5.3	Structural unit.....	30
1.5.4	Molecular structure .....	30
1.5.5	Functionality .....	31
1.5.6	Manufacturing process .....	35
1.6	Three dimensional printing (3DP).....	36
1.6.1	What is the 3DP™ process.....	38
1.6.2	Process.....	39
1.6.3	Process capabilities .....	39
1.7	Scope of the work.....	41
<b>2</b>	<b>EXPERIMENTAL .....</b>	<b>42</b>
2.1	Materials.....	42
2.1.1	Satialgine SG300 (sodium alginate).....	43
2.1.2	Unipectine PG569S (pectin).....	43
2.1.3	Unipectine PG769S (pectin).....	44
2.1.4	Satiagel KHG30 (carrageenan) .....	45
2.1.5	Satiagum CD (carrageenan) .....	45
2.2	Preparation of alginate films .....	46
2.3	Preparation of metal ion-alginate solutions.....	46
2.3.1	Preparation of stock solutions .....	46
2.3.2	Preparation of sample solutions .....	47
2.4	Preparation of sugar based metal-texturant solutions .....	47
2.4.1	Preparation of sugar solutions .....	47

2.4.2	Preparation of stock solutions .....	47
2.4.3	Preparation of solutions for viscosity measurements.....	48
2.5	Three dimensional printing (3DP).....	48
2.5.1	Primitive experiments .....	49
2.5.2	Packing density experiments.....	49
2.5.3	Printer resolution optimization.....	50
2.5.4	Effect of relative humidity (RH) on texture.....	50
2.5.5	Effect of texturants .....	50
2.6	Characterization techniques .....	51
2.6.1	Viscosity average molecular weight determinations.....	51
2.6.2	Solution viscosity measurements .....	52
2.6.3	Texture analysis.....	53
2.6.4	FTIR spectroscopy .....	53
<b>3.</b>	<b>RESULTS AND DISCUSSION .....</b>	<b>54</b>
3.1	Characterization of sodium alginate (Satialgine SG300) solutions .....	54
3.1.1	Viscosity average molecular weight determinations.....	54
3.1.2	FTIR analysis on alginate films .....	55
3.1.3	Effects of type of cations on viscosity of sodium alginate solutions .....	59
3.1.3.1	Effect of Mg <sup>2+</sup> cation.....	59
3.1.3.2	Effect of Al <sup>3+</sup> cation .....	61
3.1.3.3	Effect of Ca <sup>2+</sup> cation from different sources (CaSO <sub>4</sub> and Ca(NO <sub>3</sub> ) <sub>2</sub> ).....	63
3.1.4	Comparison of the effect of different cations on viscosity of alginate solutions.....	66
3.2	Analysis on the rheological properties of sugar based texturant solutions .....	67
3.2.1	Sodium Alginate (Satialgine SG300).....	68
3.2.2	Pectins (Unipectine PG569S and PG769S).....	71
3.2.3	Carrageenans (Satiagel KHG30 and Satiagum CD) .....	77

3.3	Three dimensional printing (3DP).....	82
3.3.1	Primitive experiments .....	82
3.3.2	Particle size analysis.....	84
3.3.3	Packing density .....	85
3.3.4	Printer resolution optimization.....	85
3.3.5	Binder solution trials .....	90
3.3.6	Texture modification studies.....	90
3.3.7	Effect of texturants .....	91
3.3.8	Further studies on promising formulations .....	95
3.4	FTIR analysis .....	99
3.4.1	Alginate .....	100
3.4.2	Carrageenans .....	101
3.4.3	Pectins .....	104
<b>4.CONCLUSIONS .....</b>		<b>107</b>
<b>REFERENCES .....</b>		<b>113</b>

## LIST OF TABLES

### TABLE

1.	FTIR peak assignments of alginate films [18] .....	56
2.	Primitive experiments with various powders and binder solutions.....	83
3.	Particle size distribution of sugar .....	84
4.	Packing density (g/cm <sup>3</sup> ) <sup>a</sup> .....	85
5.	Machine parameters and powder-type optimization .....	87
6.	Effect of particle size on resolution.....	89
7.	Properties without texturant .....	90
8.	Effect of alginate on texture .....	92
9.	Effect of carrageenans on texture.....	93
10.	Effect of pectins on texture .....	94
11.	Unipeptins based matrices with various binder solutions .....	95
12.	Texture analysis of samples at 54.1% RH chamber.....	96
13.	Texture analysis results at 77.5% RH .....	97
14.	FTIR peak assignments for different types of carrageenans.....	103

## LIST OF FIGURES

### FIGURE

1.	Possible rotations for the polysaccharide around the anomeric links .....	4
2.	Structure of the alginate chain (G=Guluronate, M=Mannuronate).....	12
3.	Portions of polysaccharide chains that make up alginate in solution.....	17
4.	Calcium ion bridges between alginate chains .....	17
5.	Representation of the alginate chains with (on the right) and without (on the left) $\text{Ca}^{2+}$ cations .....	18
6.	Structure of the carrageenan chain.....	20
7.	Production reaction of $\kappa$ -carrageenan .....	22
8.	Production reaction of $\iota$ -carrageenan .....	23
9.	Production reaction of $\theta$ -carrageenan from $\lambda$ -carrageenan.....	24
10.	Schematic representation of the gelling mechanism of carrageenan [24].....	25
11.	Structure of the pectin chain.....	29
12.	The 3DP sequence of operation [8].....	38
13.	The printing process in 3DP [32] .....	40
14.	3DP machine and its components [32].....	48
15.	FTIR spectrum of <b>a)</b> pure sodium alginate, <b>b)</b> sodium alginate + 0.01M $\text{Ca}^{2+}$ , <b>c)</b> sodium alginate + 0.1 M $\text{Ca}^{2+}$ , <b>d)</b> sodium alginate + 1 M $\text{Ca}^{2+}$ .....	57

<b>16.</b> Viscosity graphs of Mg-Alginate solutions <b>a)</b> $Mg^{2+}$ concentration is kept constant at 0.1 M while alginate concentration is varied. <b>b)</b> Alginate concentration is kept constant at 0.25% w/w while $Mg^{2+}$ concentration is varied. ....	60
<b>17.</b> Viscosity graphs of Al-Alginate solutions <b>a)</b> $Al^{3+}$ concentration is kept constant at 0.001 M while alginate concentration is varied. <b>b)</b> Alginate concentration is kept constant at 0.25% while $Al^{3+}$ concentration is varied. <b>c)</b> pH of the medium is changed at constant $Al^{3+}$ (0.001 M) and alginate concentration (0.25% w/w). ....	63
<b>18.</b> Viscosity graph of alginate solutions with $CaSO_4$ at $[Ca^{2+}]=1 \times 10^{-4} M$ .....	64
<b>19.</b> Viscosity behaviour of alginate solutions with <b>a)</b> $Ca(NO_3)_2$ at 0.25% w/w alginate, <b>b)</b> %Alginate at $[Ca^{2+}]=1 \times 10^{-4} M$ . ....	65
<b>20.</b> Effect of different cations on viscosity of alginate solutions .....	67
<b>21.</b> Viscosity vs. $Ca^{2+}$ concentration graphs of 50% sugar solution (w/w) with 0.5% (w/w) sodium alginate (Satialgine SG300) at 25 and 35 <sup>0</sup> C; <b>a)</b> at 100 rpm, <b>b)</b> at 50 rpm, <b>c)</b> at 20 rpm, <b>d)</b> at all rpms. ....	69
<b>22.</b> Viscosity vs. $Ca^{2+}$ concentration graphs of 50% sugar solution (w/w) with 0.5% (w/w) pectin (Unipectine PG569S) at 25 and 35 <sup>0</sup> C; <b>a)</b> at 100 rpm, <b>b)</b> at 50 rpm, <b>c)</b> at 20 rpm, <b>d)</b> at all rpms. ....	72
<b>23.</b> Viscosity vs. $Ca^{2+}$ concentration graphs of 50% sugar solution (w/w) with 0.5% (w/w) pectin (Unipectine PG769S) at 25 and 35 <sup>0</sup> C; <b>a)</b> at 100 rpm, <b>b)</b> at 50 rpm, <b>c)</b> at 20 rpm, <b>d)</b> at all rpms. ....	74
<b>24.</b> Viscosity vs. $Ca^{2+}$ concentration graphs of 50% sugar solution (w/w) with 0.5% (w/w) carrageenan (Satiagel KHG30) at 25 and 35 <sup>0</sup> C, <b>a)</b> at 100 rpm, <b>b)</b> at 50 rpm, <b>c)</b> at 20 rpm, <b>d)</b> at all rpms. ....	78
<b>25.</b> Viscosity vs. $Ca^{2+}$ concentration graphs of 50% sugar solution (w/w) with 0.5% (w/w) carrageenan (Satiagum CD) at 25 and 35 <sup>0</sup> C, <b>a)</b> at 100 rpm, <b>b)</b> at 50 rpm, <b>c)</b> at 20 rpm, <b>d)</b> at all rpms. ....	80

<b>26.</b> FTIR spectrum of <b>a)</b> Satialgine SG300, <b>b)</b> Satialgine SG300 in sugar solution with 0.01 M Ca <sup>2+</sup> .....	100
<b>27.</b> FTIR spectrum of <b>a)</b> Satiagum CD, <b>b)</b> Satiagum CD in sugar solution with 0.01 M Ca <sup>2+</sup> .....	101
<b>28.</b> FTIR spectrum of <b>a)</b> Satiagel KHG30, <b>b)</b> Satiagel KHG30 in sugar solution with 0.01 M Ca <sup>2+</sup> .....	102
<b>29.</b> FTIR spectrum of <b>a)</b> Unipeptine PG569S, <b>b)</b> Unipeptine PG569S in sugar solution with 0.01 M Ca <sup>2+</sup> .....	104
<b>30.</b> FTIR spectrum of <b>a)</b> Unipeptine PG769S, <b>b)</b> Unipeptine PG769S in sugar solution with 0.01 M Ca <sup>2+</sup> .....	105

## ABBREVIATIONS

3DP :	Three dimensional printing
G :	Guluronate
M :	Mannuronate
DE :	Degree of esterification
HMP :	High methoxyl pectin
LMP :	Low methoxyl pectin
RS :	Rapid set
SS :	Slow set
SFF :	Solid free-form fabrication
CAD :	Computer-aided-design
LT :	Layer thickness
CS :	Core saturation
S :	Saturation
RH :	Relative humidity

## **CHAPTER 1**

### **INTRODUCTION**

The newly evolving technology of three dimensional printing (3DP) involves the production of a complicated shapes by a software driven instrument layer by layer. The technique is well-suited to the fast production of master molds in material production and to obtain intricate shapes which are impossible to produce by standard molding operations. For example metal and metal oxide powders can easily be binded by a polymeric binder solution that is deposited from an ink-jet printer cartridge and the shape obtained can later be sintered to obtain a rigid structure, thus, reducing the time and the cost of producing a mold by machining operations [1-4].

The process can also be applied to biomaterial production where hydroxy-apatite based bone-replacement matrices can be produced in any shape to be used as the skull or bone repair elements [4-6]. In principle, not only inorganic matrices but also organic polymeric structures can be obtained in the desired shapes by a suitable combination of the powder and the binder solution.

It is also possible to apply the 3DP process to the manufacture of pharmaceutical pills which incorporates more than one drug into a single pill and arrange the dissolution of the pill as a function of time after the intake by means of layered controlled release structures [7,8].

We have worked on the production of edible objects via 3DP. The problem with the edible objects is that one needs to work basically with water based mixtures. The use of organic solvents is out of question due to food safety regulations and the public anxiety over the health effect of such products. The most suitable food products for 3DP are confectionaries which are based on sugar and sugar related materials such as starch, corn syrup etc.

Contrary to previously mentioned applications of 3DP with sugar matrices and aqueous binder solutions, the dissolution of the matrix with the binder employed creates problem of shape resolution in the finished product. One needs to slow down and reduce the dissolution and the fast impregnation of the aqueous binder solution into the matrix. The method applied to this effect is the use of food grade gelling agents such as alginates, starch and similar materials so that water is captured in the form of a gel and consequent reduction in dissolution and impregnation.

In this study, it is sought to understand the gelling behaviour of various gelling agents and the effect of various factors on the production of confectionary objects by means of 3DP process.

## **1.1 Polysaccharides; nature, occurrence and classification**

Polysaccharides may be defined as condensation polymers of high molecular weight based on simple monosaccharide units. One monosaccharide unit is joined to the next monosaccharide unit by a glycosidic linkage which may

be regarded as involving the elimination of water between the hemiacetal ( $C_{(1)}$ ) hydroxyl group of one unit and an available hydroxyl group of another. These inter-unit linkages are the same as those in oligosaccharides (disaccharides, trisaccharides, etc.), and although there is no rigorously defined division between oligo- and polysaccharides, the term polysaccharide is normally used for materials which contain more than ten sugar residues. The majority of polysaccharides, however, are substances of much higher molecular weight and several have molecular weights of more than a million [9].

Polysaccharides are natural macromolecules of almost universal occurrence in living organisms where they perform a variety of functions, many of which are not fully understood. Nevertheless, it is readily recognised that they may act as skeletal substances in the cell walls of higher land plants and seaweeds, that they provide reserve food supplies in plants, micro-organisms, and animals, and that they may function as protective substances, in plants in the form of exudate gums sealing of sites of injury, and in micro-organisms as encapsulating substances. They also function as thickening agents in the joint fluids of animals and by protecting tissues from dessication [9].

Polysaccharides are classified on the basis of their main monosaccharide components and the sequences and linkages between them, as well as the anomeric configuration of linkages, the ring size (furanose or pyranose), the absolute configuration (D- or L-) and any other substituents present.

Polysaccharides are more hydrophobic if they have a greater number of internal hydrogen bonds, and as their hydrophobicity increases there is less direct interaction with water. Carbohydrates contain alcohol groups that preferentially interact with two water molecules each if they are not interacting with other hydroxyl groups on the molecule. They will preferentially interact with water if the

hydroxyl groups are equatorial on the pyranose rings. Sugar residues have a specific conformation, often the so-called  ${}^4C_1$  chair conformation.

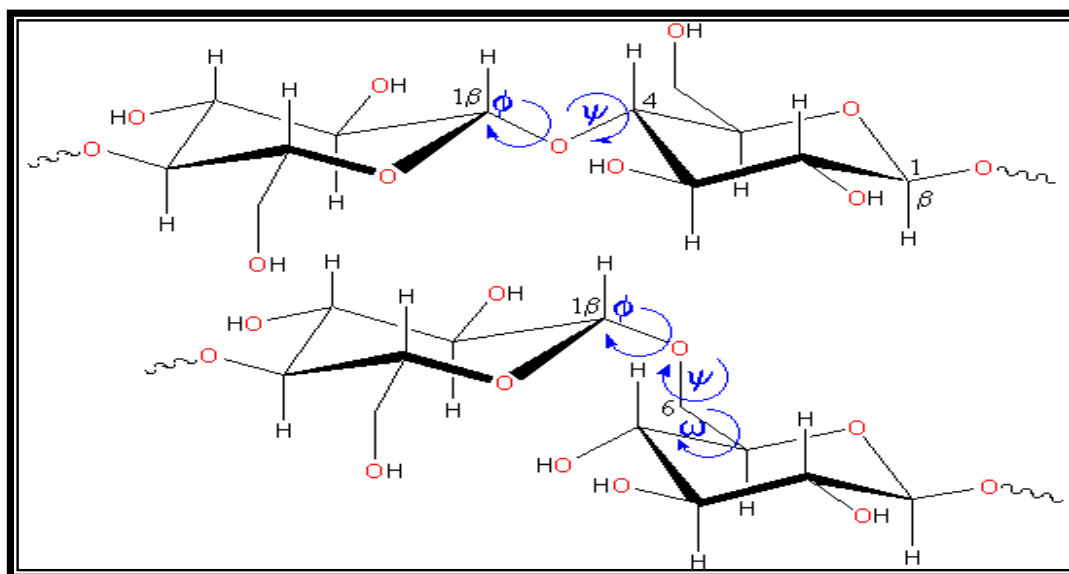


**Figure 1.** Possible rotations for the polysaccharide around the anomeric links

The flexibility of polysaccharide chains depends on the ease of rotation around the anomeric links (the torsion angles phi ( $\phi_H$ ,  $H_1C_1OC_4$  or  $H_1C_1OC_6$ ), psi ( $\psi_H$ ,  $C_1OC_4H_4$  or  $C_1OC_6C_5$ ) and omega ( $\omega_H$ ,  $OC_6C_5H_5$ ) are shown in Figure 1). Rotation changes the energy of the structure and this can be visualised in a potential energy map.

Polysaccharides are important additives in both food and non-food industries where they are widely used to thicken or immobilise aqueous solutions, and hence to control the rheological properties of the products. This control can be achieved in three distinct ways. Firstly, in common with all long chain hydrophilic molecules, polysaccharides show general properties of thickening and water immobilisation reflecting their ability to increase the viscosity of aqueous solutions. This behaviour arises because the polymer chains exist in solution in random, and continually fluctuating, shapes. It is non-specific in that a general pattern describing the dependence of solution viscosity on both concentration and

shear rate can be observed for all polysaccharides of this type and attributed to random physical entanglements between the fluctuating chains [10].

Although these commodity thickeners are widely used in industrial applications, their properties are quite different from, and they can rarely replace, the more expensive gums and thickeners. Certain of these specialist polysaccharides can control the rheology of an aqueous phase in a different way giving weak gelling properties intermediate between those of thickened solutions and those of completely rigid gels. Such systems are liquids with a finite yield stress and have some of the properties of thickened sols (pourable/flowable, shear thinning) and some of the properties of gels (excellent particle suspending). This can arise from the ability of particular polysaccharides with periodic repeating sequences to adopt ordered rod-like structures in aqueous solution which can themselves associate weakly and reversibly. The result is an incipient network which flows readily after shear disruption and reforms rapidly on standing [10].

The third sort of rheological control is shown by a range of speciality polysaccharides which can, under favourable conditions, form rigid gels. Here the origin of the structure again involves conformational ordering of extended, regular sequences of polysaccharide chains into stable microcrystalline arrays. These ordered regions are usually terminated by changes in chain covalent structure which are incompatible with the ordered association. As a consequence a single polymer chain can take part in several independent associations with different partners thus forming 3D gel network. The type of polysaccharide and the relative proportions of the polymer chains which are involved in these ordered and soluble regions are important factors in determining the final gel properties [10].

## 1.2 Hydrocolloids

The term hydrocolloid covers a fairly limited range of biopolymers (principally but not entirely polysaccharides); it nevertheless comprises a surprisingly wide coverage of polymer types, linear and branched molecules, non- and polyelectrolytes. The net effect of admixing water with hydrocolloids, particularly when accompanied by changes in temperature, is to cause some rearrangement of the polymer and water molecules, the actual result being a function of the hydrocolloid-water interactions as well as the temperature and concentration regimes [11].

Hydrocolloids are hydrophilic polymers, of vegetable, animal, microbial or synthetic origin, that generally contain many hydroxyl groups and may be polyelectrolytes. They are naturally present or added to control the functional properties of aqueous foodstuffs. Most important amongst these properties are viscosity (including thickening and gelling) and water binding but also significant are many others including emulsion stabilization and organoleptic properties. Foodstuffs are very complex materials and this together with the multifactorial functionality of the hydrocolloids have resulted in several different hydrocolloids being required; the most important of which are listed below:

Alginate, arabinoxylan, carrageenan, carboxymethylcellulose, cellulose, gelatin, b-glucan, guar gum, locust bean gum, pectin, starch, xanthan gum.

Each of these hydrocolloids consists of mixtures of similar, but not identical, molecules and different sources, methods of preparation, thermal processing and foodstuff environment (e.g. salt content, pH and temperature) all affect the physical properties they exhibit. Descriptions of hydrocolloids often present idealized structures but it should be remembered that they are natural products (or derivatives) with structures determined by stochastic enzymic action,

not laid down exactly by the genetic code. They are made up of mixtures of molecules with different molecular weights and no one molecule is likely to be conformationally identical or even structurally identical (cellulose excepted) to any other.

All hydrocolloids interact with water, reducing its diffusion and stabilizing its presence. Generally neutral hydrocolloids are less soluble whereas polyelectrolytes are more soluble. Such water may be held specifically through direct hydrogen-bonding or the structuring of water or within extensive but contained inter- and intra-molecular voids. Interactions between hydrocolloids and water depend on hydrogen-bonding and therefore on temperature and pressure in the same way as water cluster formation.

As hydrocolloids can dramatically affect the flow behavior of many times their own weight of water, most hydrocolloids are used to increase viscosity, which is used to stabilize foodstuffs by preventing settling, phase separation, foam collapse and crystallization.

Many hydrocolloids also gel, so controlling many textural properties. Gels are liquid-water-containing networks showing solid-like behavior with characteristic strength, dependent on their concentration, and hardness and brittleness dependent on the structure of the hydrocolloid(s) present. Hydrocolloids display both elastic and viscous behaviour where the elasticity occurs when the entangled polymers are unable to disentangle in time to allow flow. Mixtures of hydrocolloids may act synergistically, associating to precipitate, gel or form incompatible biphasic systems; such phase confinement affecting both viscosity and elasticity. Hydrocolloids are extremely versatile and they are used for many other purposes including;

(a) production of pseudoplasticity (i.e. fluidity under shear) at high temperatures to ease mixing and processing followed by thickening on cooling,

- (b) liquefaction on heating followed by gelling on cooling,
- (c) gelling on heating to hold the structure together (thermogelling),
- (d) production and stabilization of multiphase systems including films.

The behaviour of a hydrocolloid in aqueous solution will depend on the interactions which occur between hydrocolloid and solvent molecules, between individual hydrocolloid molecules and between hydrocolloid and other solute molecules in the solution. In addition to these direct effects there are, what may be termed, indirect effects such as competition between the hydrocolloid and other solutes for the available water molecules [12].

Hydrocolloids find wide application because of their ability to thicken, or increase the viscosity of the medium in which they are dissolved. In very dilute solutions the optimum properties are obtained from the hydrocolloid by maximising the hydrocolloid-solvent interactions and minimising the intramolecular hydrocolloid-hydrocolloid interactions. This should result in maximum extension of the hydrocolloid molecule and give high values for the intrinsic viscosities. As the concentration of the hydrocolloid solution is increased then intermolecular interactions may develop between neighbouring hydrocolloid molecules and the viscosity of the solution shows a substantial increase [12].

The development of intermolecular interaction leads to increasing departure from Newtonian behaviour, as the apparent viscosity is now sensitive to shear rate. Intermolecular interactions involving polyanionic hydrocolloids may show some differences compared with the intermolecular interactions of neutral hydrocolloids. Thus the presence of charge on each polyanion may inhibit intermolecular interactions, while cations which are inevitably present, or are deliberately added to the solution, may have a specific role to play in the development of intermolecular interactions [12].

### 1.2.1 Some aspects of hydrocolloid gelation

Gels are dual-natured substances, because they exhibit properties that are typical of both liquids and solids. Thus, while they display vapor pressure, compressibility, and electrical conductivity typical of fluids, they may also show rigidity commonly associated with solids. This unusual combination of properties is caused by the physical structure of gels: long-chain molecules linked by primary or secondary bonds at widely separated sites along the molecule [13].

It is convenient to classify gels into two categories: elastic and nonelastic. Elastic gels can be partially dehydrated to give typically elastic solids. Replacement of the loss water, sometimes with heating, readily regenerates the original gel. Hence, the gel system can be considered as reversible. On the other hand, nonelastic gels are nonreversible. Such gels become glassy or crumble into a powder upon dehydration and cannot be regenerated by the simple addition of water [13].

The start of gelation is first manifested by the gradual decrease in the Brownian movement. This may be caused by the hydration and coherence of the particles, as long-range forces between molecules begin to exert their actions. The viscosity begins to increase and the solvent is immobilized or absorbed by the swelling solute. As the action continues, a three-dimensional network is gradually built up containing “*pores*” of solvent. At the gel point, the rigidity is still small and most of the polymerizable material is still in monomeric, dimeric, and trimeric form. As the reaction proceeds, the smaller fragments continue to react with each other to form what is essentially one large molecule. The rigidity may become considerable at this point. Parts of the large molecule can still further react with other parts to form more crosslinks and thus increase the rigidity. If the molecular segments between linking points are relatively long and flexible, the gel tends to be rubbery and to have a greater tendency to imbibe solvent [13].

To establish a suitable technique for measurement of the transition to a gel it is necessary to fundamentally define a gel. The majority of prior studies make reference to the theoretical work of Flory. Flory states that a gel is a solid like structure that at the instant of gelation, has a structure in the fluid which extends over the entire sample volume. Flory demonstrates that at the gel point, the effective molecular weight of a polymer solution goes to infinity. Physical interpretation suggests that at the gel point the shear viscosity extends to infinity ( $\eta_0 \rightarrow \infty$ ) and the equilibrium modulus is 0 ( $G_{\infty} = 0$ ). In terms of polymer solutions, it is considered that during gelation a material changes from one in which connectivity extends from a single molecular scale to one in which connectivity extends throughout the entire sample. For the application of Flory's definition of a gel, it is necessary that the connectivity throughout the sample is continuous over any timescale and therefore the crosslinking process must be permanent. A concentrated solution of high initial molecular weight polymer is complicated by the presence of molecular entanglements, which contribute to the overall elasticity of the system [14].

A gel is a system with small proportions of a substance dispersed in relatively large proportions of liquid, which behaves in certain respects as a rigid solid and yet retains many properties characteristic of fluids. Polysaccharide gels contain in general a few or less than 1% of polysaccharide and 99% of water and low molecular weight solids. The gel nature can be based on the existence of a crosslinked polysaccharide network; the gelation takes place by crosslinking of the dissolved polysaccharide macromolecules to a 3D network. This process is considered very specific, because only a few polysaccharides can form true thermoreversible gels [15].

The high molecular weight of the polysaccharide molecules is the most important and limiting factor for any crosslinking reaction, such as the gelation

process. The importance of a high molecular weight has been proved for practically every polysaccharide gel mixture [15].

The shape of the polysaccharide molecules, also not fully investigated, might have another important influence on the gelation properties. Linear chain molecules show in general much better gelation properties than branched ones. Heavily coiled molecules will obviously react preferentially with different segments of the same molecule; uncoiled molecules will react preferentially with each other. The coiling of the molecules is influenced by charged groups and side groups on the chain molecules, restricted free rotation of the glycosidic bonds, etc. Side groups or some kind of molecular branching of chain molecules may hinder the contact of two molecules for steric reasons and therefore hinder a crosslinking [15].

The gelation reaction itself involves changes of solvent-solute and solute-solute forces. These changes are brought about by (a) additions of sugar or salt to the gel mixture, causing dehydration of the macromolecules (salt also suppresses the dissociation of dissociated groups, decreasing the repelling action of the molecules) and (b) by dropping the temperature, causing a decrease of the kinetic energy of the particles. These changes cause the relative interactions of the functional groups of the macromolecules with the solvent to become weaker than those between the functional groups of two macromolecules-association (gelation) occurs [15].



- Fucales: *ascophyllum nodosum* and *fucus serratus*

The useful properties of brown seaweeds were known to both the ancient Chinese and the Romans, who used them for medical cosmetic purposes. Production of alginates on an industrial scale began in the United States in the 1930s. Originally, alginates were produced for the manufacture of canned food used at sea [16].

### 1.3.3 Structural unit

Alginates are linear unbranched polymers containing  $\beta$ -(1 $\rightarrow$ 4)-linked D-mannuronic acid (M) and  $\alpha$ -(1 $\rightarrow$ 4)-linked L-guluronic acid (G) residues. Although these residues are epimers (D-mannuronic acid residues being enzymatically converted to L-guluronic after polymerization) and only differ at C5, they possess very different conformations; D-mannuronic acid being  ${}^4C_1$  with diequatorial links between them and L-guluronic acid being  ${}^1C_4$  with diaxial links between them. Bacterial alginates are additionally O-acetylated on the 2 and/or 3 positions of the D-mannuronic acid residues. The bacterial O-acetylase may be used to O-acetylate the algal alginates, so increasing their water-binding.

### 1.3.4 Molecular structure

Alginates are not random copolymers but, according to the source algae, consist of blocks of similar and strictly alternating residues (i.e. MMMMMM, GGGGGG and GMGMGMGM), each of which have different conformational preferences and behavior. The monomers are arranged along the chains in a block-wise fashion with homopolymeric blocks of the G and M residues, together with blocks containing both monomers arranged in, preferentially, an alternating (MG) type of structure. A considerable amount of work has been carried out to characterize the physical properties of the three types of blocks, and their contribution to the physical properties of alginate molecules with different block

composition. Conformational energy calculations have indicated that the relative extension (stiffness) of the three types of blocks increases in the order [17]:

$$\text{MG-blocks} < \text{MM-blocks} < \text{GG-blocks}$$

This order was verified experimentally, although a lack of high molecular weight alginates with all the extreme compositions and the limited knowledge of block composition and block length distribution made any quantitative comparison difficult. The solubility at low pH was found to increase in the order GG-blocks < MM-blocks < MG-blocks, resulting in reduced gel strength and increased swelling of acid gels in that same order. The selective binding of divalent metal ions and the corresponding gel strength were found to increase in the order MM-blocks  $\leq$  MGblocks  $\ll$  GG-blocks. The basic problem in relating the physical properties to the molecular structure has been the limited knowledge of the monomer sequence within the alginate molecule. They may be prepared with a wide range of average molecular weights (50-100000 residues) to suit the application [17].

Poly  $\beta$ -(1 $\rightarrow$ 4)-linked D-mannuronic acid prefers intra-molecular hydrogen bonding between the hydroxyl group in the 3 position and the subsequent ring oxygen (i.e. O3-H $\rightarrow$ O'). Poly  $\alpha$ -(1 $\rightarrow$ 4)-linked L-guluronic acid forms stiffer chains preferring intra-molecular hydrogen bonding between the hydroxyl groups and the carboxyl group in the prior residue. The free carboxylic acids (without counterion) have a water molecule H<sub>3</sub>O<sup>+</sup> firmly hydrogen bound to carboxylate. Ca<sup>2+</sup> ions can replace this hydrogen bonding, zipping chains together stoichiometrically in a supposedly egg-box like conformation (the ions being the eggs in the puckered box of the polysaccharides). Under similar conditions, poly-mannuronic acid blocks take up a less-gelling ribbon conformation. Alternating (MG) structures contain both equatorial-axial and axial-equatorial links and take up dissimilar rather disorderly conformations. *'Designer'* alginates may be

available in the future by the 5-epimerization of  $\beta$ -(1 $\rightarrow$ 4)-linked D-mannuronic acid residues to  $\alpha$ -(1 $\rightarrow$ 4)-linked L-guluronic acid residues in algal alginates using bacterial epimerases. An available natural alternative is to harvest the seaweed from exposed seaboards (more G giving the kelp strength) or sheltered bays (more M).

### 1.3.5 Functionality - structuring using alginates

In solution alginates can be used as thickening or gelling agents. These properties depend on the presence or absence of calcium ions.

- *Calcium-induced gelation of alginates*

The primary function of the alginates are as thermally stable cold setting gelling agents in the presence of calcium ions; gelling at far lower concentrations than gelatin. Such gels can be heat treated without melting, although they may eventually degrade. Gelling depends on the ion binding ( $\text{Mg}^{2+} \ll \text{Ca}^{2+} < \text{Sr}^{2+} < \text{Ba}^{2+}$ ) with the control of the dication addition being important for the production of homogeneous gels (e.g. by ionic diffusion or controlled acidification of  $\text{CaCO}_3$ ).

Alginates are well known for their ability to form gels with divalent cations such as  $\text{Ca}^{2+}$ , and they have found widespread application in the food and pharmaceutical industries. The high absorbency and the haemostatic properties of alginates make them of particular use for wound dressings [18].

The guluronic segments of alginate chains can adopt the form of a buckled ribbon. In the presence of calcium ions, segments that are homogeneous can associate to form aggregates similar to an "eggbox". Within these junction zones the chains are in a regular pleated structure which is stabilized by calcium ions, each neutralizing a negative charge on two different chains. As a result, alginates

richer in these blocks form stronger gels. When the calcium-induced crosslinks are strong and numerous, an alginate gel will be thermally irreversible [16].

G sequences organize by selectively binding  $\text{Ca}^{2+}$  and other divalent cations to form ordered domains which are responsible for gelation. Monovalent cations and  $\text{Mg}^{2+}$  ions do not induce gelation. Since M sequences in the chain do not form an “*egg-box*”, the content of G in the alginate determines the properties of the gels. Alginates with high content of G produce rigid gels that are subject to syneresis, while alginates with high content of M form more elastic gels. The molecular weight and the M/G ratio are important structural factors in the complexing with divalent ions [19].

High G content produces strong brittle gels with good heat stability (except if present in low molecular weight molecules) but prone to water weepage (syneresis) on freeze-thaw, whereas high M content produces weaker more-elastic gels with good freeze-thaw behavior. However, at low or very high  $\text{Ca}^{2+}$  concentrations high M alginates produce the stronger gels. So long as the average chain lengths are not particularly short, the gelling properties correlate with average G block length (optimum block size~12) and not necessarily with the M/G ratio which may be primarily due to alternating MGMG chains. The future prospects are excellent as recombinant epimerases with different specificities may be used to produce novel designer alginates.

Alginate is a mixture of such polysaccharide chains. The ratio of guluronate (G) and mannuronate (M) units and the proportion of the various polysaccharide chains depend upon the source of alginate and the processing conditions (Figure 3).

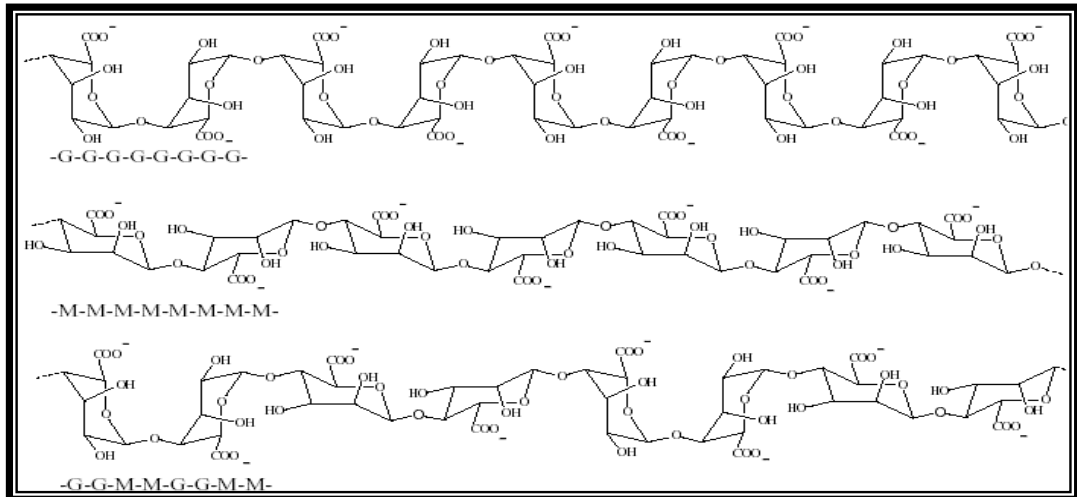


**Figure 3.** Portions of polysaccharide chains that make up alginate in solution

Positively-charged calcium ions,  $\text{Ca}^{2+}$ , are attracted to the negatively-charged carboxylic acid groups,  $\text{COO}^-$  of the alginate polysaccharide chains.  $\text{Ca}^{2+}$  ions fit into guluronate structures like eggs in an eggbox (Figure 4).

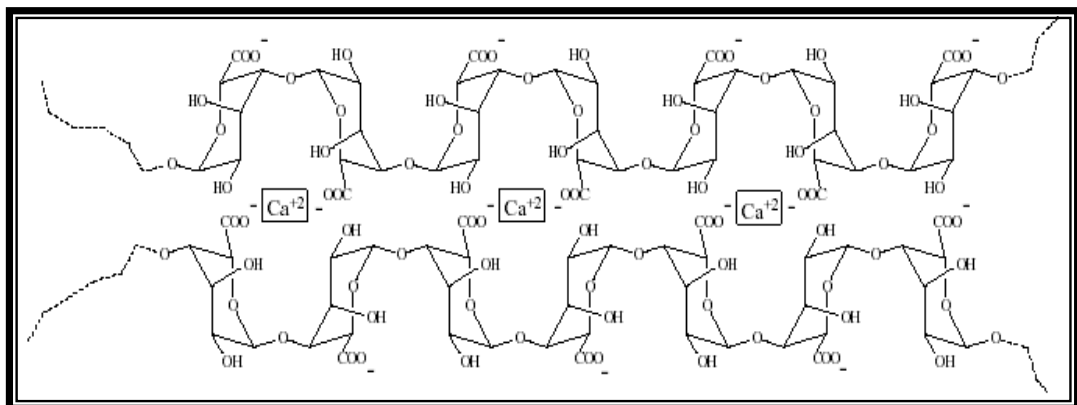


**Figure 4.** Calcium ion bridges between alginate chains

Regions of guluronate units in one alginate polysaccharide chain can be linked to a similar region in another alginate polysaccharide chain through calcium ion bridges (Figure 4).

In the absence of calcium ions, alginate chains remain in solution. However, in the presence of calcium ions, alginate chains become bound together

at the guluronate units, forming an insoluble network of alginate polysaccharides. This network is called a gel (Figure 5).

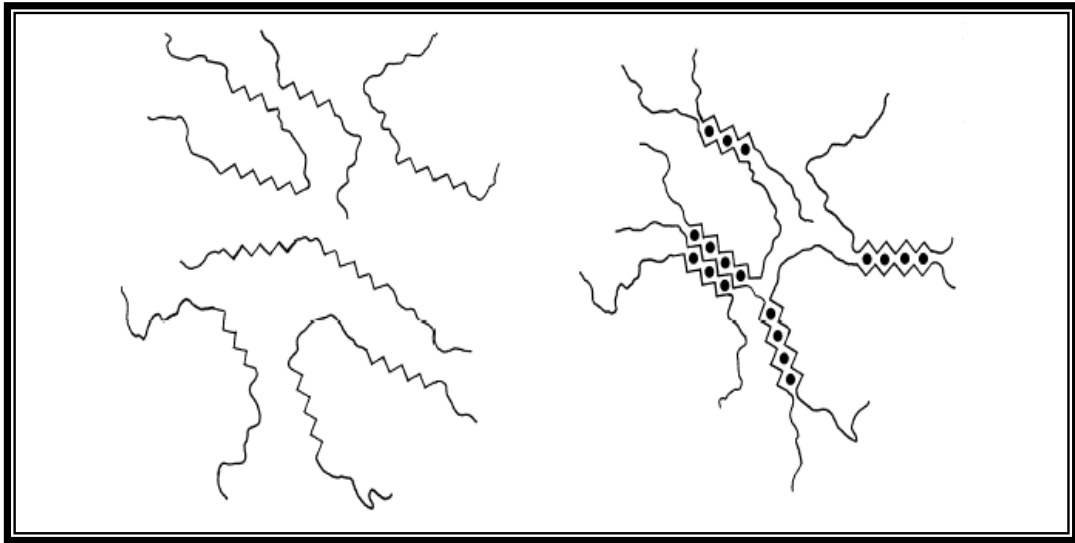


**Figure 5.** Representation of the alginate chains with (on the right) and without (on the left)  $\text{Ca}^{2+}$  cations

- *Thickening*

Alginate's solubility and water-holding capacity depend on pH (precipitating below about pH 3.5), ionic strength (low ionic strength increasing the extended nature of the chains) and the nature of the ions present. Generally alginates show high water absorption and may be used as low viscosity emulsifiers and shear-thinning thickeners. They can be used to stabilize phase separation in low fat fat-substitutes e.g. as alginate/caseinate blends in starch three-phase systems. When a soluble alginate is dissolved, the acid groups are entirely ionized and a viscous solution is obtained. With high viscosity and shear-thinning properties, its rheology is typical of solutions of flexible coil macromolecules. These two properties are proportional to the concentration and the molecular weight. As the temperature rises, the viscosity decreases. This is reversible [16].

### 1.3.6 Manufacturing process

The process is based on the following two properties:

- sodium and potassium alginates are soluble in water;
- alginic acid and its calcium salt have very low water solubility.

The manufacturing process includes 4 main steps:

- Demineralization
- Extraction
- Precipitation of alginic acid
- Neutralization and obtention of alginates [16].

#### Main Applications

- Dairy:  
Creams and whipped creams, dessert creams, mixes for dessert creams, processed cheese, ice creams
- Powder products:  
Baking bakery creams, batter mix, béchamel sauce
- Restructured products:  
Meat, fruits, vegetables, fishes (internal/external gelation)
- Technical applications:  
Textile (color fixing), welding rods, water treatment, cosmetics (masks, dental prints) [16].

## 1.4 Carrageenans

### 1.4.1 Source

Carrageenan is a collective term for polysaccharides prepared by alkaline extraction (and modification) from red seaweed (rhodophyceae).

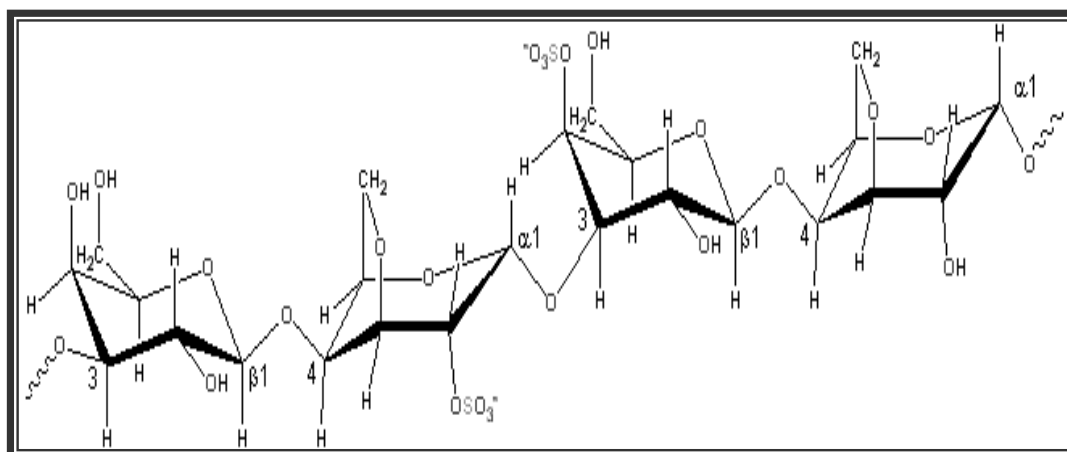


**Figure 6.** Structure of the carrageenan chain

### 1.4.2 Raw materials

Carrageenans are extracted from various types of red seaweeds (rhodophyceae) of the gigartinales group, the main types being:

- Gigartina (France, Argentina/Chili, Morocco)
- Chondrus (France, North Atlantic)
- Iridaea (Chili)
- Eucheuma (Philippines/Indonesia) [16].

### 1.4.3 Structural unit

Carrageenan consists of alternating 3-linked-β-D-galactopyranose and 4-linked-α-D-galactopyranose units (Figure 6).

#### 1.4.4 Molecular structure

Carrageenans are linear polymers of about 25,000 galactose derivatives with regular but imprecise structures, dependent on the source and extraction conditions [20]. They are polysaccharides (galactose) with a varying degree of sulfatation (between 15% and 40%) and extracted from red seaweeds and are used as thermoreversible gelling and thickening agents mainly in the food industry [16]. Idealized structures are given in Figures 7, 8, and 9.

#### 1.4.5 Functionality - structuring using carrageenan

The carrageenan family is extremely diverse; it can be broadly classified into 3 main "*ideal*" types of carrageenan, split into two groups:

- *Gelling Carrageenans: kappa and iota*

After heat treatment required for dissolution, the macromolecules have a tendency to spontaneously associate during cooling, thus creating junction zones required for a gel. The  $\iota$ -carrageenan network is formed by a series of double-helices and kinks, that form a transparent, elastic gel. This loosely connected network can easily be destroyed by mechanical action. However, it reforms quickly once the mechanical action has stopped. This property is called "*thixotropy*" and is very useful in certain applications, such as cold-filled dairy desserts [16].

Gelation of  $\kappa$ -carrageenan is particularly enhanced by the potassium ion. It induces gel formation at very low concentrations. Because of its small size when hydrated, it fits into the coil and partially neutralizes the sulfate groups. Thus, the double-helices can cluster together and form aggregates which create a strong, brittle gel [16].

- *κ-carrageenan (kappa-carrageenan)*

-(1→3)-β-D-galactopyranose-4-sulfate-(1→4)-3,6-anhydro-α-D-galactopyranose-(1→3)-

κ-carrageenan is produced by alkaline elimination from μ-carrageenan (mu-carrageenan) (Figure 7). The experimental charge/dimer is 1.03 rather than 1.0 with 0.82 molecules of anhydrogalactose rather than one.

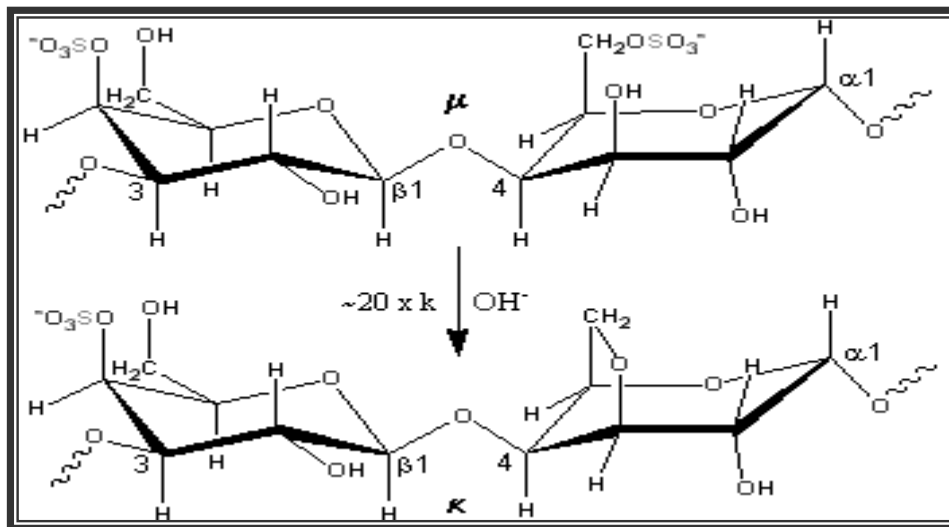


**Figure 7.** Production reaction of κ-carrageenan

- *ι-carrageenan (iota-carrageenan)*

-(1→3)-β-D-galactopyranose-4-sulfate-(1→4)-3,6-anhydro-α-D-galactopyranose-2-sulfate-(1→3)-

ι-carrageenan is produced by alkaline elimination from ν-carrageenan (nu-carrageenan) (Figure 8). The experimental charge/dimer is 1.49 rather than 2.0 with 0.59 molecules of anhydrogalactose rather than one.

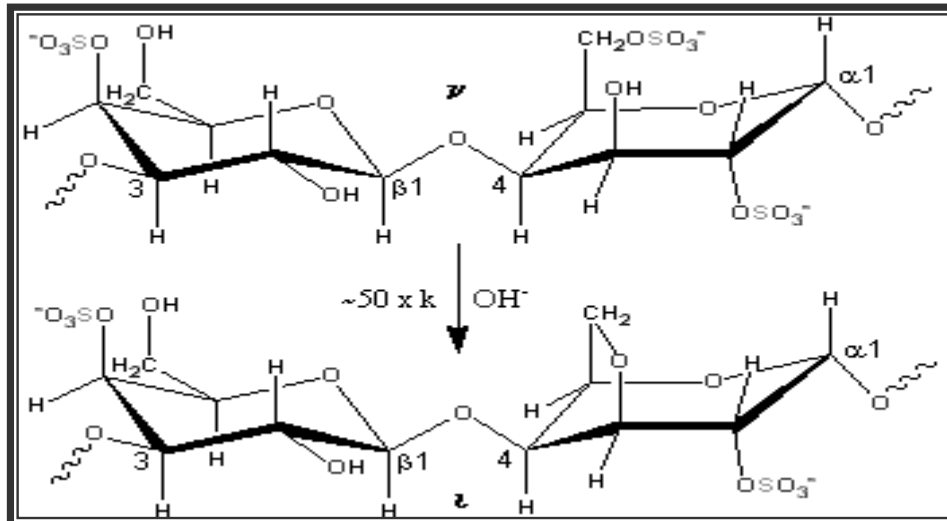


**Figure 8.** Production reaction of  $\iota$ -carrageenan

The 3D structure of the  $\iota$ -carrageenan double helix has been determined [21,22] as forming a half-staggered, parallel, threefold, right-handed double helix, stabilized by interchain O2-H...O-5 and O6-H...O-2 hydrogen bonds between the  $\beta$ -D-galactopyranose-4-sulfate units.

- Thickening Carrageenans: lambda

Mainly because of electrostatic repulsion, the chains of lambda carrageenan do not have a tendency to self-associate and can easily be separated from each other. Thus, lambda carrageenan acts simply as a thickening agent [16].

- $\lambda$ -carrageenan (lambda-carrageenan)

-(1→3)- $\beta$ -D-galactopyranose-2-sulfate-(1→4)- $\alpha$ -D-galactopyranose-2,6-disulfate-(1→3)-

$\lambda$ -carrageenan is converted into  $\theta$ -carrageenan (theta-carrageenan) by alkaline elimination, but at a much slower rate than causes the production of  $\iota$ -carrageenan and  $\kappa$ -carrageenan (Figure 9). The experimental charge/dimer is 2.09 rather than 3.0 with 0.16 molecules of anhydrogalactose rather than zero.

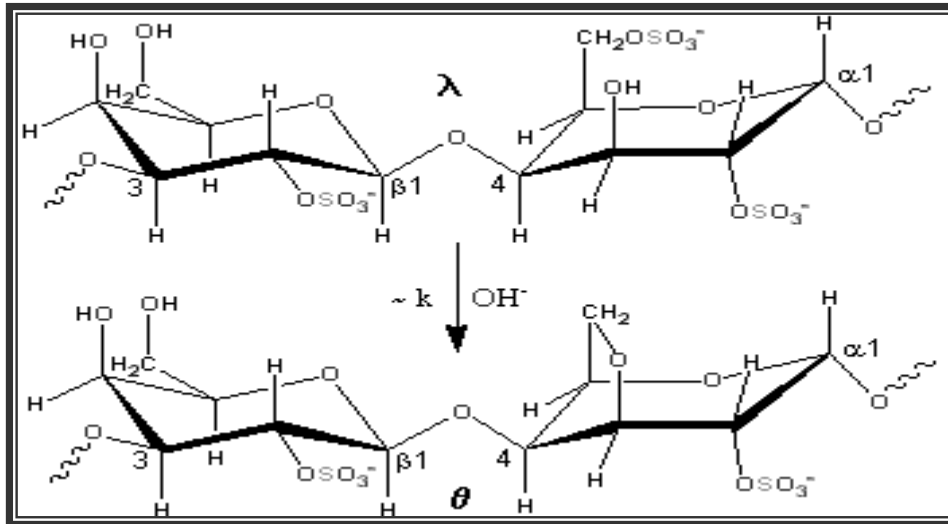


**Figure 9.** Production reaction of  $\theta$ -carrageenan from  $\lambda$ -carrageenan

The structures described above are idealized, implying that different carrageenans are perfect chains made up of identical repetitive units. In reality, carrageenan macromolecules are not homogeneous. They are heterogeneous either due to differing molecular structures within the chains or due to differing chains within the seaweed [16].

The chemical reactivity of carrageenans is primarily due to half-ester sulfate groups that are strongly ionic. Carrageenan is usually employed as either a sodium, potassium or calcium salt or a mixture of these. The association of the cations together with the conformation of the units of the polysaccharide determine the physical properties of the carrageenans [23]. For example, potassium carrageenate, as prepared commercially, is a mixture of  $\lambda$ - and  $\kappa$ -carrageenan and is soluble in hot water but only  $\lambda$ -carrageenan is gel forming. Sodium carrageenate is soluble in cold water and does not gel [24].

Carrageenan gels are all thermally reversible. The formation of the gels is based upon the double helix structure which is lacking at high temperatures. On cooling, a polymer network is formed with double helices forming the junction points which then undergo further aggregation (Figure 10)[24].

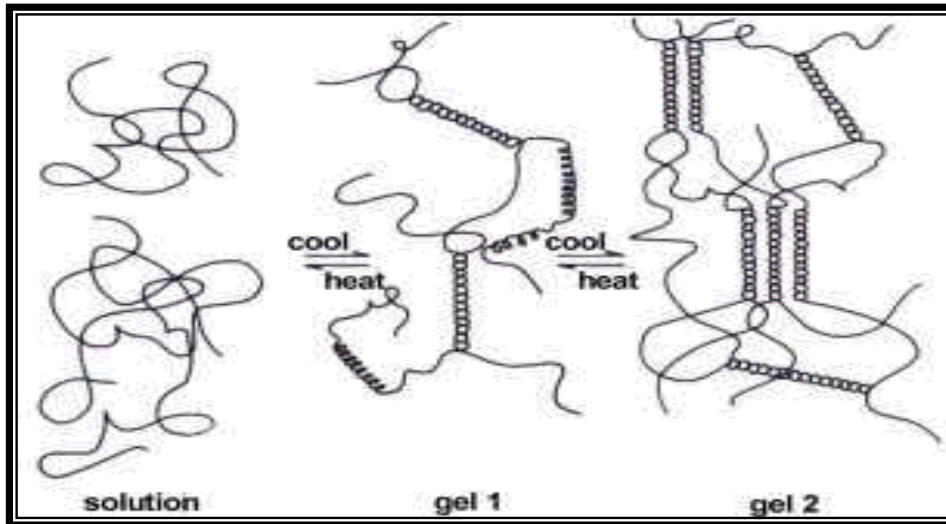


**Figure 10.** Schematic representation of the gelling mechanism of carrageenan [24]

All carrageenans are highly flexible molecules which, at higher concentrations, wind around each other to form double-helical zones. Gel formation in  $\kappa$ - and  $\iota$ -carrageenans involves helix formation on cooling from a hot solution together with gel-inducing  $K^+$  or  $Ca^{2+}$  cations respectively (not  $Na^+$ ) which link between the helices forming the junction zones.

In an appropriate condition,  $\kappa$ -carrageenan and  $\iota$ -carrageenan in aqueous solutions undergo thermoreversible sol-gel transition, while no gelation takes place in  $\lambda$ -carrageenan having more electrolyte groups. Carrageenan is widely applied to food industry as gel or viscous agents, and also exhibits some physiological effect such as anti-tumor activities. Such a wide application and an interest in sol-gel transition phenomenon have promoted many fundamental studies on the aqueous solution of carrageenan [25].

It is widely accepted that the gelation of carrageenan is based on the formation of double helix structure. The structural model of a double helix was first deduced from the X-ray diffraction image of carrageenan fibrils, and other results, for example, the comparison of experimental results with the calculated optical rotation or the dimerization of carrageenan segments investigated by light scattering support this model indirectly. Carrageenan assumes a random coil conformation in sol state, and low temperature induces anhydro-galactose sequences to twist in a double helical manner. The further aggregation is also promoted among formed double helical parts. A part of hydrated sequences function as a helix breaker. Subsequently the aggregation of double helices forms a cross-linking domain and leads the infinite network structure enough to complete gelation. Since the carrageenan repeat units possess the electrical charge in sulfate groups, the counter ions are found to play a role in gelation. Morris et al. suggested the modified gelation model by including the counter ions mediated between double helices [25].

Both  $\kappa$ - and  $\iota$ -carrageenans are polyions and, consequently, salts affect their conformational transitions and gelation behaviour. Moreover, the behaviour of low charged  $\kappa$ -carrageenan is very sensitive to the presence of monovalent ions [26].

Note that the gelling hydrocolloid agar is produced from the same family of seaweeds and consists of a mixture of branched but only slightly sulfated (~2%) polymers based on the  $-(1\rightarrow3)\text{-}\beta\text{-D-galactopyranose-(1}\rightarrow4\text{)-3,6-anhydro-}\alpha\text{-L-galactopyranose}$  unit; the major difference being the presence of L-rather than D-3,6-anhydro- $\alpha$ -galactopyranose units.

Carrageenans are used mainly for thickening, suspending and gelling.  $\kappa$ - and  $\iota$ -carrageenans form thermoreversible gels on cooling in the presence of appropriate counterions.  $\kappa$ -carrageenan forms a firm clear, if brittle, gel with poor

freeze-thaw stability; the coil-helix transition being followed by a  $K^+$ -induced aggregation of the helices.  $\kappa$ -carrageenan gels may be softened (and is generally regarded to be synergistically strengthened) with locust bean gum.  $\iota$ -carrageenan has less specific ionic binding but increased ionic strength allows helices to form junction zones in soft elastic gels with good freeze-thaw stability.  $\lambda$ -carrageenan is non gelling as the lack of the  $^1C_4$  3,6-anhydro-link allows the galactose residues to revert to their  $^4C_1$  conformation which does not allow the initial double helix formation required for gelling.  $\lambda$ -carrageenan has been found to act as a cryoprotectant and improves the freeze-thaw behavior of locust bean gum.

Only a limited number of studies have been made on the effect of divalent cations on the gelation mechanisms of carrageenans. Moreover, the information about the effect of calcium on the  $\kappa$ -carrageenan gels is confusing and contradictory. Morris and Chilvers found that calcium gave rise to stronger gels than potassium, whereas the opposite was found by Watase and Nishinari. However, the results were obtained under different experimental conditions. The importance of these experimental conditions has been discussed by Clark and Ross-Murphy, Hermansson et al., Richardson and Goycoolea. These authors have pointed out the importance of polymer concentration, cation type and concentration, rate of cooling on the rheological properties of carrageenan [26].

#### **1.4.6 Manufacturing process for refined carrageenan**

Industrial production of carrageenan consists of three main steps:

- Extraction in alkaline conditions
- Purification by separating the gum from insoluble impurities
- Carrageenan recovery (precipitation in alcohol or gelation of filtrate by addition of potassium chloride) [16].

### Main Applications

Alone or in combination with other hydrocolloids (especially locust bean gum) carrageenans are used in:

- Dairy:

Stabilization of chocolate drinks and creams, dairy desserts, like gelled milks, flans, multi-layered desserts, mousses

- Meat (and fish) products:

Injections (hams, poultry), fat reduction (hamburgers), canned foods: in combination with locust bean gum for human and pet food

- Powder products:

Homemade flans, dessert, custard and bakery creams, water gel desserts, glazings

- Ice cream:

In combination with guar gum, locust bean gum and alginates

- Non-Food Applications:

Toothpaste and cosmetics, air fresheners, pharmaceuticals [16].

## 1.5 Pectins

### 1.5.1 Source

Pectin is a structural polysaccharide, found in fruit and vegetables and prepared from citrus peel.

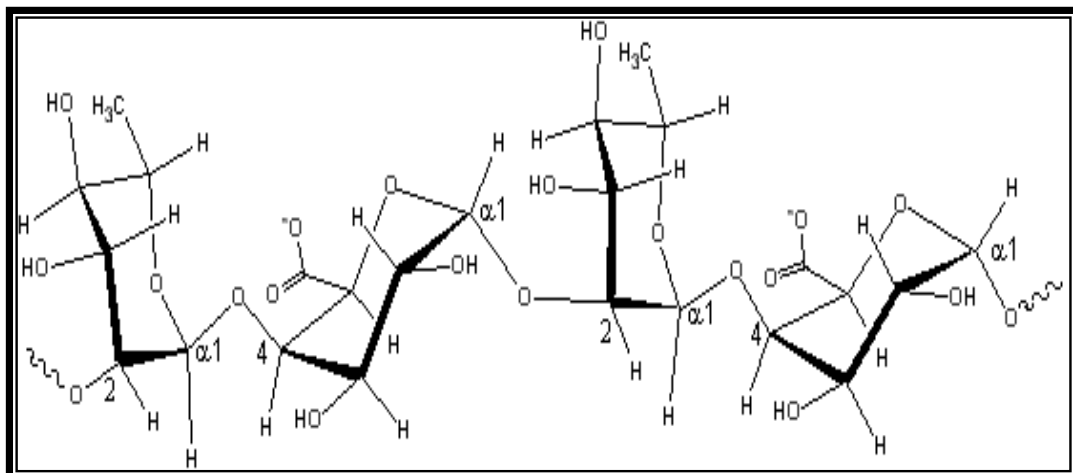
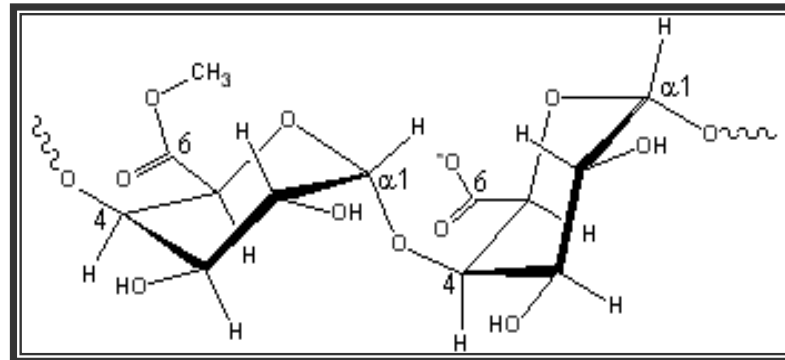


**Figure 11.** Structure of the pectin chain

### 1.5.2 Raw materials

Pectin is present in all higher plants, but is mainly extracted from apple pomace and citrus peel.

### 1.5.3 Structural unit

The majority of the structure consists of partially methylated poly- $\alpha$ -(1 $\rightarrow$ 4)-galacturonic acid residues ('*smooth*', see Figure 11 above) but there are substantial '*hairy*' areas (see Figure 11 below) of alternating  $\alpha$ -(1 $\rightarrow$ 2)-L-rhamnosyl  $\alpha$ -(1 $\rightarrow$ 4)-D-galacturonosyl sections containing branch-points with mostly neutral side chains (1-20 residues) of mainly L-arabinose and D-galactose but may also contain other residues such as D-Xylose, L-Fucose and D-glucuronic acid.

### 1.5.4 Molecular structure

Generally, pectins do not possess exact structures. D-galacturonic acid residues form most of the molecules, in blocks of '*smooth*' and '*hairy*' regions. The molecule does not adopt a straight conformation in solution, but is extended and curved ('*worm like*') with a large amount of flexibility. The '*hairy*' regions of pectins are even more flexible and may have pendant arabinogalactans. The carboxylate groups tend to expand the structure of pectins as a result of their charge (unless they interact through divalent cationic bridging). Methylation of these carboxylic acid groups forms their methyl esters, which take up a similar space but are much more hydrophobic and consequently have a different effect on the structuring of the surrounding water. The properties of pectins depend on the degree of esterification (DE), which is normally about 70%. Low-methoxyl pectins (LMP's) (<40% esterified) gel by calcium di-cation bridging between adjacent two-fold helical chains forming '*egg-box*' junction zone structures so long as a minimum of 14-20 residues can cooperate. It may well be that the two carboxylate groups have to cooperate together in prizing the bound water away from the calcium ions to form the salt links that make up these junction zones. The gelling ability of the di-cations is similar to that found with the alginates ( $\text{Mg}^{2+} \ll \text{Ca}^{2+}, \text{Sr}^{2+} < \text{Ba}^{2+}$ ) with  $\text{Na}^+$  and  $\text{K}^+$  not gelling. If the methoxyl esterified content is greater than about 50%, calcium ions show some interaction but do not

gel. The controlled removal of methoxyl groups, converting high-methoxyl pectins (HMPs) to LMPs, is possible using pectin methylesterases but the reverse process is not easily achieved.

Pectin is a natural component of plants. It is especially abundant in fruit such as apples and citrus. Pectin is associated with cellulose in plant tissues, where it plays a fundamental role in determining their mechanical properties [16].

In plant cells, pectin is linked to cellulose to form protopectin, which has the ability to absorb large amounts of water. Cellulose gives the supporting tissues their rigidity, whilst the pectic components give the plant its flexibility. Pectin has only been produced industrially since early in the 20<sup>th</sup> century, but has long been used by housewives for gelling jams [16].

In industry and at home, pectin is well known for its gelling, thickening and stabilizing properties. Today, it is used in such diverse applications as yogurt, confectionery and acid milk drinks. It has the image of a natural product and has acknowledged nutritional benefits. For all those reasons, new uses are constantly found for pectin in the food industry, and also in pharmaceutical and cosmetic applications [16].

HMPs (>43% esterified) gel by the formation of hydrogen-bonding and hydrophobic interactions in the presence of acids and sugars.

### **1.5.5 Functionality**

Pectins are mainly used as gelling agents, but can also act as thickener, water binder and stabilizer. LMPs (<50% esterified) form thermoreversible gels in the presence of calcium ions and at low pH (3-4.5) whereas HMPs rapidly form thermally irreversible gels in the presence of sufficient (e.g. 65% by weight)

sugars such as sucrose and at low pH (<3.5); the lower the methoxyl content, the slower the set. The DE can be (incompletely) reduced using commercial pectin methylesterase, leading to a higher viscosity and firmer gelling in the presence of  $\text{Ca}^{2+}$  ions.

In the fruit, pectin has a very high DE. During the acid hydrolysis used to extract it, some of the esters are converted into the free acid form, that is to say they are saponified. By careful control of this process, HMPs with different degrees of esterification are obtained. The higher the DE, the faster the setting rate, so these pectins are classified as rapid set (RS), or slow set (SS) for example [16].

In general, LMPs can be obtained either by acid or alkaline hydrolysis. However, amidated LMPs can only be produced by hydrolyzing under alkaline conditions using an ammonia solution. Under these conditions, some of the esters are converted to amide groups, which alters the pectin's rheology and calcium reactivity [16].

Correct preparation of the pectin solution is a key first step in its use. Incomplete dissolution is a frequent cause of unsatisfactory performance. A pectin which is easy to handle must have: good dispersibility, high dissolution rate and maximum solubility [16].

Pectin solutions are stable under acid conditions (between pH 3.2 and 4.5), even at high temperatures. They are also stable for several hours at room temperature under more alkaline conditions, but degrade rapidly at high temperature [16].

HMPs form thermostable gels when the pH is low (less than 3.5) and the sugar concentration is high (dry matter content greater than 60 %). When the dry matter is less than 60%, LMPs have to be used. The pH and the dry matter content

affect the rate of gelation, more than the gel strength. LMPs are generally thermoreversible. However, non-amidated LMPs can form thermostable gels [16].

Gel formation is not the only function of pectins: HMPs are excellent stabilizers of acid milk drinks. They coat the casein particles, stopping them from aggregating and so preventing sedimentation problems. LMPs can provide a wide range of textures and rheological properties, depending on the calcium concentration and the calcium reactivity of the pectin chosen [16].

The gelling ability of pectin depends on its solubility and viscosity, which are a measure of its molecular weight. The viscosity depends not only on the concentration of the polymer but also on the molecular weight and shape, pH and ionic strength. Higher the molecular weight, the higher is its viscosity and hence, the better is its grade and hence, there is a need to measure the molecular weight of pectin solutions. The pectin molecule can contain from a few hundred units up to approximately one thousand units corresponding to molecular weights of up to 150000, depending on the raw materials used [27].

Pectins are used in a wide variety of food products. For many products, native fruit pectins are released by heating and gelled at low pH; additional HMPs and sugar may be introduced to enhance gelling. Low sugar jams and jellies are made with LMPs that gel with calcium. Pectins are also used to produce fruit flavored jelly candies, to enhance the quality of some frozen fruits and ice pops, to improve the mouthfeel of yogurt, to impart improved cloud characteristics to beverages, and to limit lipid migration through edible coatings on confectionery products [28].

At the molecular level, pectins are complex polysaccharides with heterogeneous structure and a range of molecular weights. The primary structure consists of d-galacturonic acid and rhamnogalacturonan. Various carboxyl groups

of the galacturonic acid may be esterified with methyl groups. Typically, pectins contain both branched and unbranched regions; branched regions contain a higher percentage of rhamnose units, which cause kinks in the chain, and which may carry other neutral sugar side chains. Pectins are classified as LM or HM according to their degree of esterification. The former contain between 25–50% methoxylated carboxyl groups; the latter between 50–80%. The specifics of the molecular structure determine the properties exhibited by various pectin fractions. For example, HMPs gel in the presence of cosolutes such as sucrose when subjected to heating. In contrast, LMPs gel in the presence of cations such as calcium [28].

Pectins are classified as hydrocolloids due to their high molecular weight coupled with the abundance of polar and ionic groups on their sidechains. One of the crucial properties of any food hydrocolloid is its ability to interact with water. The hydrocolloid may bind, immobilize, or otherwise interact with water near its surface. In turn, water acts as a plasticizer for such polymers, that is, it increases the free volume for molecular motions. At the macroscopic level, such interactions will influence water binding capacity, juiciness, gelation, and textural properties of the material [28].

The desire to add value to under-used agricultural commodities has led us to search for new uses for pectin, co-product of fruit juice, sunflower oil and sugar from sugar beet. Pectin is a major structural component of cell walls consisting mainly of partially methyl esterified poly( $\alpha$ -(1→4)D-galacturonic acid) containing rhamnose inserts in the backbone and neutral sugar side chains. It is both water soluble and biodegradable [29].

When blended with starch and plasticized with glycerol, pectin forms edible and biodegradable films which have a wide range of good mechanical properties and excellent oxygen barrier properties. Pectin is also miscible with

poly(vinyl alcohol) in all proportions, and together they form films which also have excellent mechanical properties. Potential industrial uses for the pectin/starch/glycerol (PSG) and pectin/poly(vinyl alcohol) films include water soluble pouches for detergents and insecticides, flushable liners and bags, and medical delivery systems and devices. In addition edible bags for soup and noodle ingredients can be fabricated from PSG films [29].

### **1.5.6 Manufacturing process**

Depending on the type of raw material used, whether apple or citrus, different types of pectins, HM and LM, with specific properties, will be obtained. There are four main steps in the production of pectin:

- Hydrolysis
- Purification
- Separation
- Standardization [16].

#### Main Applications

- Dairy
  - HMP; stabilization of acid dairy drinks
  - LMP; yogurts, fruit preparations for yogurt, and dessert creams
- Fruit applications
  - HMP; traditional jams, and fruited beverages
  - LMP; low calorie jams, fruit preparations for yogurts, preparations for baking/pastry fillings
- Confectionery
  - HMP; fruit paste (combined with gelatine), gelled articles (combined with gelatine)
  - LMP; miscellaneous [16].

## **1.6 Three dimensional printing (3DP)**

Solid free-form fabrication (SFF) methods are techniques which create complex objects directly from computer models. A computer-aided design (CAD) of a desired part is used to direct the fabrication of the component. These methods have primarily been applied to engineering components with shapes that are too complicated to use conventional numerical control machining. Several SFF methods have been developed in recent years, such as stereolithography, selective laser sintering, ballistic particle manufacturing, and 3DP. All of these methods build components in a laminated fashion [8].

3DP fabricates complex structures by ink-jet printing liquid binder onto loose, fine powder in a laminated printing fashion. The printing pattern is derived from CAD models. A large number of material combinations can be processed because the liquid and powder phases can have different compositions. The computerized X-Y positioning system directs the 2D horizontal motion of the printhead, which delivers the liquid binder droplets. Binding occurs only where binder droplets contact the binder material below. The local composition can be manipulated by specifying the appropriate printhead to deposit a predetermined volume of binder. The local microstructure can be controlled by either modulating the binder composition, or by altering the printing parameters during component construction [4].

These features make 3DP an attractive manufacturing technology for biomedical devices. Dense, defect-free structures are required for most drug delivery devices in which uncontrolled defects may lead to adverse complications. Highly dense structures are also necessary for many orthopedic fixation devices in which random defects can deteriorate mechanical integrity and result in premature clinical failures. Highly porous matrices with interconnected microporosity and controlled channel dimensions are critical for successful engineering of thick

tissues. The ability to control feature size, or print resolution, is critical for all types of devices. The common theme for controlling feature size, microstructure, and spatial distribution of printed matter is to understand the fundamental binding mechanisms during 3DP [4].

The predominant binding mechanism is dissolution-reprecipitation, in which four stages have been identified: droplet impact, binder imbibition and drainage, particle dissolution/swelling, and reprecipitation. In the 3DP process, droplets impact the loose powder bed at typical speeds of 10 m/s, creating a crater and an initial core of binder-powder mixture. Binder imbibition/drainage commences as the liquid in the initial core migrates away from the saturated pores, and drains into surrounding empty pores. Smaller pores tend to exert larger capillary forces for the binder, while larger pores tend to offer less resistance against binder drainage. Neighbouring loose particles are partially or completely dissolved by the solvent droplets, and 3D structures are produced by reprecipitation of the solvent-polymer gel-mix as a result of solvent evaporation [4].

3DP is one such technology that build parts in thin, sequential layers of fine powder. Each cycle begins with fine powder spread into a thin layer, typically 170 microns thick. A slicing algorithm draws detailed information for every layer from a CAD model. Then a raster-scan printhead applies a binder material to join particles where the object is to be formed. The supporting piston lowers the powder bed so that the next layer of powder can be spread. This building cycle repeats until the part is complete. Removal of the unbound powder reveals the finished product (Figure 12) [30].

The use of powder as the building medium enables 3DP to address a wide range of materials includes ceramics, metals and polymers. However, the compressibility of powder raises concerns for dimensional accuracy in the vertical

direction. Loads applied from above a layer may cause it to displace downward from its original position with respect to the powder bed floor [30].

The 3DP fabrication technique has proven its versatility by being able to process many types of powders, including metals, ceramics, polymers, and hydrogels. It is particularly useful for constructing parts in applications where control over microstructure and where internal device features are required, as in degradable tissue engineering matrices or drug delivery devices [7].

### 1.6.1 What is the 3DP™ process

3DP is a process under development at Massachusetts Institute of Technology (MIT) for the rapid and flexible production of prototype parts, end-use parts, and tools directly from a CAD model. 3DP has unprecedented flexibility. It can create parts of any geometry, and out of any material, including ceramics, metals, polymers and composites. Furthermore, it can exercise local control over the material composition, microstructure, and surface texture [31].

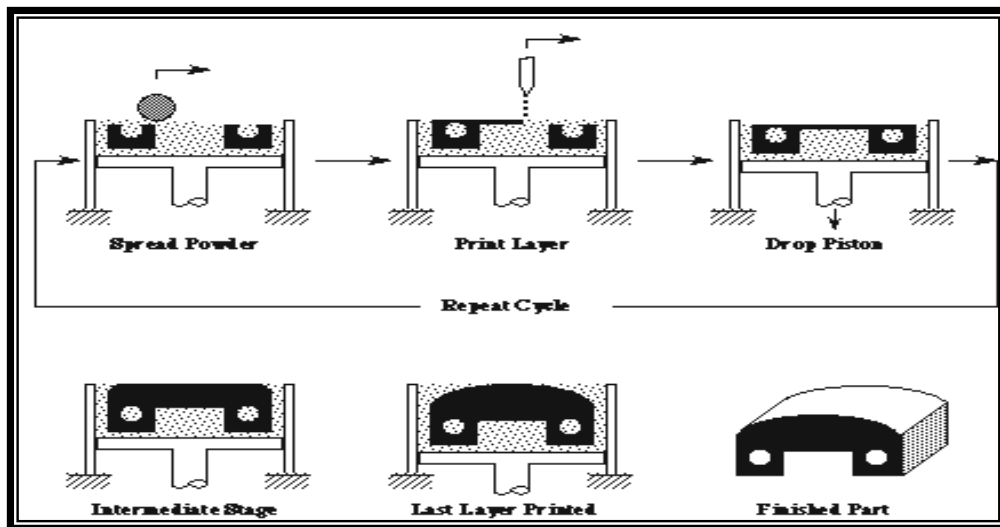


**Figure 12.** The 3DP sequence of operation [8]

### 1.6.2 Process

3DP functions by building parts in layers. From a CAD model of the desired part, a slicing algorithm draws detailed information for every layer. Each layer begins with a thin distribution of powder spread over the surface of a powder bed. Using a technology similar to ink-jet printing, a binder material selectively joins particles where the object is to be formed. A piston that supports the powder bed and the part-in-progress lowers so that the next powder layer can be spread and selectively joined. This layer-by-layer process repeats until the part is completed (Figure 13). Following a heat treatment, unbound powder is removed, leaving the fabricated part. The sequence of operations is depicted below [31]:



### 1.6.3 Process capabilities

The 3DP process combines powders and binders with unprecedented geometric flexibility. The support gained from the powder bed means that overhangs, undercuts and internal volumes can be created (as long as there is a hole for the loose powder to escape). 3DP can form any material that can be obtained as a powder-which is just about any material. Further, because different materials can be dispensed by different print heads, 3DP can exercise control over local material composition. Material can be in a liquid carrier, or it can be applied as molten matter. The proper placement of droplets can be used to create surfaces of controlled texture and to control the internal microstructure of the printed part.

The 3DP process surpasses conventional powder processing because while the 3DP components rival the performance of those made by conventional methods, there are no tooling or geometric limitations with 3DP. Because of its great flexibility in handling a wide range of materials and because of the unique ability to locally tailor the material composition, 3DP offers potential for the direct manufacture of structural components with unique microstructures and capabilities. 3DP is also readily scaled in production rate through the use of multiple nozzle technology which has been commercially developed for printing images on paper [31].

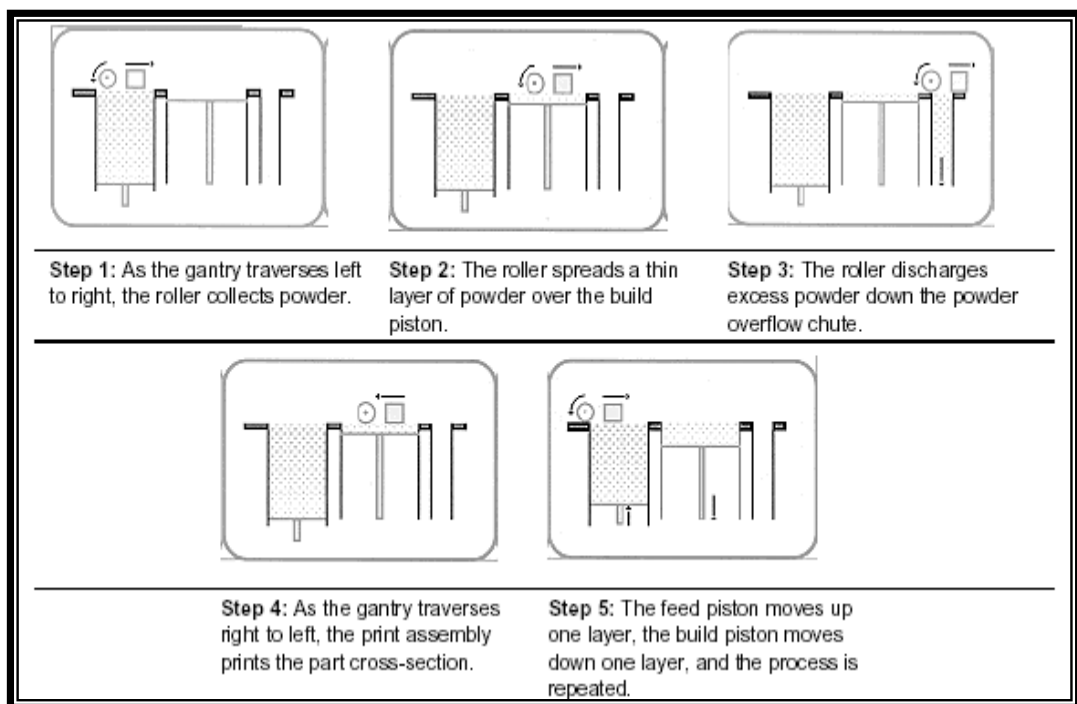


**Figure 13.** The printing process in 3DP [32]

## **1.7 Scope of the work**

In this study, basically the effect of gelling agents (alginates, carrageenans and pectins) in the production of three dimensional (3D) sugar based objects are studied.

The main aim in the formation of 3D objects is to prevent the impregnation and the dissolution the sugar matrix with the aqueous binder solution used and to keep the binder solution localized where it is deposited through the printing ink-jet head, otherwise, it will be impossible to obtain sharp, well-defined shapes by means of 3DP operations.

To this purpose the effects of the divalent cations on the viscosities of gelling agents are studied. A spectroscopical investigation is performed to understand the changes in molecular interaction as gelling proceeds. The amount of binded mass as a function of porosity of the sugar based matrix and the volume of binder liquid are investigated through primitive formation experiments. Finally, 3D objects are produced and their shape resolution and texture changes as a function of various experimental parameters are determined.

## **CHAPTER 2**

### **EXPERIMENTAL**

#### **2.1 Materials**

The gelling polysaccharides (Satialgine SG300 (sodium alginate), Unipectine PG569S and PG769S (pectins), Satiagel KHG30 and Satiagum CD (carrageenans)) were supplied from Degussa Texturant Systems and used without further purification. Modified starches, T468, T470 and G463 were supplied from A.E.Staley Manufacturing Company. Triple distilled water was used for all of the viscosity measurements, FTIR analysis and 3DP experiments. Commercial powdered sugar was supplied from Gimat. Reagent grade metal salts ( $\text{CaSO}_4$ ,  $\text{Ca}(\text{NO}_3)_2$ ,  $\text{Mg}(\text{NO}_3)_2$ ,  $\text{Al}(\text{NO}_3)_3$ ) were obtained from Riedel De Haen. Below are some basic informations about the texturant materials that were focused on:

### **2.1.1 Satialgine SG300 (sodium alginate)**

#### Description :

It is a food additive used as a texturant extracted from brown seaweeds. It is a thickener and/or gelling agent (in acid and/or calcium medium) particularly suited to various food applications [16].

#### Characteristics :

- Rheology : Viscosity in a 1% aqueous solution : 110-230 cP measured at 20<sup>0</sup>C on a Brookfield RVT viscometer, N 1 spindle, 20 rpm.
- pH: 6 to 8.5 - measured in a 1% aqueous solution
- Aspect, flavour : A creamy-white to light-brown powder, of neutral odour and flavour
- Particle size : At least 98% less than 200 microns
- Loss on drying : Not more than 15% [16].

### **2.1.2 Unipectine PG569S (pectin)**

#### Description :

It is a food additive used as a texturant and a gelling agent (in an acid and very sweetened medium; SS>76%, pH=3.2-3.5).

#### The product consists of :

- HMP
- Sodium citrate
- Sodium polyphosphate [16].

#### Characteristics :

- Esterification degree : 58 to 64%

- pH: 5.2 to 5.9 - measured in a 1% aqueous solution
- Aspect, flavour : A creamy-white to light-brown powder, of neutral odour and flavour
- Particle size : At least 99% less than 315 microns
- Loss on drying : Not more than 12% [16].

### **2.1.3 Unipectine PG769S (pectin)**

#### Description :

It is a food additive used as a texturant and a gelling agent ( in an acid and very sweetened medium; SS>76 %, pH=3.2-3.5).

#### The product consists of :

- HMP
- Sodium and potassium tartrate
- Sodium polyphosphate [16].

#### Characteristics :

- Esterification degree : 59 to 65%
- pH: 4.1 to 4.6-measured in a 1% aqueous solution
- Aspect, flavour : A creamy-white to light-brown powder, of neutral odour and flavour
- Particle size : At least 99% less than 315 microns
- Loss on drying : Not more than 16% [16].

#### **2.1.4 Satiagel KHG30 (carrageenan)**

##### Description :

It is a food additive used as a texturant which is an extract of red seaweeds. It is a gelling agent particularly suited to the manufacture of neutral or slightly acid souces. At a dosage between 0.20 to 0.50% : it behaves like a thickener in cold-prepared souces and like a slightly gelling agent in hot-prepared souces. It increases the viscosity in cold conditions, which facilitates industrial packaging of ready meats and ensures good stability during storage and after thawing [16].

##### Characteristics :

- Rheology : Strength of a gel at 1.5% in water + 0.75% NaCl : RES=170–210 measured at 10<sup>0</sup>C, on a PNR 6 penetrometer, piston 35 g. plunger 15 g. penetration during 3 seconds.
- pH: 7 to 10 - measured in a 1% aqueous solution
- Aspect, flavour : A creamy-white to light-brown powder, of neutral odour and flavour
- Particle size : At least 98% less than 250 microns
- Loss on drying : Not more than 12% [16].

#### **2.1.5 Satiagum CD (carrageenan)**

##### Description :

It is a food additive used as a texturant which is an extract of red seaweeds. It is a thickener particularly suited to food and para-pharmaceutical applications [16].

##### Characteristics :

- Rheology : Viscosity in a 1% aqueous solution : 320-380 cP measured at 25<sup>0</sup>C on a Brookfield RVT viscometer, N 2 spindle, 20 rpm.

- pH: 7 to 10 - measured in a 1% aqueous solution
- Aspect, flavour : A creamy-white to light-brown powder, of neutral odour and flavour
- Particle size : At least 98% less than 250 microns
- Loss on drying : Not more than 12% [16].

## **2.2 Preparation of alginate films**

Only alginates could be produced as films and their FTIR analysis were done. 5ml 1% (w/w) satialgine solutions were put in petri dishes and then they were dipped into the 90 ml solutions with four different  $\text{Ca}^{2+}$  concentrations (0, 0.1, 0.01, 0.001 M) for 1 hour. The resulting gels were dried in a vacuum oven for 2 hours at 75<sup>0</sup>C 400 mm Hg. Resulting thin films around 10  $\mu\text{m}$  thick were used for FTIR analysis.

## **2.3 Preparation of metal ion-alginate solutions**

At first, investigations were done on alginate interactions with different metal salts with no sugar content.

### **2.3.1 Preparation of stock solutions**

Stock solutions of 0.125%, 0.250%, 0.500%, 1.0% (w/w) alginate solutions were prepared by dissolving appropriate amount of alginate in triple distilled water at room temperature. Polymer solutions require longer equilibration times, and hence the resulting solutions were stirred for 24 hours by magnetic stirrer.

For all metals studied, appropriate amounts of metallic salts ( $\text{CaSO}_4$ ,  $\text{Ca}(\text{NO}_3)_2$ ,  $\text{Mg}(\text{NO}_3)_2$ ,  $\text{Al}(\text{NO}_3)_3$ ) were dissolved in triple distilled water at room

temperature, to achieve concentrations of  $1 \times 10^{-1}$  and  $1 \times 10^{-3}$  M. The concentrations of  $1 \times 10^{-2}$  M and  $1 \times 10^{-4}$  M were prepared by the dilution of these two solutions.

### **2.3.2 Preparation of sample solutions**

5 ml of both alginate and metal ion solutions were mixed and stirred for 30 minutes in order to equilibrate the metal-alginate sample. Two sets of sample solutions for each metallic salt were prepared. In the first set, alginate concentration was kept constant (0.250% w/w) while the metal ion concentration was varied. In the second set, metal ion concentration was kept constant ( $1 \times 10^{-4}$  M) while alginate concentration was varied. For the case of  $\text{Mg}^{2+}$ , 0.1 M stock solution was used because the behavior of  $\text{Mg}^{2+}$  at low concentrations is not very effective.

## **2.4 Preparation of sugar based metal-texturant solutions**

In these experiments all of the texturant materials were investigated in sugar containing solution.

### **2.4.1 Preparation of sugar solutions**

Commercial powdered sugar was dissolved in the triple distilled water to obtain 50% (w/w) sugar solution.

### **2.4.2 Preparation of stock solutions**

To this sugar solutions,  $\text{Ca}^{2+}$  ions (from  $\text{Ca}(\text{NO}_3)_2$ ) were introduced to obtain four different  $\text{Ca}^{2+}$  ion content (0, 0.01, 0.001, 0.0001 M) respectively. These stock solutions were used for further experiments.

### 2.4.3 Preparation of solutions for viscosity measurements

From each of the stock solutions, 25 ml solution was taken and texturant materials were introduced separately to achieve the final concentration of 0.5% (w/w) in texturants. To dissolve the materials, the contents were stirred vigorously at room temperature for 24 hours by means of a magnetic stirrer.

### 2.5 Three dimensional printing (3DP)

In this part of the study, control and optimization of the parameters of the 3DP machine (see Figure 14), changing the texture of the desired products by changing the binder-powder formulations and parameters of the machine in sugar based matrices were studied generally. The mechanism of the 3DP machine depends on layer by layer building of a 3D shape that exists in the memory of the computer that drives the machine. Layer thickness can be adjusted depending on the characteristics of the powder and the binder solution used.

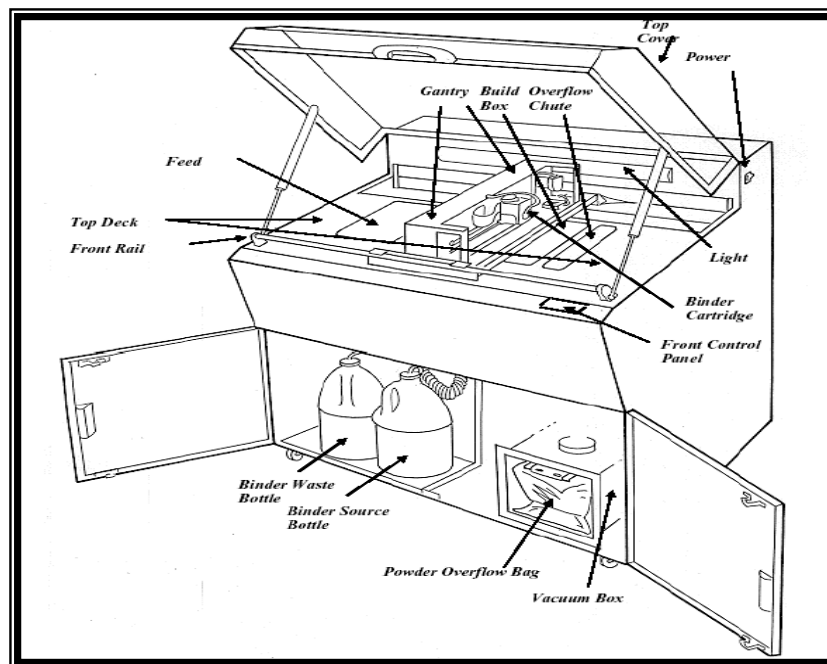


**Figure 14.** 3DP machine and its components [32]

For 3DP process, there are three basic parameters used for determining the product's texture. The first one is the layer thickness (LT) that means the thicknesses of the powder layers to be spread at each time and this parameter is given in inches. The second one is the saturation (S). It describes the amount of binder used for the outer surface of the product. The last one is core saturation (CS), which shows the amount of binder used for the inner surfaces of the desired specimen.

### **2.5.1 Primitive experiments**

To have rough idea about the performance of the powders and binders, primitive formation experiments were carried out. For these experiments, different powder formulations were prepared and tapped into the petri dishes with 5.5 cm in diameter and 1.2 cm in height and their porosities were measured from the geometric volume of the container and the true density of the powder. Cutter knife was used to get rid of the excess powder and tapping was continued up to obtaining the maximum packing density. Different binder formulations were prepared and a calibrated micropipette was used to deposit 50  $\mu\text{L}$  binder onto the powders.

### **2.5.2 Packing density experiments**

Trials were made to understand the effect of powder compression in the feed section on the powder density in the build section of the 3DP machine. For this purpose the packing densities of the two sections are measured by a cylindrical, sharp-edged brass bore. The absolute densities of the powder materials and the geometric volumes were used to calculate the porosities.

### **2.5.3 Printer resolution optimization**

In this part, optimization studies were done on the machine parameters (LT, S, CS), powder composition in terms of types of starches, pre-drying of powders, effect of powder particle size and relative humidity (RH) on the spreading of the powder and the resolution (and quality) of the dumbbell shaped specimens produced.

### **2.5.4 Effect of relative humidity (RH) on texture**

Dumbbell shaped specimens with no texturant were placed in humidity adjusted dessicators for 48 hours and the texture analysis were made quickly. Desired RH values were obtained by using the saturated solutions of suitable salts.

### **2.5.5 Effect of texturants**

For these set of experiments, texturant materials were used and a cylindrical sample geometry with 2 cm diameter and 1 cm height was constructed by 3DP instead of dumbbell shaped ones. To correlate with the previous studies, force values were given in g/cm. Also different RH chambers were again applied to the specimens prior to the texture analysis.

## 2.6 Characterization techniques

### 2.6.1 Viscosity average molecular weight determinations

Viscosity average molecular weight of only alginate (Satialgine SG300) was determined from solution viscosity measurements by using a Cannon E212 type Ubbelohde capillary viscometer. Constant temperature was maintained by using a thermostated water bath fixed at 25<sup>0</sup>C. Stock solutions of sodium alginate were prepared in the concentrations of 1x10<sup>-3</sup> g/ml to 5x10<sup>-3</sup> g/ml. Appropriate amount of NaCl was added to achieve a total concentration of 0.1 M NaCl. All viscosity measurements were performed triple. First, the flow time of solvent was measured. The flow time of solvent is high enough to ignore the Hagenbach-Coutte corrections.

The relative viscosities,  $\eta_r = t/t_0$  were measured; where  $t$  and  $t_0$  are the flow times for the solution and solvent respectively. The intrinsic viscosity  $[\eta]$  is obtained from the reduced viscosity  $\eta_{red}$  and inherent viscosity  $\eta_{inh}$  versus concentration plots by extrapolation to zero concentration [33].

The reduced viscosity and the inherent viscosity are described by the Huggins and Kraemer equations respectively:

$$\eta_{red} = \eta_{sp}/C = [\eta] + K'[\eta]^2C \quad (1)$$

$$\eta_{inh} = \ln\eta_r/C = [\eta] - K''[\eta]^2C \quad (2)$$

where;

$\eta_{sp}$  is the specific viscosity and  $\eta_{sp} = \eta_r - 1$

$\eta_r$  is the relative viscosity

$C$  is the concentration (g/dl)

$[\eta]$  is the intrinsic viscosity (dl/g)

$K'$  is the Huggins constant  
 $K''$  is the Kraemer constant

The Huggins and Kraemer constants are related as shown below:

$$K' - K'' = 0.5 \quad (3)$$

The Huggins and Kraemer equations provide the most common procedure for evaluation of  $[\eta]$  from experimental data. This involves a dual extrapolation according to these equations and gives  $[\eta]$  as the mean intercept of the lines of both equations. The intrinsic viscosities were obtained from the mean intercepts [33].

From the data obtained, viscosity average molecular weight of sodium alginate was determined according to Mark-Houwink-Sakurada equation [34,35]:

$$[\eta] = K M_v^a \quad (4)$$

Where  $[\eta]$  is intrinsic viscosity and  $M_v$  is the viscosity average molecular weight. Average molecular weight of our sample was calculated by using values of  $K=7.3 \times 10^{-5}$  and  $a=0.92$  determined by Martinsen et. al. [35,36].

## 2.6.2 Solution viscosity measurements

For viscosity measurements, Brookfield RV DV II+ model viscometer was used and SC-28 spindle was chosen. From the prepared solutions described before, 10 ml of solution was taken to the disposable cell and it was placed in a thermocell of the viscometer to control the temperature. Viscosity measurements were done three times at different compositions, temperatures, pH, and spindle speeds (rpm). Viscosity readings were taken after 30 minutes to achieve thermal equilibrium.

### **2.6.3 Texture analysis**

Samples produced by 3DP machine has the shapes of dumbbell, cylinder and bar. Production was done at different compositions of binder and powder content. The resulting specimens were cleaned by pressurized air to get rid of the excess powder. Also effects of different RH chambers on the specimens were studied.

Texture analysis were done by using the Stable Micro Systems TA XT2 model texture analyser. Sharp cutter knife type probe was used and the results were given as maximum force average (g/cm) of three measurements at failure. Suitable conversions were done to compare the texture analysis results of the different shaped specimens.

### **2.6.4 FTIR spectroscopy**

A Nicolet 510 model FTIR spectrophotometer was used to get the spectrum of the samples. The spectrum of the film samples were taken as they were. The solution samples were dropped onto the KBr pellets and these pellets were dried prior to the FTIR analysis.

## CHAPTER 3

### RESULTS AND DISCUSSION

#### 3.1 Characterization of sodium alginate (Satialgine SG300) solutions

In this part of the study, only sodium alginate was investigated. The main aspects were determination of viscosity average molecular weight ( $M_v$ ), rheological and spectroscopic analysis on sodium alginate at different alginate concentrations, different metal cations and their concentrations, pH and temperature.

##### 3.1.1 Viscosity average molecular weight determinations

The capillary viscometer (ubbelohde) analysis is one of the most important tools for the determination of molecular weight of polymers. The molecular weight is directly proportional to the intrinsic viscosity with the equation below;

$$[\eta] = K M_v^a \quad (4)$$

where:

$[\eta]$  is the intrinsic viscosity  
K and a are the constants  
 $M_v$  is the viscosity average molecular weight.

From the flow times of solvent and solution; first  $[\eta]$ , then viscosity average molecular weight of sodium alginate (Satialgine SG300) was determined.

Average molecular weight of sodium alginate was calculated by using values of  $K=7.3 \times 10^{-5}$  and  $a=0.92$  at 0.1 M NaCl concentration determined by Martinsen et.al. [36];  $[\eta]$  was found as 3.217 dl/g and  $M_w$  was calculated as  $1.1 \times 10^5$  g/mole by using the above equation and constants.

### **3.1.2 FTIR analysis on alginate films**

Films were produced according to the procedure described in 2.2. Then these films with 10  $\mu\text{m}$  average thickness were analyzed by FTIR spectroscopy (Figure 15). Peak assignments of sodium alginate films are given in Table 1.

**Table 1.** FTIR peak assignments of alginate films [18]

Wavenumber (cm <sup>-1</sup> )	Intensity-Shape	Assignment
3360 - 3380	Very strong-broad	O-H stretching
2930 - 2935	Weak-broad	C-H stretching
1608 - 1611	Very strong-sharp	COO <sup>-</sup> stretching (asymmetric)
1413 - 1415	Medium-sharp	COO <sup>-</sup> stretching (asymmetric)
1317	Weak-broad	C-O stretching
1294	Weak-shoulder	C-O stretching
1176	Weak-shoulder	C-O stretching C-C stretching C-C-C bending
1124 - 1126	Medium-sharp	C-C stretching C-O stretching
1090 - 1094	Medium-sharp	C-O stretching C-O-C stretching
1030 - 1035	Medium-broad	?
947 - 950	Weak-sharp	C-O stretching C-C-H stretching
903	Weak-sharp	?
810 - 815	Weak-broad	?
781	Weak-broad	C-O internal rotation C-C-O bending C-C-H bending

From the fingerprint region of sodium alginate, (reference is COO<sup>-</sup> asymmetric stretching peak around 1610 cm<sup>-1</sup>) the bands of shoulders around 1410, 1320, 1130, 1090, 1020, 1000, and 950 cm<sup>-1</sup> are of greater intensity in high G alginate. These wavenumbers are characteristic of guluronate, so our alginate can be assigned as a high G alginate by the help of the IR spectrum.

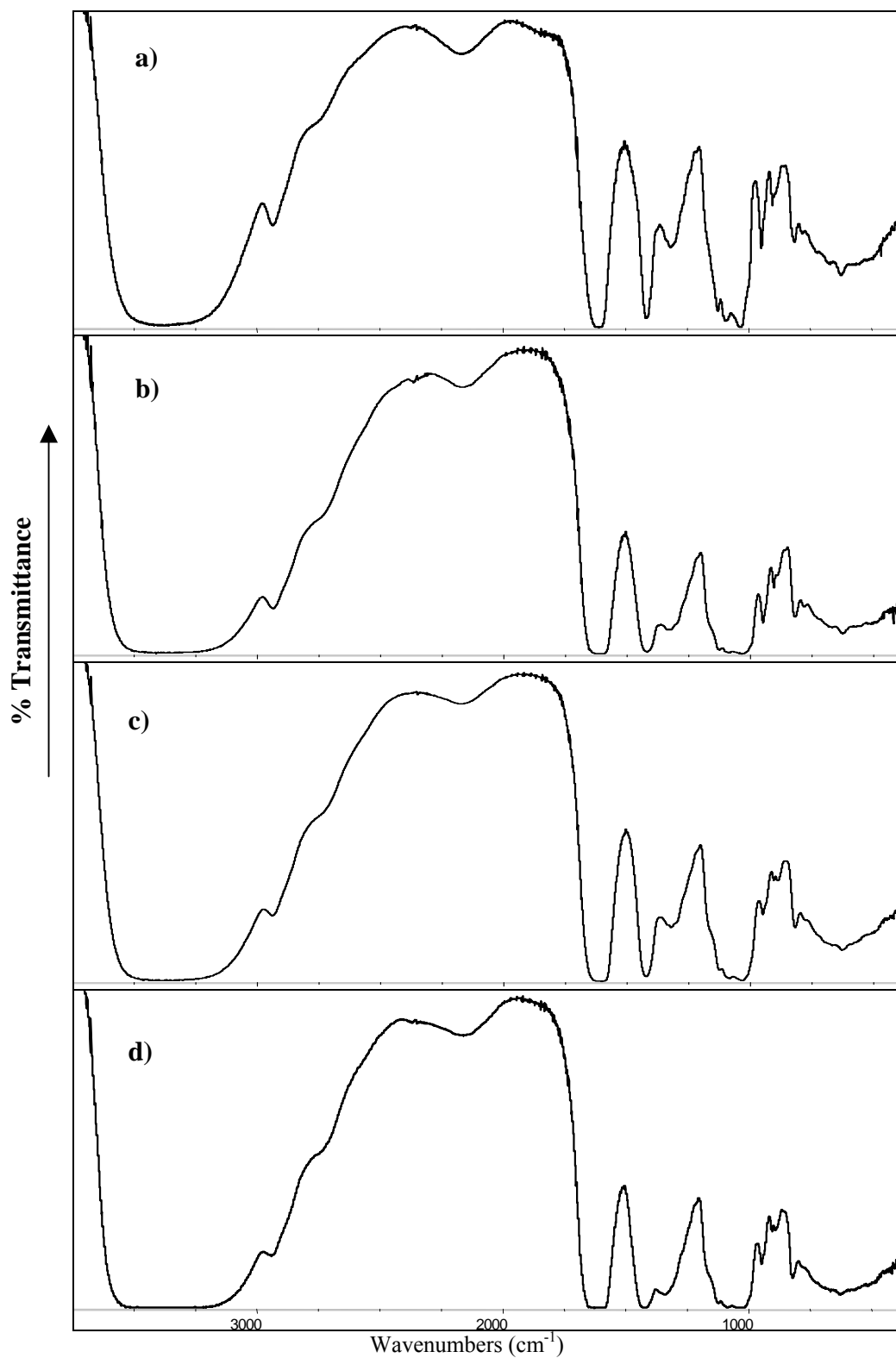


**Figure 15.** FTIR spectrum of **a)** pure sodium alginate, **b)** sodium alginate + 0.01M Ca<sup>2+</sup>, **c)** sodium alginate + 0.1 M Ca<sup>2+</sup>, **d)** sodium alginate + 1 M Ca<sup>2+</sup>.

FTIR spectra can give direct information about the ion exchange process between sodium and calcium for alginate. As the solution concentration of  $\text{Ca}^{2+}$  increases, the O-H stretching peak ( $3300\text{-}3400\text{ cm}^{-1}$ ) becomes broader and of greater intensity.

The  $\text{COO}^-$  peaks at  $1610$  and  $1415\text{ cm}^{-1}$  assigned for the asymmetric and symmetric stretching become broader with an increase in  $\text{Ca}^{2+}$  concentration. The intensities are also decreased for both at some extent. For the latter peak, the decrease in intensity means that there is a decrease in the ionic bonding. As calcium cations replace sodium ions in the alginate blocks, the charge density, the radius and the atomic weight of the cation changed around the carbonyl group. Therefore, little shift can be seen for this peak.

Three sets of sharp peaks between the regions of  $1150\text{-}1000\text{ cm}^{-1}$  can be seen easily. The first two peaks have been assigned to C-O and C-C stretching, but no assignment is done for the third peak. These bonds being shared with the calcium ion. As a result of the weakening in these bonds, these peaks shift towards lower wavenumbers as the calcium content increases. At  $1030\text{ cm}^{-1}$ , the shoulders become more dominant, suggesting that stronger O-H bending vibration and stronger binding of the calcium to the guluronate blocks. The broadening may also be the result of the metal-oxygen-metal bonds, which are commonly appears at  $1010\text{ cm}^{-1}$  (partial covalent bonding between calcium and oxygen atoms).

For the guluronic acid segments, there is a peak assigned at  $781\text{ cm}^{-1}$ . The band around  $948\text{ cm}^{-1}$  is assigned to  $\alpha\text{-}1\rightarrow4$  linkage, and the band at  $903\text{ cm}^{-1}$  is attributed to the  $\alpha\text{-L-gulopyranuronic}$  asymmetric ring vibration. The peak at  $814\text{ cm}^{-1}$  appears at all polyguluronate enrich materials.

### 3.1.3 Effects of type of cations on viscosity of sodium alginate solutions

Preparation of the solutions is described in part 2.3, 2.3.1 and 2.3.2. All viscosity measurements were done by Brookfield viscometer at a spindle speed of 50 rpm.

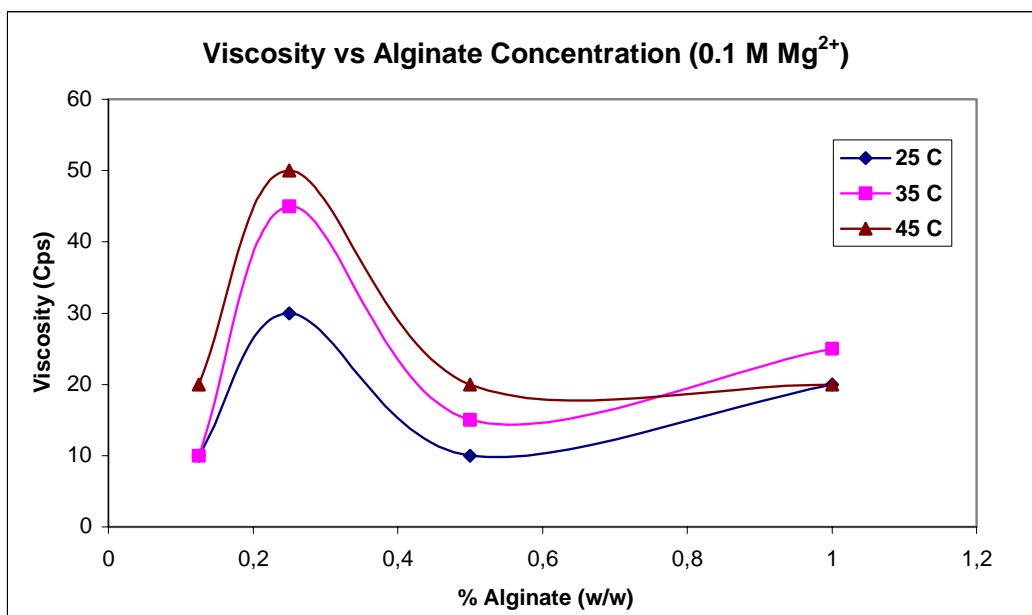
#### 3.1.3.1 Effect of $Mg^{2+}$ cation

Besides high gelling property of  $Ca^{2+}$ ,  $Mg^{2+}$  does not form cooperative binding [37]. The strength and selectivity of cooperative binding is determined by two factors, the size of the metal ion and ease of packing of the alginate chains around the metal ion.

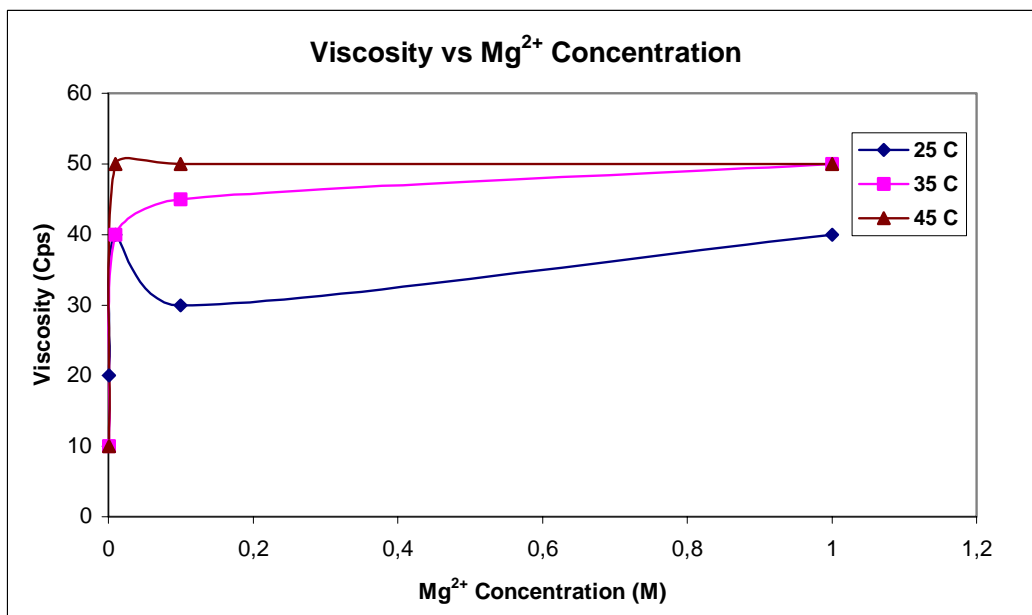
As mentioned before for the  $Mg^{2+}$  ion, no gels were formed or intellect interactions occurred. These weak interactions are easily destroyable with an application of little mechanical force (eg.spindle rotation). We expect to see a decrease in viscosity with increasing temperature. However we have seen that viscosity has increased slightly with increasing temperature. A linear behaviour between concentration and viscosity was expected. For  $Mg^{2+}$ , linearity has not been observed (Figure 16). This non-linearity also suggests that interaction between  $Mg^{2+}$  ions and alginate monomers is very weak.

Previous studies performed on this subject also have shown that magnesium does not form inner-sphere complexes with alginates even at high metal loadings [38].  $Mg^{2+}$  with an ionic radius  $0.65 \text{ \AA}$ , may not be sufficient enough to fit into the cavities in the alginate network and may not be able to crosslink the two alginate chains. From the graphs in Figure 16, it is obvious that temperature change did not affect the rheological behaviour of the gel very much. Also, one can conclude that viscosity increase is not too much with an increase in the temperature and alginate concentration. At 0.25% w/w alginate concentration,

maximum viscosity was achieved.  $Mg^{2+}$  concentration effects viscosity at low concentrations, however further increase in the concentration made no sense.



(a)



(b)

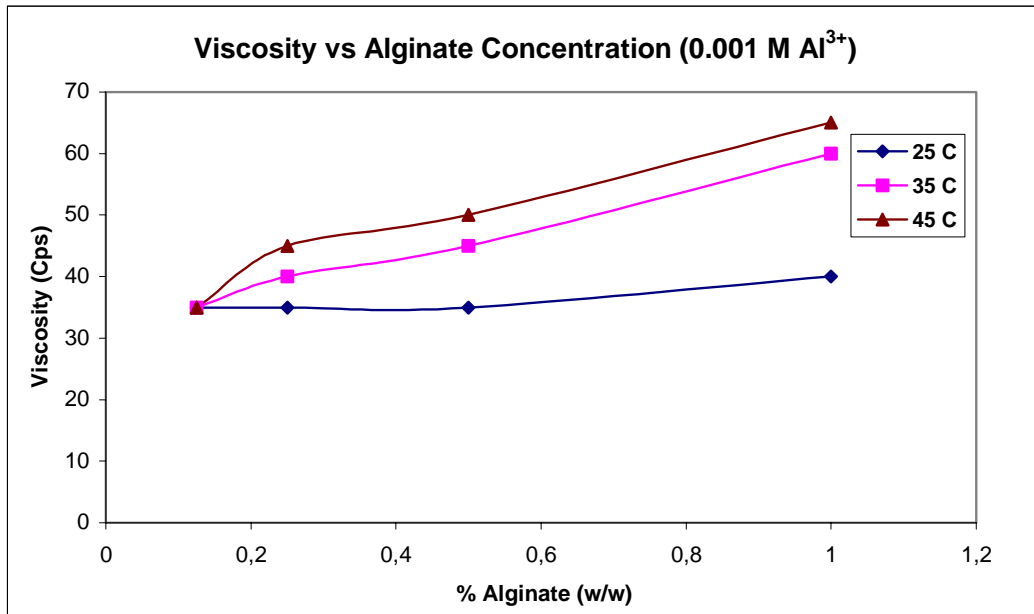
**Figure 16.** Viscosity graphs of Mg-Alginate solutions **a)**  $Mg^{2+}$  concentration is kept constant at 0.1 M while alginate concentration is varied. **b)** Alginate concentration is kept constant at 0.25% w/w while  $Mg^{2+}$  concentration is varied.

### 3.1.3.2 Effect of Al<sup>3+</sup> cation

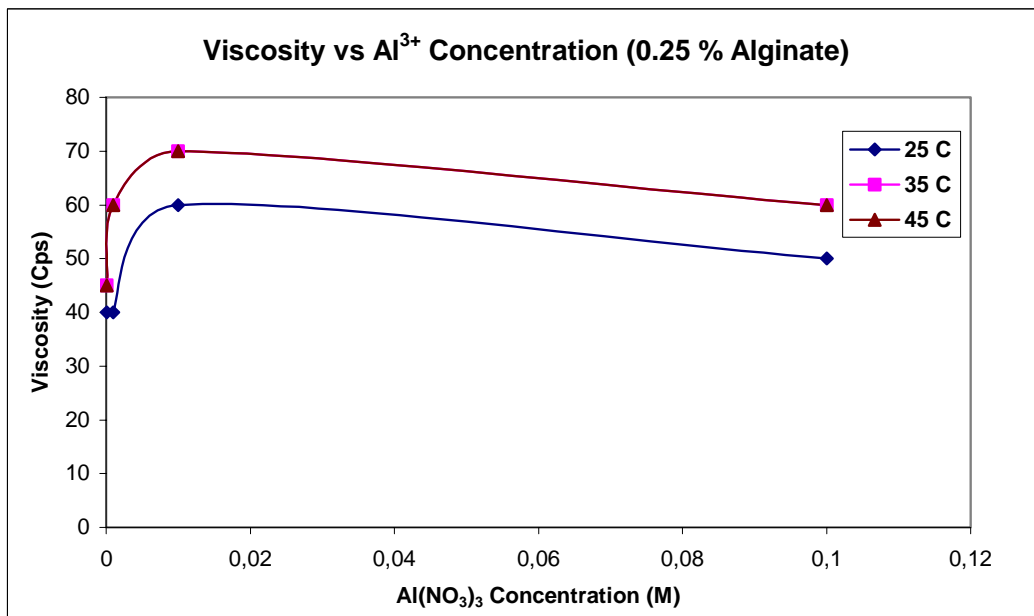
For Al(NO<sub>3</sub>)<sub>3</sub> again an increase in viscosity with increasing temperature was observed. That slight increase in the temperature enhances the interaction between the di- and trivalent metal cations with highly G alginate chains. Therefore, increase in viscosity is seen in both Mg<sup>2+</sup> and Al<sup>3+</sup> trials. Also, viscosity of the solution increases with increasing the amount of alginate (Figure 17(a)).

In Figure 17(b), one can see the increase in viscosity with Al<sup>3+</sup> cation concentration. After a critical concentration of metal cation, slight decrease in viscosity is observed. That may rise from the reaction equilibrium between the metal cation and alginate segments. At 0.01 M concentration of Al<sup>3+</sup> cation, maximum viscosity is obtained at constant alginate concentration (0.25% w/w).

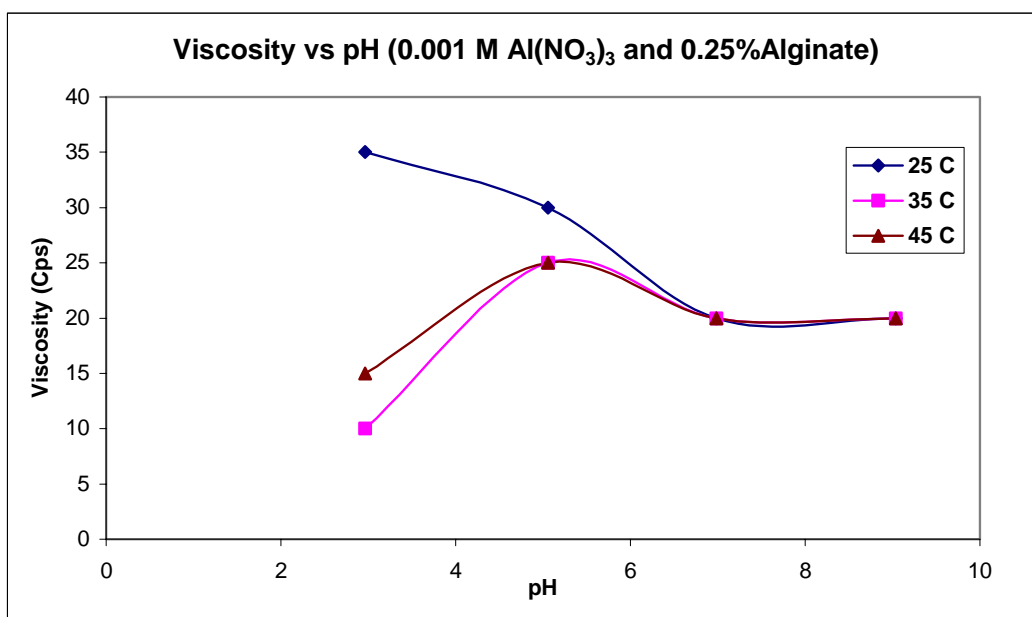
In Figure 17(c), the less acidic medium cause an increase in viscosities of 35 and 45<sup>0</sup>C up to the neutral region, however, there is a decrease in the case of 25<sup>0</sup>C. Where at pH~5, maximum viscosity is achieved for the former case. Less acidic medium enhances the bonding between Al<sup>3+</sup> cation and alginate segments at COO<sup>-</sup> groups, therefore increase in viscosity is expected behaviour. This effect can easily be attributed to the H-bonding interactions between the Na-alginate chains. At low temperature, H-bonding, which is directional, can take place at a higher level, which imparts a rigid, rod like structure to the alginate chains. Due to this effect chain alignment at a shear field (flow regime) gives rise to lower viscosity. When the temperature is increased, the formation of H-bonding is more difficult due to thermal motion of the polymer segments, hence, the viscosity increases. Then, slight decrease is seen for all cases near the neutralization range. At basic medium, viscosity stays constant.



(a)



(b)



(c)

**Figure 17.** Viscosity graphs of Al-Alginate solutions **a)**  $\text{Al}^{3+}$  concentration is kept constant at 0.001 M while alginate concentration is varied. **b)** Alginate concentration is kept constant at 0.25% while  $\text{Al}^{3+}$  concentration is varied. **c)** pH of the medium is changed at constant  $\text{Al}^{3+}$  (0.001 M) and alginate concentration (0.25% w/w).

### 3.1.3.3 Effect of $\text{Ca}^{2+}$ cation from different sources ( $\text{CaSO}_4$ and $\text{Ca}(\text{NO}_3)_2$ )

From the graph of viscosity vs. alginate concentration (see Figure 18), where  $\text{CaSO}_4$  was used, a decreasing behavior of viscosity with temperature is expected. Generally, viscosity decreases with increasing temperature. There are several reasons for this behavior. Intramolecular crosslinkings, which are formed by the metal cation, are the main reason for viscosity increase and gel formation. At lower temperatures the mobility of these segments is weak and the networks formed by the entanglements of polychains are very stable. If intramolecular crosslinking is present, it could have been destroyed by the increased mobility of chain segments. That is why we may see the decrease in viscosity. We can correlate the decrease in viscosity to the volume increase with increasing temperature, which in turn decreases the density. The linear relationship between viscosity and increasing alginate concentration, also indicates that the interaction between  $\text{Ca}^{2+}$

ions and alginate monomers is relatively stable and could not be destroyed by heating.

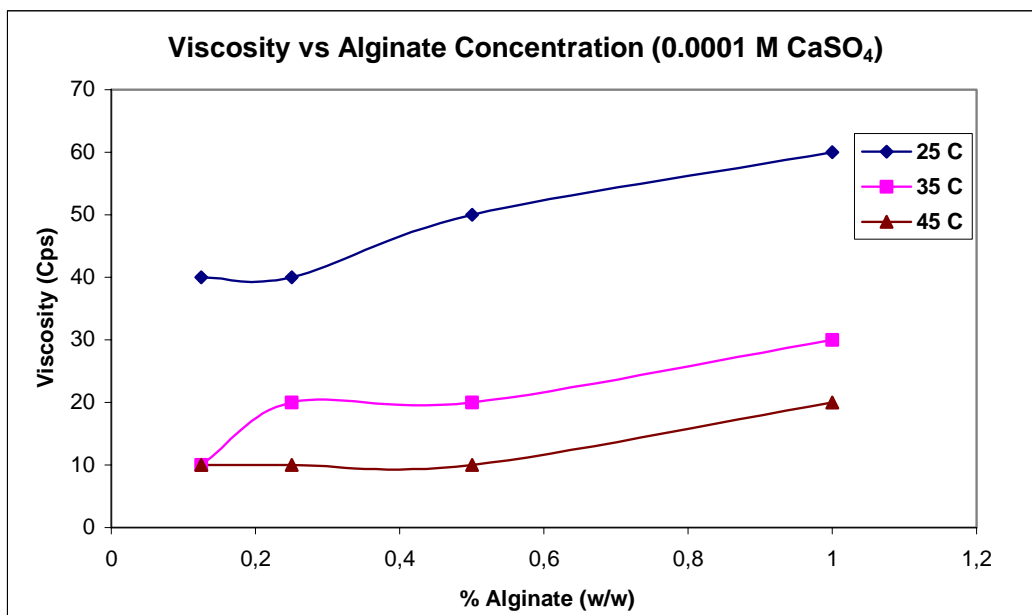
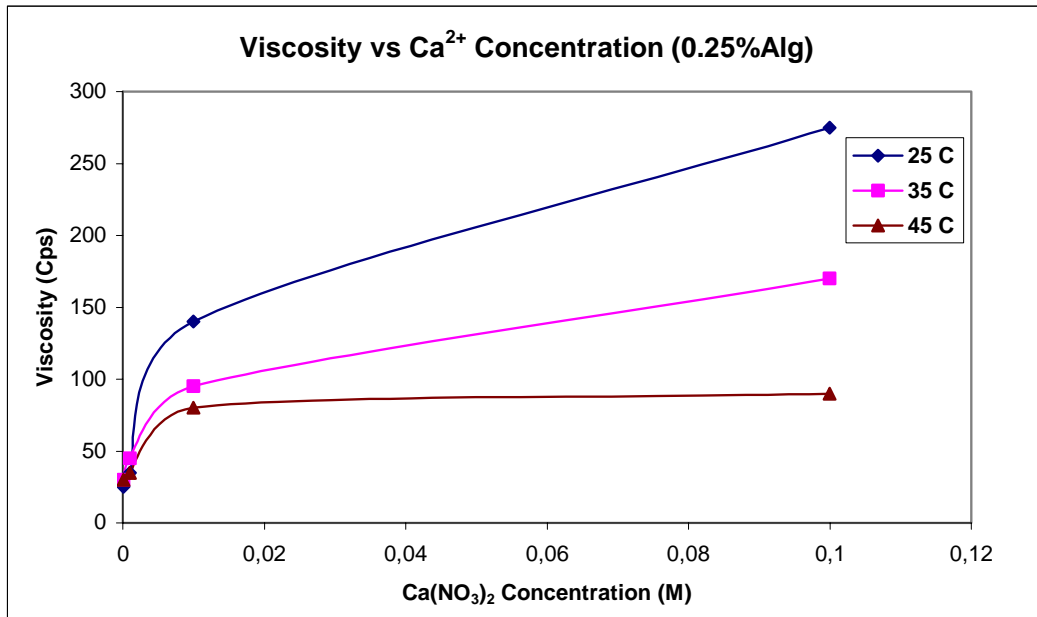
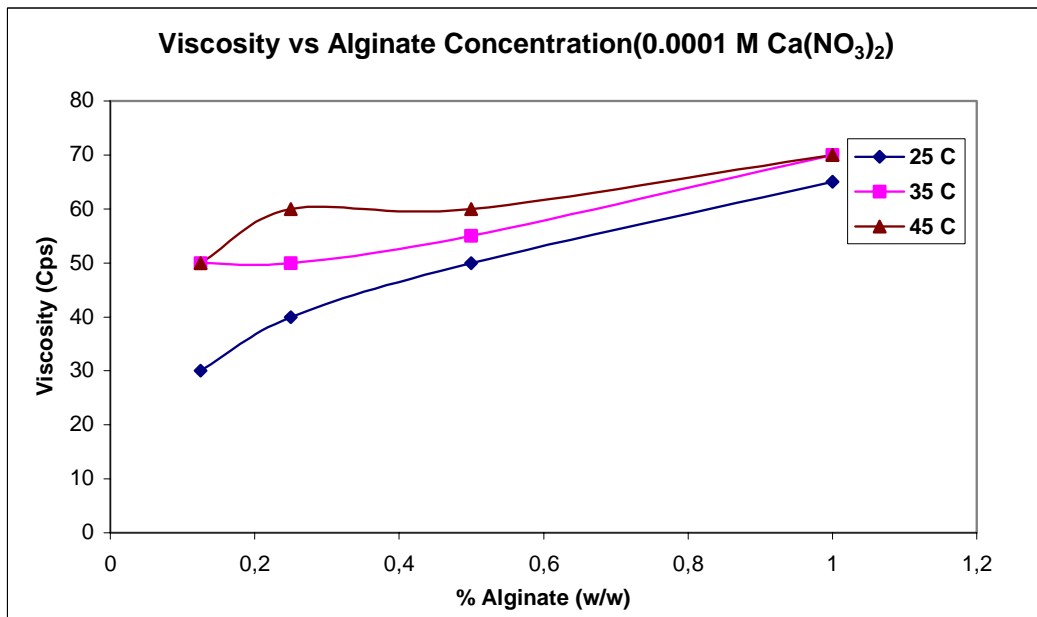


**Figure 18.** Viscosity graph of alginate solutions with  $\text{CaSO}_4$  at  $[\text{Ca}^{2+}] = 1 \times 10^{-4} \text{M}$

It has been shown that GG-blocks are more equipped by  $\text{Ca}^{2+}$  ions than MM-blocks. The diaxial linkage pattern of G structure results in deep cavities for metal ions to occupy while the M residues are linked diequatorially, resulting in a flat, ribbon-like structure [39]. The linear charge density of the polyanion also influences the strength in binding metal ions. The smaller distance between negatively charged carboxylate groups in guluronate sequences result in a higher charge density and stronger interaction with positively charged metal ion.



(a)



(b)

**Figure 19.** Viscosity behaviour of alginate solutions with **a)** Ca(NO<sub>3</sub>)<sub>2</sub> at 0.25% w/w alginate, **b)** %Alginate at [Ca<sup>2+</sup>]=1x10<sup>-4</sup> M.

A similar behaviour was observed for  $\text{Ca}(\text{NO}_3)_2$ . Again a linear behavior of viscosity indicates formation of thermally stable gels. As seen from the graphs (see Figure 19(a) and (b)), at low concentrations of  $\text{Ca}^{2+}$ , a better viscosity behaviour is achieved. In case of 0.1 M  $\text{Ca}^{2+}$  ion loading, the viscosity data has been varied between a range. This behaviour was due to the large mass of cross-linked gel network produced. Different calcium cation sources are not effective on viscosity basically.

### **3.1.4 Comparison of the effect of different cations on viscosity of alginate solutions**

Complexation of alginates with metallic cations is dependent on different factors. Divalent cations show a preference on GG-blocks to form crosslinked networks.  $\text{Ca}^{2+}$  ion forms more stable gel networks compared to  $\text{Mg}^{2+}$  and  $\text{Al}^{3+}$ . Graphs corresponding to  $\text{Ca}^{2+}$  show linearity and this linearity is not ruined upon temperature change. This indicates the strong interaction between calcium ions and alginate residues.

The preference of cations of calcium over magnesium can be explained in terms of alginic acid secondary structure and ionic radius of the relevant cations. The extent of binding increases with increasing the cation radius.

Temperature affects the viscosity inversely for salts other than  $\text{Ca}^{2+}$  because of the ease of formation of H-bonding at low temperatures and flow alignment of the polymeric chains.

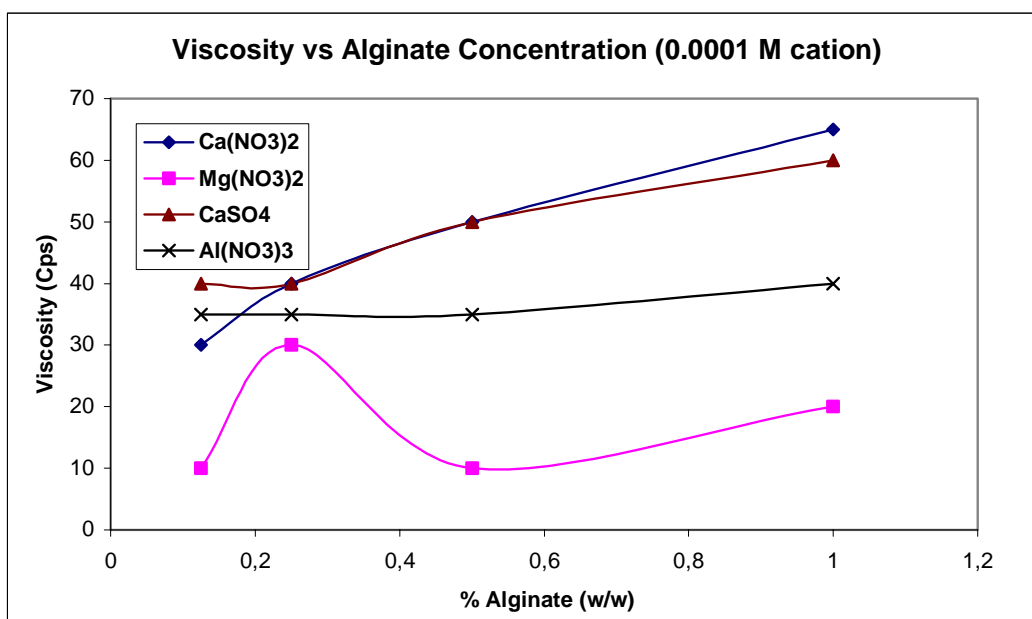


**Figure 20.** Effect of different cations on viscosity of alginate solutions

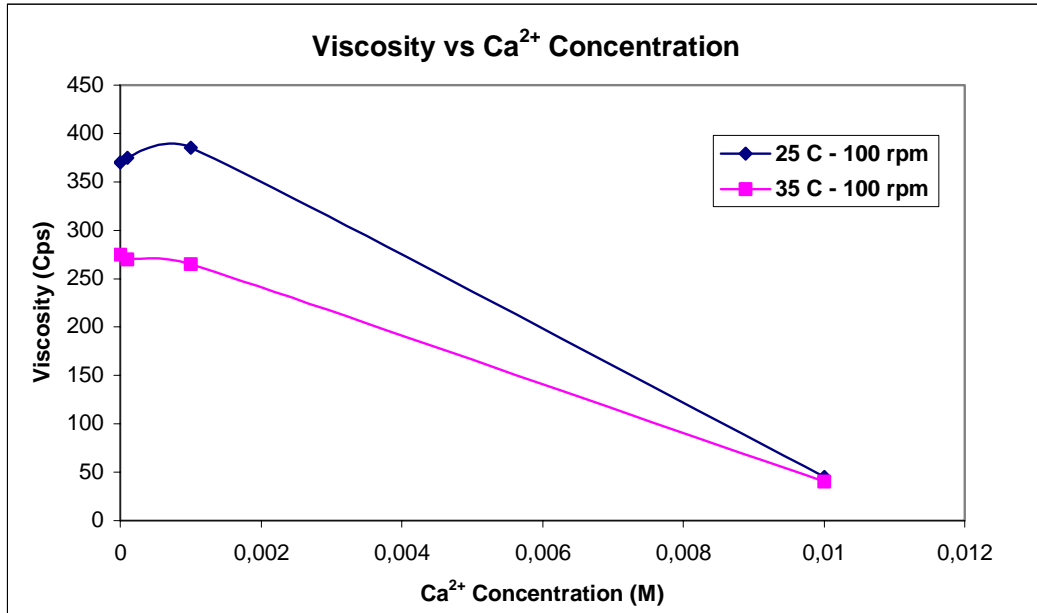
In Figure 20, the effect of different multivalent cations on alginate viscosity at different alginate concentration is shown. The salt concentrations are kept constant at  $1 \times 10^{-4}$  M. Calcium salts are found to be more effective in increasing viscosity which is more dramatic at higher salt concentrations.

### 3.2 Analysis on the rheological properties of sugar based texturant solutions

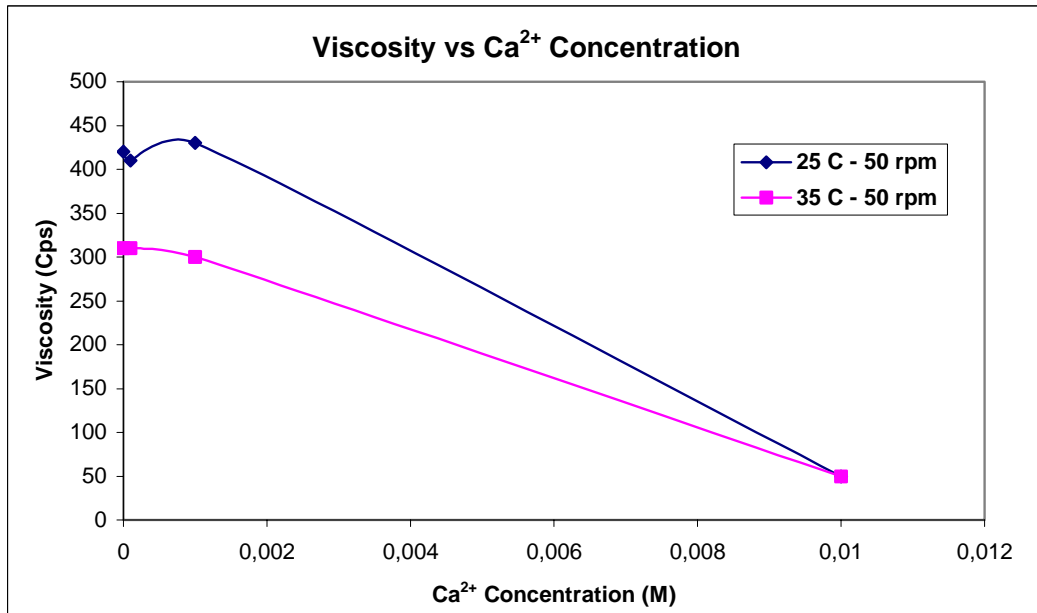
In this part of the study, all of the texturant materials' (alginate, pectins, and carrageenans) behaviour in sugar solutions was investigated.  $\text{Ca}(\text{NO}_3)_2$  was used as a  $\text{Ca}^{2+}$  cation source. Preparation of the solutions was described in sections 2.4, 2.4.1, 2.4.2 and 2.4.3.

### 3.2.1 Sodium Alginate (Satialgine SG300)

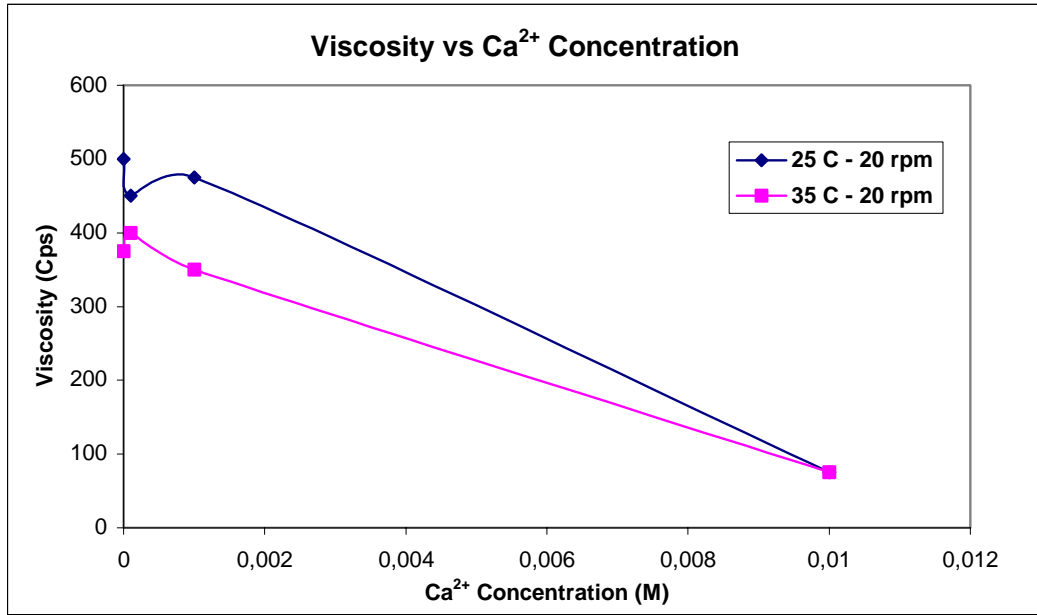
Viscosity measurements of sugar solutions with sodium alginate and  $\text{Ca}^{2+}$  cation were done at different temperatures and rpm (Figure 21).



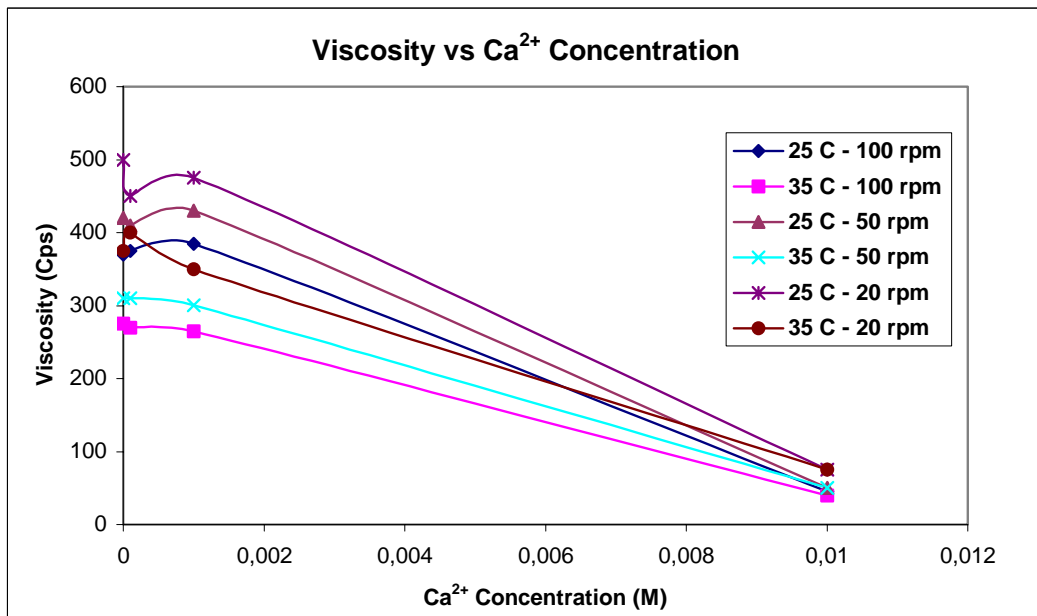
(a)



(b)



(c)



(d)

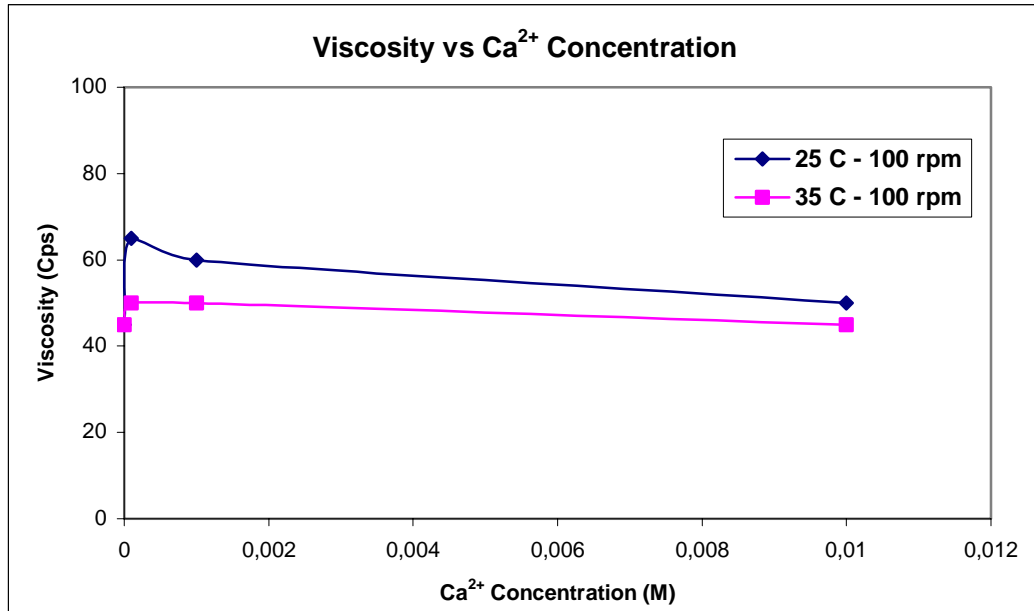
**Figure 21.** Viscosity vs. Ca<sup>2+</sup> concentration graphs of 50% sugar solution (w/w) with 0.5% (w/w) sodium alginate (Satialgine SG300) at 25 and 35°C; a) at 100 rpm, b) at 50 rpm, c) at 20 rpm, d) at all rpms.

As explained before, while the addition of the divalent cation ( $\text{Ca}^{2+}$  in this case), viscosity of the solution increases and irreversible gelation takes place when enough cation is added. Initially, divalent cation and sodium alginate concentration was held at possible minimum value to prevent the spherical gel bead formation. However, in all the graphs (Figure 21), viscosity increases with cation concentration up to nearly 0.001 M and then starts to decrease to the same viscosity interval between 45-75 Cps. That cation concentration can be assigned as the critical concentration of gel beads formation for this experimental parameters. This decrease may resulted from starting of a gel bead formation and decreasing in the distribution of alginate chains in the solution. Also temperature increase causes viscosity to decrease at all rpms and concentrations. The non-Newtonian behaviour of the solutions gives higher viscosities at slower spindle speeds (Figure 21(d)).

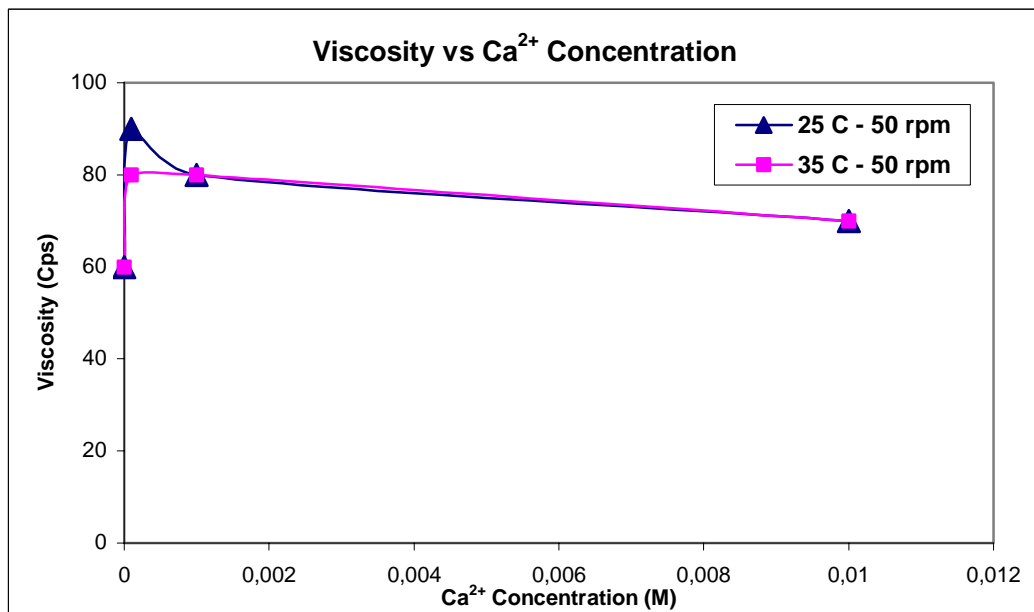
The results clearly show that above 0.001 M  $\text{Ca}^{2+}$  concentration morphological change in the sugar, alginate solutions occur which has not been observed in the alginate alone solution. A significant decrease in viscosity is observed possibly due to the spherical gel-bead formation of sugar alginates agglomerates.

### 3.2.2 Pectins (Unipectine PG569S and PG769S)

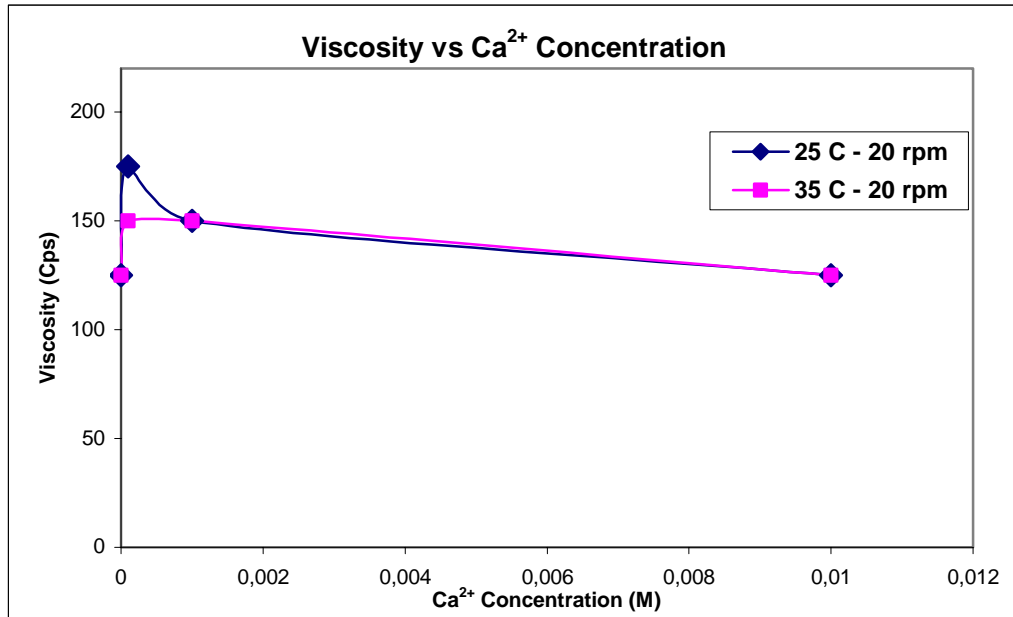
Viscosity measurements of sugar solutions with pectins and  $\text{Ca}^{2+}$  cation were done at different temperatures and rpm (Figure 22, Figure 23).



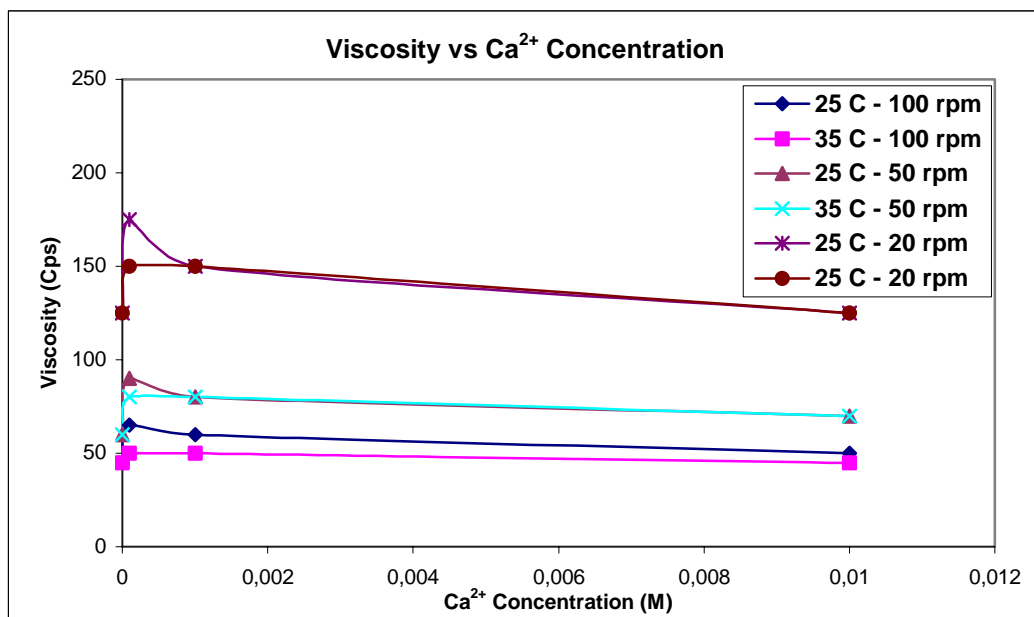
(a)



(b)

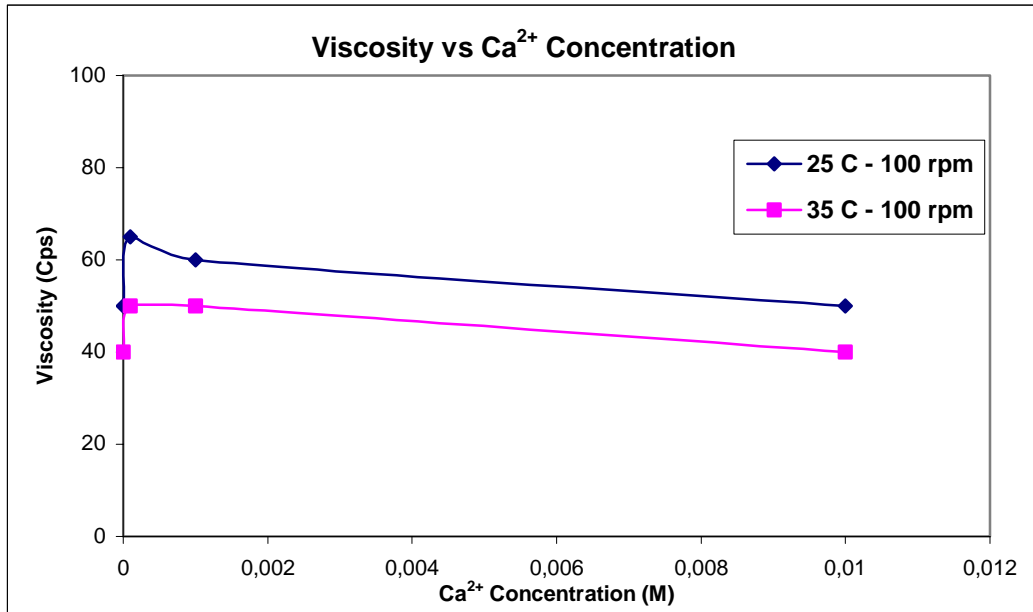


(c)

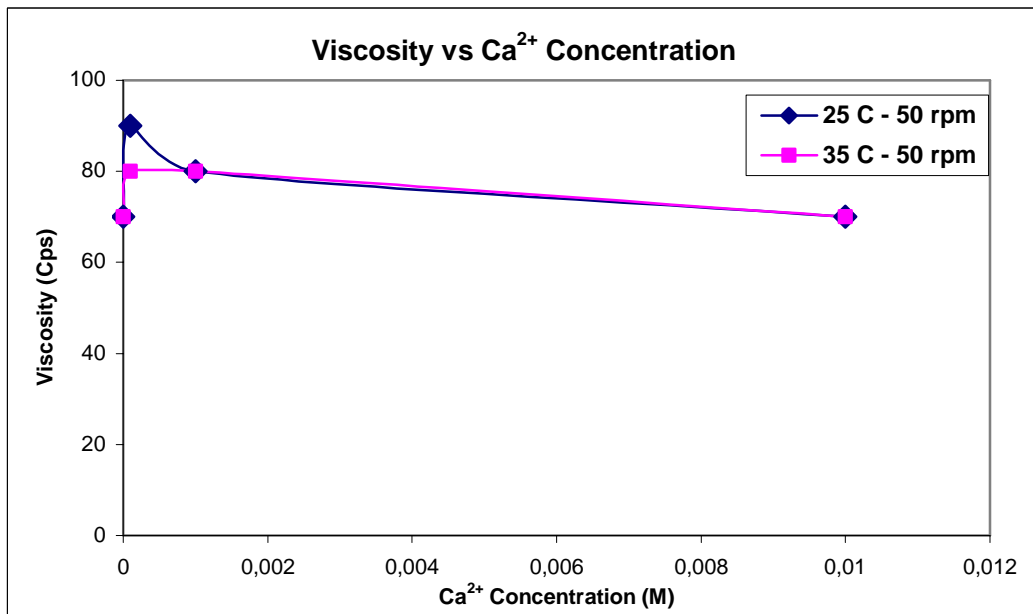


(d)

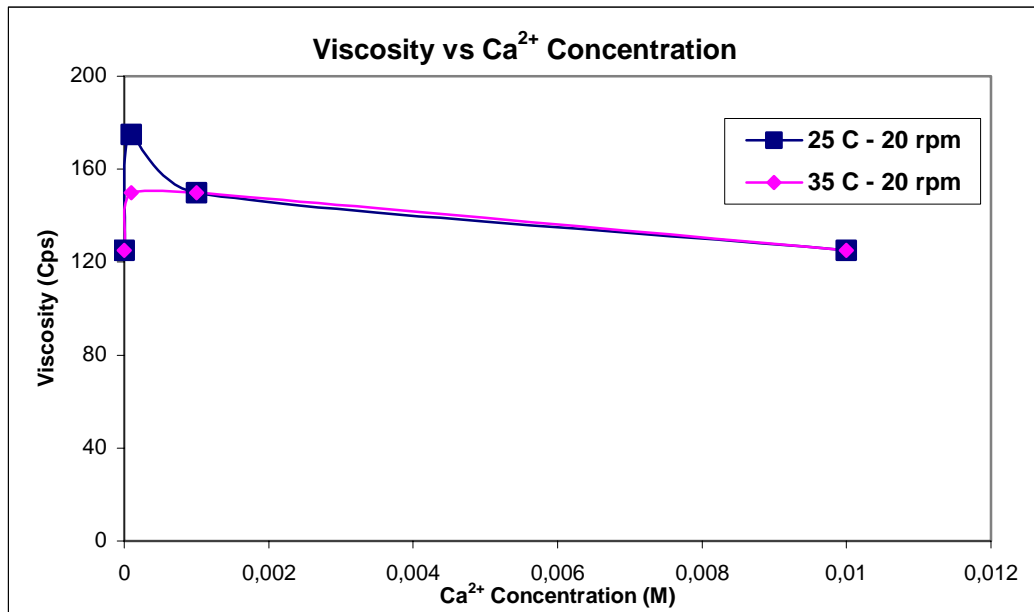
**Figure 22.** Viscosity vs. Ca<sup>2+</sup> concentration graphs of 50% sugar solution (w/w) with 0.5% (w/w) pectin (Unipectine PG569S) at 25 and 35°C; **a)** at 100 rpm, **b)** at 50 rpm, **c)** at 20 rpm, **d)** at all rpms.



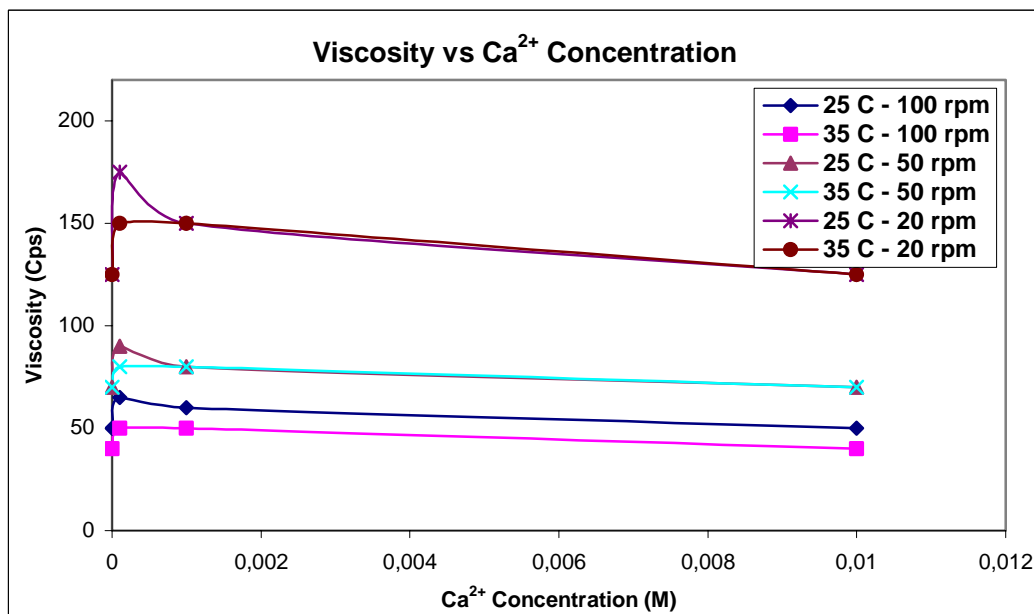
(a)



(b)



(c)



(d)

**Figure 23.** Viscosity vs. Ca<sup>2+</sup> concentration graphs of 50% sugar solution (w/w) with 0.5% (w/w) pectin (Unipectine PG769S) at 25 and 35°C; **a)** at 100 rpm, **b)** at 50 rpm, **c)** at 20 rpm, **d)** at all rpms.

Pectin solutions generally show lower viscosities with respect to other plant gums and thickeners. Their esterification degree plays an important role on rheological properties and gel characterization. Also, at higher pH values or temperatures,  $\beta$ -elimination starts and degradation of pectin chains occurs. These two kind of pectins are HMPs, so they are stable only at room temperature and near to neutralization pH (5 to 6). If these two factors increases, chain cleavage occurs as hydrolysis of  $\beta$ -linkage and loss of viscosity and gelling properties is observed.

In the Figures 22 and 23, viscosity was increased slightly with an  $\text{Ca}^{2+}$  addition at first, but then it decreased and reached nearly a constant plateau. The viscosity values were very smaller with respect to alginate and carrageenans. Increase in the viscosity was observed with decreasing the spindle speed as a result of non-Newtonian behaviour of polymer solutions. Temperature change within 25 to 35<sup>0</sup>C was not seemed so important on viscosities for both kind of pectins. Also, viscosity vs.  $\text{Ca}^{2+}$  concentration graphs of both pectins were very similar to each other.

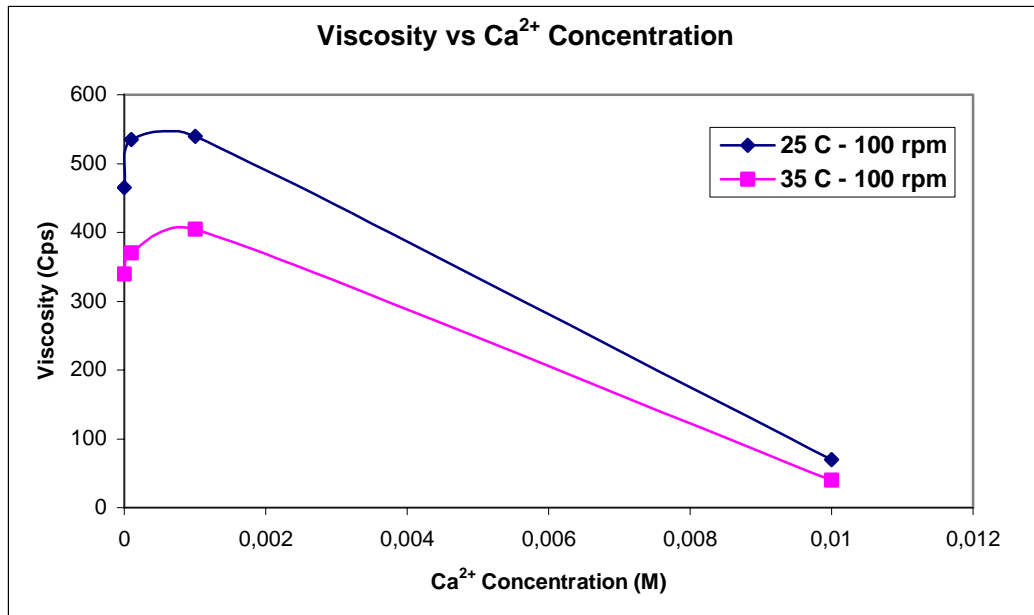
The carboxylate groups on the pectin chains tend to expand the structure of pectins as a result of their charge unless they interact through a divalent cation bridging ( $\text{Ca}^{2+}$ ). For these pectins, HM content decreased the efficiency of divalent cation bridging between the chains. Therefore, slight increase in the viscosity with an addition of  $1 \times 10^{-4} \text{M}$   $\text{Ca}^{2+}$  was an expected result. Lower viscosities with compared to alginate and carrageenans were the result of the higher esterification degree of these pectins. After a critical point, further  $\text{Ca}^{2+}$  additions caused viscosity to decrease slightly. Initial stages of the gel formation may cause this decrease. However, this formation was very limited within the HMPs, so viscosity values became nearly constant after that slight decrease. Hydrogen bonding formation or controlled removal of methoxyl groups are necessary to increase the

rheological properties of pectin solutions with  $\text{Ca}^{2+}$  additions. Without these modifications, viscosity change was not seemed so important.

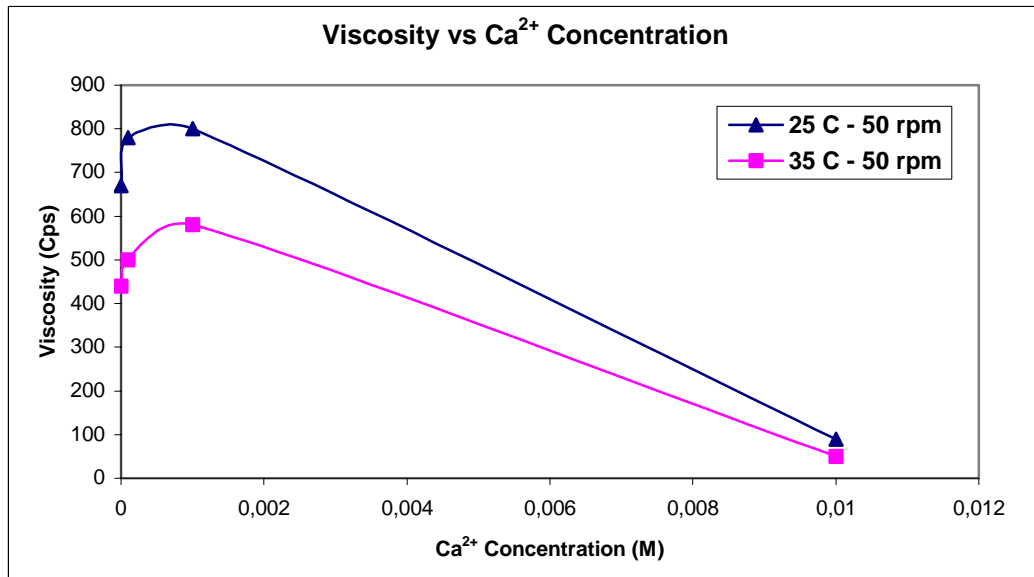
Sugar content of the solution was effective to dehydrate the pectin molecules in the solution. At higher content of sugar caused less water to act as a solvent for pectin, therefore, tendency to crystallize or gelation was favoured.

### 3.2.3 Carrageenans (Satiagel KHG30 and Satiagum CD)

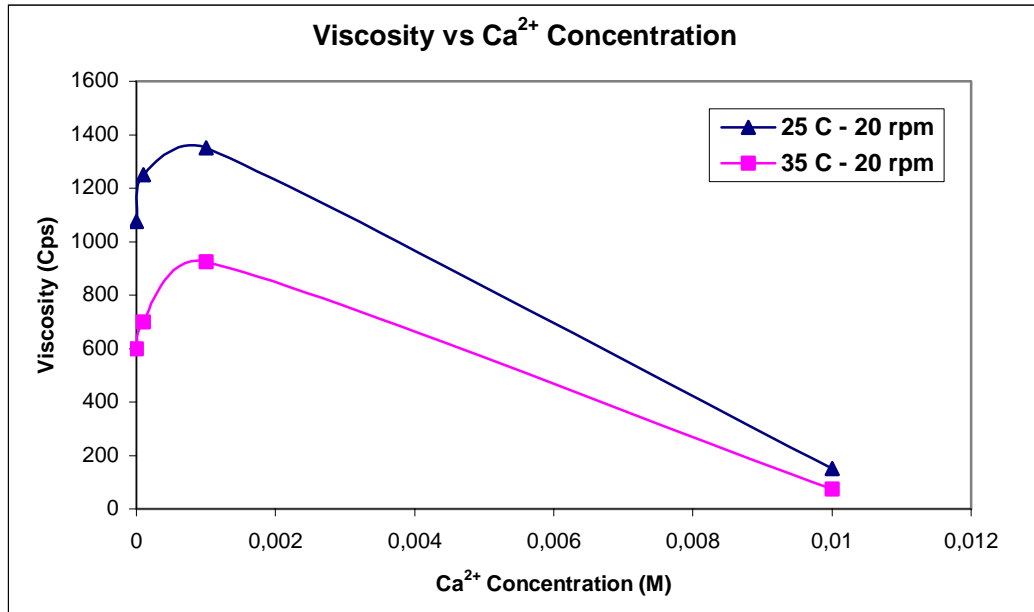
Viscosity measurements of sugar solutions with carrageenans and  $\text{Ca}^{2+}$  cation were carried at various temperatures and rpm (Figure 24, Figure 25). Similar behaviour as in alginates are observed for carrageenans. A decrease in viscosity after about 0.001 M  $\text{Ca}^{2+}$  indicates the formation of gel-beads.



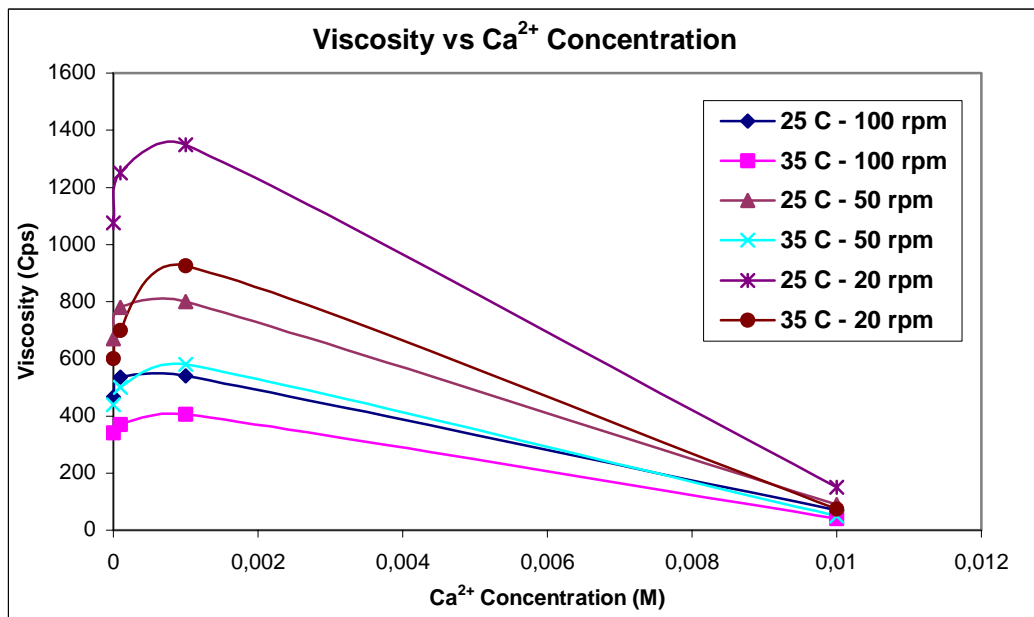
(a)



(b)

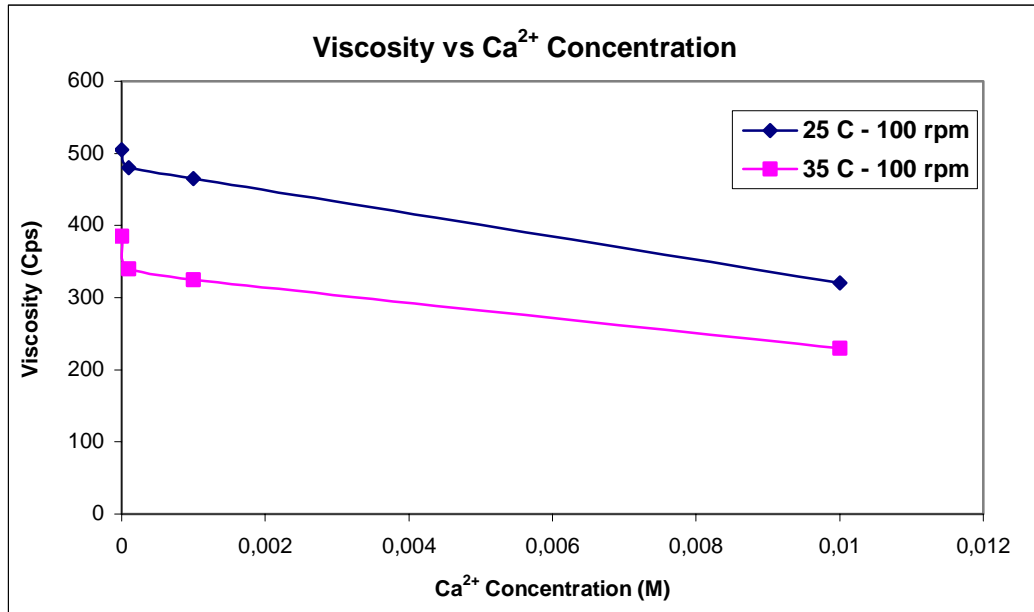


(c)

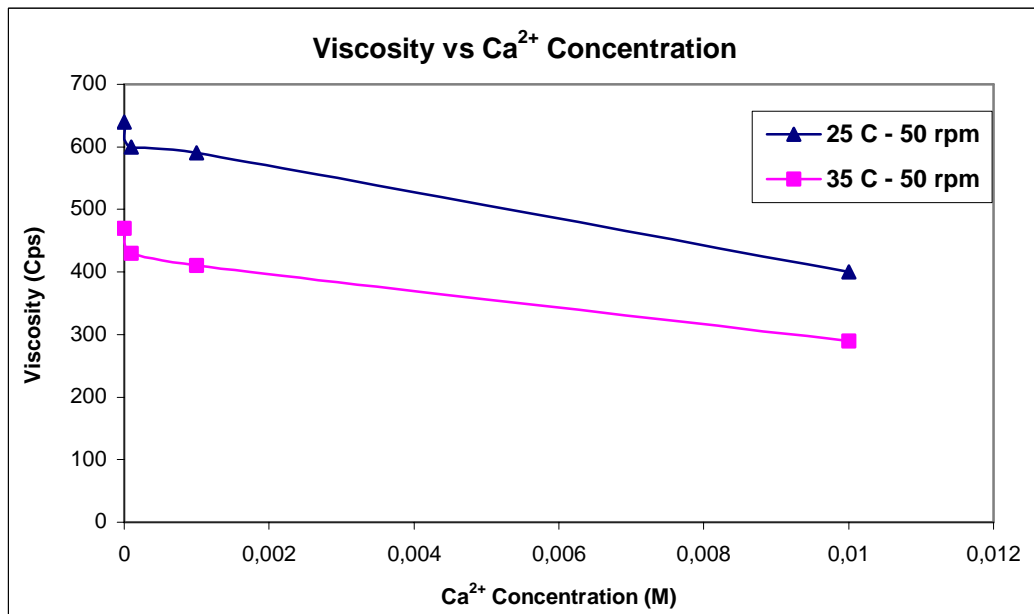


(d)

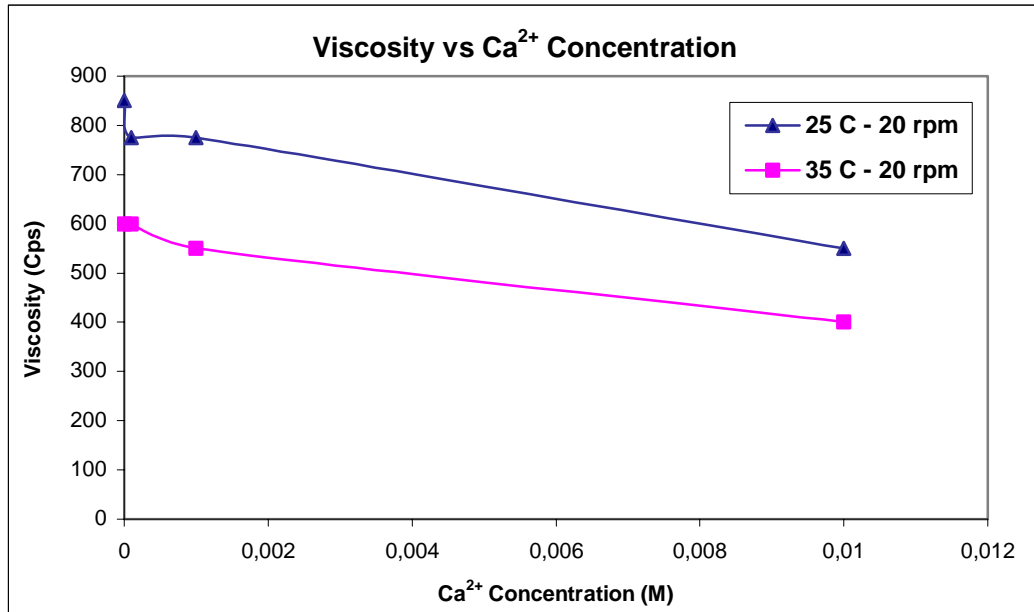
**Figure 24.** Viscosity vs. Ca<sup>2+</sup> concentration graphs of 50% sugar solution (w/w) with 0.5% (w/w) carrageenan (Satiagel KHG30) at 25 and 35<sup>0</sup>C, **a)** at 100 rpm, **b)** at 50 rpm, **c)** at 20 rpm, **d)** at all rpms.



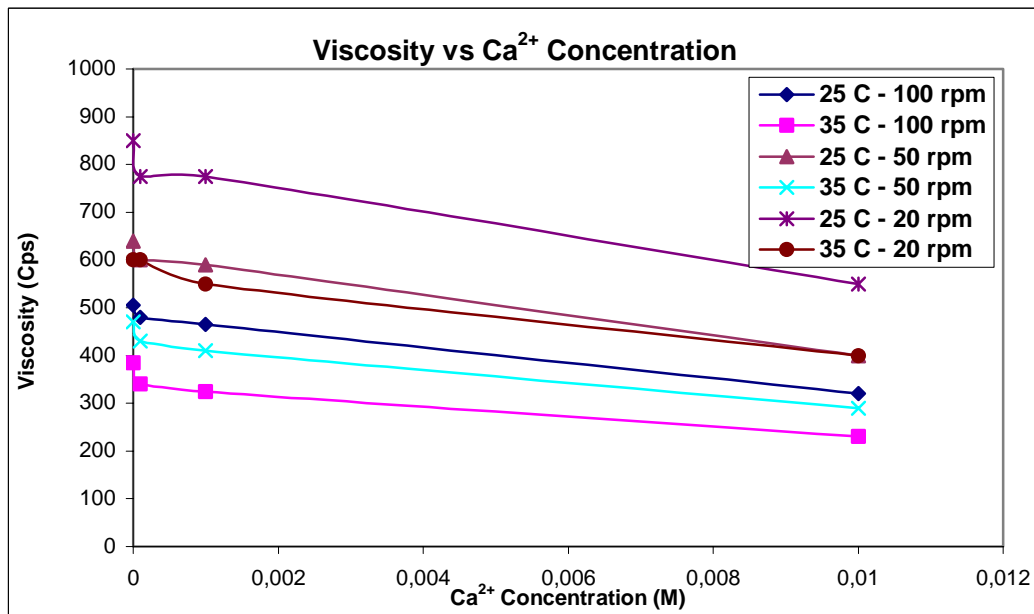
(a)



(b)



(c)



(d)

**Figure 25.** Viscosity vs. Ca<sup>2+</sup> concentration graphs of 50% sugar solution (w/w) with 0.5% (w/w) carrageenan (Satiagum CD) at 25 and 35<sup>0</sup>C, **a)** at 100 rpm, **b)** at 50 rpm, **c)** at 20 rpm, **d)** at all rpms.

The different types of carrageenan differ only in the position and the number of ester sulphate groups. Gelling ability mainly comes from the kappa and iota carrageenans. First double helix formation and then gel network formation with the help of the cations is responsible for increasing the viscosity and gel formation ability. Carrageenan is a thermoreversible gelling agent and gel formation is obtained only in the presence of potassium ions (for  $\kappa$ - and  $\iota$ -carrageenan) or calcium ions (for  $\iota$ -carrageenan). It should be noticed that carrageenan is not just a single polymer, but rather family of gelling and non-gelling sulfated galactans.

In Figure 24, the viscosity of satiagel KHG30 was increased up to the critical  $\text{Ca}^{2+}$  loading; and then viscosity decreased to very low values. That meant, gel beads started to form and this viscosity value belonged to the remaining solution. The highest viscosity values were reached by using this texturant at same parameters with all the other texturants applied. Decreasing the spindle speed caused the viscosity to increase, also decreasing the temperature had the increasing effect on the viscosity. These two parameters had much more effective in the carrageenans with respect to alginate and pectins.

The non-Newtonian behaviour of these solution is apparent as the shear rate with rpm increases the viscosity of the solution decreases (Figure 24(d), Figure 25(d)).

In Figure 25, viscosity values of satiagum CD was decreased slightly with  $\text{Ca}^{2+}$  addition. After adding 0,001 M  $\text{Ca}^{2+}$ , decreasing rate became linear. However, final viscosity value was much more higher than the other carrageenan. Temperature and the spindle speed had almost the same effect in viscosity with satiagel KHG30.

### **3.3 Three dimensional printing (3DP)**

After studying the rheological properties of all the texturant materials, in the presence or absence of sugar, that changes with the metal cations, especially with  $\text{Ca}^{2+}$  ion, analysis on the 3DP machine were done. These analysis were basically about the solid mixture of the sugar, starches and texturants as the powder bed in the 3DP machine and by using a binder solution, then the texture analysis of the specimens formed are carried out. Prior to that, some experiments were done to give an idea, so that to improve the resolution and textural properties of the specimens. Also optimization of the 3DP machine parameters was necessary for that purpose.

#### **3.3.1 Primitive experiments**

To have a rough idea about the performance of the powders and the binders, primitive formation experiments are carried out (Table 2) with some of the selected material. No effort was made to calculate the porosities in individual experiments, but, as in previous experiments porosities are in the vicinity of 0.60 and 50  $\mu\text{L}$  of binder is deposited in experiments. Table 2 shows that use of starch and alginates decreases the impregnation considerably in primitive weight, reducing to half and when used together 1/4 of the sugar only matrice. Among the starches, Gel 463 starch is different than the other two (T470 and T468). It has a very large primitive (0.33 g) compared to T470 and T468, both giving primitives of about 0.19 g.

Among carrageenans, satiamum CD gives small primitives as alginate but satiamum KHG30 is not effective in preventing the formation of large primitives. Pectins also form large primitives. In terms of binder properties when water percentage is decreased primitives get smaller as expected in dissolution type matrices. The possible choices of binder are water, sucrose solution, ethyl alcohol, glycerol (not over 10 % because of drying problem) containing solutions.

**Table 2.** Primitive experiments with various powders and binder solutions

<b>Powder Composition</b>	<b>Binder Composition</b>	<b>Avg. Weight(g)</b>
Sugar	water	0.5742
<b>Alginates</b>		
Sugar + Satialgine (1%)	water	0.2582
Sugar + Satialgine (1%) (dried)		0.2034
Sugar + Satialgine (0.5%)		0.3927
Sugar + Satialgine (0.5%) (dried)		0.3722
Sugar + T468 (5%)		0.1936
Sugar + T468 (5%) (dried)		0.1762
Sugar + T468 (5%) + Satialgine (1%)		0.0763
Sugar + T468 (5%) + Satialgine (1%) (dried)		0.0795
Sugar + T468 (5%) + Satialgine (0.5%)		0.1059
Sugar+ T468 (5%) + Satialgine (0.5%) (dried)		0.1112
Sugar + G463 (5%)		0.3314
Sugar + G463 (5%) (dried)		0.3182
Sugar + G463 (5%) + Satialgine (1%)		0.1232
Sugar + G463 (5%) + Satialgine (1%) (dried)		0.0990
Sugar + G463 (5%) + Satialgine (0.5%)		0.1290
Sugar+ G463 (5%) + Satialgine (0.5%) (dried)		0.1430
Sugar + T470 (5%)		0.1854
Sugar + T470 (5%) (dried)		0.1747
Sugar + T470 (5%) + Satialgine (1%)		0.0764
Sugar + T470 (5%) + Satialgine (1%) (dried)		0.0689
Sugar + T470 (5%) + Satialgine (0.5%)	0.1152	
Sugar +T470 (5%) + Satialgine (0.5%) (dried)	0.1155	
<b>Carrageenans</b>		
Sugar + Satiagum (1%)	CaAc(25mg/100ml water)	0.2309
Sugar + Satiagum (1%)	water	0.1860
Sugar + Satiagum (0.5%)	CaAc(25mg/100ml water)	0.3533
Sugar + Satiagum (0.5%)	water	0.3075
Sugar + Satiagel (1%)	CaAc(25mg/100ml water)	0.4911
Sugar + Satiagel (1%)	water	0.4708
Sugar + Satiagel (0.5%)	CaAc(25mg/100ml water)	0.5404
Sugar + Satiagel (0.5%)	water	0.6110
<b>Pectins</b>		
Sugar + Unipeptine PG569S (1%)	Citric acid (pH=3.12)	0.5466
Sugar + Unipeptine PG569S (1.5%)		0.5566
Sugar + Unipeptine PG769S (1%)		0.4715
Sugar + Unipeptine PG769S (1.5%)		0.4957

**Table 2.** Continued...

<b>Sugar+starch</b>		
Sugar	Sugar soln.(40%) 85% Ethyl alcohol 15%	0.4147
Sugar + T468 (5%)		0.1782
Sugar + T470 (5%)		0.1868
Sugar + G463 (5%)		0.2495
Sugar	Sugar soln.(40%) 85% Ethyl alcohol 10% Glycerol 5%	0.3761
Sugar + T468 (5%)		0.1709
Sugar + T470 (5%)		0.1817
Sugar + G463 (5%)		0.2459

Screening tests of some confectionary powders and the binder solutions were carried out to determine their material properties. A good understanding of the properties and the problems associated with regards to material properties was achieved as far as the primitive formation is concerned.

### 3.3.2 Particle size analysis

Sugar is sieved and particle size distribution of sugar is given in Table 3 (Malvern Master Sizer).

**Table 3.** Particle size distribution of sugar

Above 80 Mesh (177 $\mu\text{m}$ )	8.55 %
Above 120 Mesh (120 $\mu\text{m}$ )	24.82 %
Above 170 Mesh (88 $\mu\text{m}$ )	30.61 %
Fines (88 $\mu\text{m}$ )	36.02 %

Starch has quite a narrow distribution of size with an average diameter  $d(\text{G463})=34.5 \mu\text{m}$ ,  $d(\text{T468})=40.0 \mu\text{m}$ , and  $d(\text{T470})=57.5 \mu\text{m}$  with tails towards 10  $\mu\text{m}$  in particle diameter. Samples produced with 120 and 170 mesh powders give in general better resolution.

### 3.3.3 Packing density

Trials were made to understand the effect of powder compression in the feed section on the powder density in the build section of the 3DP machine.

Packing density in the storage section of the 3DP machine does not significantly affect the density in the build section. It is thought that the roller homogenizes the density of the spread layer (Table 4).

The packing densities of the two sections are measured by a cylindrical, sharp-edged brass bore. The absolute densities of the powder materials and the geometric volumes are used to calculate the porosities. The values are given in Table 4. In the experiments with 3DP machine, no special effort was made except tapping and leveling the powder in the feed part of the instrument due to this finding.

**Table 4.** Packing density (g/cm<sup>3</sup>)<sup>a</sup>

<b>Experiment no.<sup>b</sup></b>	<b>Feed</b>	<b>Build</b>	<b>Porosity<sup>c</sup></b>
1a	0.809	0.606	0.60
1b	0.804	0.641	0.58
2a	0.894	0.615	0.60
2b	0.892	0.645	0.58

<sup>a</sup>After 50 spreads

<sup>b</sup>1a, 1b at low compression, and 2a, 2b at high compression

<sup>c</sup>Density of sugar is taken as 1.521 g/cm<sup>3</sup>.

### 3.3.4 Printer resolution optimization

This part deals with optimization studies of the machine parameters such as layer thickness (LT), saturation (S), core saturation (CS), and the powder composition in terms of types of starches and pre-drying of powders, effect of powder particle size and relative humidity on the spreading of the powder and the

resolution (and quality) of the dumbbells produced. The resolution was graded from 1 (for the best) to 5 (for the worst).

The texture analysis using the sharp knife probe shows that the samples were brittle. The maximum force and displacement at maximum force were reported.

In general, much lower S and CS values are needed with the dissolution type matrices used in this study. With regards to texture, since the binding of the sugar particles occur via fusion, brittle texture was obtained. To generate chewy and softer textures dissolution should be reduced and binding should be produced by gummy additives. Also, viscosity and RH adjustment were studied with suitable additives in the powder and the binder solution.

In the following experiments (Table 5) starch T468 is used to optimize the machine parameters. The sugar in these tests was not sieved unless otherwise is noted.

Inspection of Table 5 reveals that, with water as the binder, S value greater than 1 was detrimental to resolution and layer thickness of 0.005" seemed to be optimum. CS value did not change resolution at S is 1, so an average 0.43 value was employed in most of the following trials. Pre-drying of powder before trials did not have a significant effect on sample resolution so powders were used as is in the remaining experiments.

Table 6 summarizes the effect of using sieved powder with different types of starches. A narrow particle size distribution around 100  $\mu\text{m}$  (120 mesh and 170 mesh) had a dramatic effect on the improvement of resolution. There was also effect of the starch on resolution. A more regular impregnation pattern due to the regularity of pore sizes should be the main reason for the improvement in

resolution. Particle size and its distribution could be singled out as the most effective means of having a good resolution.

**Table 5.** Machine parameters and powder-type optimization

Starch type : T468  
 Starch composition : 5%  
 LT : 0.004 ”  
 CS : 0.34 (Binder/Volume ratio : 5.9%)  
 Binder : water

Sample No.	Saturation	Binder/Volume ratio (%)	Predry	Resolution rating*
1	1.0	17.5	No	3
2	1.5	26.2	No	5
3	2.0	35.0	No	5
4	1.0	17.5	Yes	3

Starch type : T468  
 Starch composition : 5%

Sample No.	LT	S	Binder/Volume ratio (%)	CS	Predry	Resolution rating*
1	0.004 ”	1.00	17.5	0.34	No	3
4	0.004 ”	1.00	17.5	0.34	Yes	3
5	0.006 ”	1.25	14.6	0.52	No	4
6	0.008 ”	1.50	13.1	0.69	No	4
7	0.005 ”	1.00	14.0	0.43	No	2

Starch type : T468  
 Starch composition : 5 %  
 LT : 0.005 ”  
 S : 1.00 (Binder/Volume ratio : 14.0 %)  
 Binder : water

Sample No.	CS	Binder/Volume ratio (%)	Predry	Resolution rating*
7	0.43	6.0	No	2
8	0.35	4.9	No	2
9	0.30	4.2	No	2
10	0.50	7.0	No	2
11	0.60	8.4	No	2
12	0.30	4.2	Yes	2
13	0.43	6.0	Yes	2
14	0.50	7.0	Yes	2
15	0.60	8.4	Yes	2

**Table 5.** Continued...

LT : 0.005 ”  
S: 1.00  
Starch composition : 5%  
Binder : water  
Pre-dried

<b>Sample No.</b>	<b>Starch Type</b>	<b>CS</b>	<b>Binder/Volume ratio (%)</b>	<b>Resolution rating*</b>
12	T468	0.30	4.2	2
13	T468	0.43	6.0	2
15	T468	0.60	8.4	2
16	G463	0.30	4.2	2
17	G463	0.43	6.0	2
18	G463	0.60	8.4	3
19	T470	0.30	4.2	2
20	T470	0.43	6.0	2
21	T470	0.60	8.4	2

\* Rating was done out of 5; 1 stands for the best and 5 for the worst.

In Table 6, sieved powders were used at the above saturation levels. For 120 and 170 mesh powders and starches T470 and G463, the best resolution was obtained.

**Table 6.** Effect of particle size on resolution

Particle size of sugar : 120 mesh  
 LT : 0.005 ”  
 S : 1.0  
 CS : 0.43  
 Starch Composition : 5%  
 Predried.

Sample No.	Starch Type	Resolution rating*
22	T468	2
23	T470	1
24	G463	1

Particle size of sugar : 170 mesh  
 LT : 0.005 ”  
 S : 1.0  
 CS : 0.43  
 Starch composition : 5%  
 Predried.

Sample No.	Starch Type	Resolution rating*
25	T468	3
26	T470	1
27	G463	1

\* Rating was done out of 5; 1 stands for the best and 5 for the worst.

### 3.3.5 Binder solution trials

To decrease the spreading of the binder and dissolution of the matrix, 45% sugar solution was used in combination with ethyl alcohol and glycerol (Table 7). At S value 1 (sample 54), very good resolution was obtained. S value 1.5 was detrimental to resolution (sample 55). Unfortunately this binder formulation was difficult to work with in the 3DP machine. The crystallization of sugar in the binder at the capillaries blocked the ink-jet head frequently; therefore, no more trials were carried out with this particular binder formulation.

**Table 7.** Properties without texturant

Sample no	Powder	Machine Parameters	Binder	Maximum Force Average (g/cm)	Rating
34	95% Sugar 5% T470	S : 1 CS : 0.43 LT : 0.005"	Water	4088	2
54	95% Sugar 5% T470	S : 1 CS : 0.43 LT : 0.005"	85% Sugar soln(45%) 10% EtOH 5% Glycerol	3734	1
55	95% Sugar 5% T470	S : 1.5 CS : 1 LT : 0.005"	85% Sugar soln(45%) 10% EtOH 5% Glycerol	14000	5

### 3.3.6 Texture modification studies

In order to change texture the fusion of the sugar particles has to be prevented to a large extent, fusing of sugar is basically an irreversible phenomenon in 3-D process that is it can not be undone by evaporating water. Basically there are various ways of reducing sugar fusing;

- i- Coating the sugar particles with non-soluble or hydrophobic layer.

- ii- To accomplish binding of powder particle with inert solvents other than water that contain a preferable natural polymeric binder.
- iii- To reduce the amount of water in the binder which is limited to for example glycerol and ethyl alcohol inclusion which may or may not be enough to prevent fusion.
- iv- To employ concentrated sugar solution to reduce the dissolution of sugar particles, this remedy may not work because extra sugar is introduced into the matrix which can fuse the sugar particles after water is evaporated. (This factor is more helpful in increasing the resolution because of reduction in the dissolution process).
- v- To introduce gel forming additives, alginates, carrageenans, pectins or gums into the powder to trap some of the binder water in a way that will prevent fusing of sugar particles.

In this work (iii),(iv), and (v) were studied. The results are discussed below:

### **3.3.7 Effect of texturants**

For these sets of experiments, a cylindrical sample geometry with 2 cm diameter and 1 cm height was used. To correlate with the previous studies force values were given in g/cm which can be compared directly with the "*body*" force values of the dumbbells which have 1 cm width.

#### **Alginate (Satialgine SG300):**

The results are given in Table 8. Reducing starch percentage and increasing alginate percentage gave rise to stronger cohesion (samples 28, 29, and 30). When sugar percentage was reduced and alginate increased, a slight increase in maximum force value was recorded. All of these samples were brittle. Since, in these experiments the effect on texture was investigated, no special effort to obtain

high resolution was sought in these series. To have gelling, binder solution was prepared with calcium acetate (50 mg/100 ml water).

**Table 8.** Effect of alginate on texture

*Satialgine SG300*

Sample No.	Powder	Binder	Maximum Force Average (g/cm)	Rating
28	95% Sugar 4.5% T470 0.5% Satialgine	85% water 10% EtOH 5% Glycerol CaAc (50mg/100ml soln)	4836	3
29	95% Sugar 4% T470 1% Satialgine	85% water 10% EtOH 5% Glycerol CaAc (50mg/100ml soln)	7404	3
30	95% Sugar 3% T470 2% Satialgine	85% water 10% EtOH 5% Glycerol CaAc (50mg/100ml soln)	9060	2
31	94% Sugar 5% T470 1% Satialgine	85% water 10% EtOH 5% Glycerol CaAc (50mg/100ml soln)	5266	3
32	93.5% Sugar 5% T470 1.5% Satialgine	85% water 10% EtOH 5% Glycerol CaAc (50mg/100ml soln)	5964	3
33	93% Sugar 5% T470 2% Satialgine	85%water 10%EtOH 5%Glycerol CaAc (50mg/100ml soln)	5482	2
34	95% Sugar 5% T470	water	4089	2
35	95% Sugar 4.5% T470 0.5% Satialgine	water CaAc (50mg/100ml soln)	4210	3

**Carrageenans (Satiagum CD, Satiagel KHG30):**

With Satiagum CD and Satiagel KHG30, the results displayed in Table 9 are obtained. In general, hard and brittle texture is observed, a maximum with Satiagel and water only binder is recorded.

**Table 9.** Effect of carrageenans on texture

*Satiagum CD*

Sample No.	Powder	Binder	Maximum Force Average (g/cm)	Rating
36	95% Sugar 4.5% T470 0.5% Satiagum	Water	4872	2
37	95% Sugar 4.5% T470 0.5% Satiagum	85% water 10% EtOH 5% Glycerol	9344	3
38	95% Sugar 4% T470 1% Satiagum	85% water 10% EtOH 5% Glycerol	6435	3
39	95% Sugar 3% T470 2% Satiagum	85% water 10% EtOH 5% Glycerol	6250	2

*Satiagel KHG30*

Sample No.	Powder	Binder	Maximum Force Average (g/cm)	Rating
40	95% Sugar 4.5% T470 0.5% Satiagel	Water	11634	2

**Pectins (Unipectine PG 569S, Unipectine PG 769S):**

With Unipectine PG569S, interesting changes in texture was observed. For sample 44 in Table 10, a gummy or chewy material with low maximum force and medium resolution was produced at 1% pectin concentration. The other pectin, Unipectine PG769S, gave similar results as the previous brittle material. Unipectine PG569S gave a soft texture at 0.5% and an even softer one at 1% usage.

**Table 10.** Effect of pectins on texture*Unipectine PG569S*

<b>Sample No.</b>	<b>Powder</b>	<b>Binder</b>	<b>Maximum Force Average (g/cm)</b>	<b>Rating</b>
41	95% Sugar 4.5% T470 0.5% Unipectine569S	Water	6310	4
42	95% Sugar 4.5% T470 0.5% Unipectine569S	Water + Citric Acid pH : 3.075	3041	3
43	95% Sugar 4.5% T470 0.5% Unipectine569S	85%water+10%EtOH + 5%Glycerol+citric acid pH : 3.415	7166	3
44	95% Sugar 4% T470 1% Unipectine569S	85%water+10%EtOH + 5%Glycerol+citric acid pH : 3.415	1761	3

*Unipectine PG769S*

<b>Sample No.</b>	<b>Powder</b>	<b>Binder</b>	<b>Maximum Force Average (g/cm)</b>	<b>Rating</b>
45	95% Sugar 4.5% T470 0.5% Unipectine769S	Water	6177	4
46	95% Sugar 4.5% T470 0.5% Unipectine769S	Water + Citric Acid pH : 3.075	5472	2
47	95% Sugar 4.5% T470 0.5% Unipectine769S	85%water+10%EtOH + 5%Glycerol+citric acid pH : 3.415	7094	2
48	95% Sugar 4% T470 1% Unipectine769S	85%water+10%EtOH + 5%Glycerol+citric acid pH : 3.415	4032	3

### 3.3.8 Further studies on promising formulations

In the following series of experiments Unipectins which gave rise to largest texture change in the previous experiments were tested with various types of binders. The samples were tested under conditions of no humidity control (~ 30 % RH) and at 54.1 % RH (Table 11 and Table 12).

**Table 11.** Unipectins based matrices with various binder solutions

Sample No	Powder	Binder	Maximum Force Average (g/cm)	Rating
60	95% Sugar 4.5% T470 0.5% Unipectine769S	Water + Citric acid pH : 3.121	2449 (Body) 7673 (Head)	2
61	95 % Sugar 4.5 % T470 0.5 %Unipectine769S	85%Water+10%EtOH+ 5%Glycerol+Citricacid pH: 3.402	2431 (Body) 3205 (Head)	3
62	95 % Sugar 4 % T470 1 %Unipectine769S	85%Water+10%EtOH+ 5%Glycerol+Citricacid pH: 3.402	4725 (Body) 5053 (Head)	2
63	95% Sugar 4.5% T470 0.5% Unipectine569S	Water + Citric acid pH: 3.121	3919 (Body) 8075 (Head)	3
64	95 % Sugar 4 % T470 1 %Unipectine569S	85%Water+10%EtOH+ 5%Glycerol+Citricacid pH: 3.402	1752 (Body) 1829 (Head)	3
65	95 % Sugar (Sieved) 4 % T470 1 %Unipectine569S	85%Water+10%EtOH+ 5%Glycerol+Citricacid pH: 3.402	1607 (Body) 3166 (Head)	1
66	94 % Sugar 5 % T470 1 %Unipectine769S	85%Water+10%EtOH+ 5%Glycerol+Citricacid pH: 3.463	3138 (Body) 3745 (Head)	3
67	93 % Sugar 5 % T470 2 %Unipectine769S	85%Water+10%EtOH+ 5%Glycerol+Citricacid pH: 3.463	2191 (Body) 4093 (Head)	2
68 color	94 % Sugar 5 % T470 1 %Unipectine569S	85%Water+10%EtOH+ 5%Glycerol+Citricacid pH: 3.463	5261 (Body) 6182 (Head)	3

\* Texture analysis were done on the body and head parts of the dumbbell shaped specimens.

Unipeptine 569S can be called chewy at 1% concentration with the binder solution used (sample 65) at 30% RH.

**Table 12.** Texture analysis of samples at 54.1% RH chamber

Sample No	Powder	Binder	Maximum Force Average (g/cm)	Rating
71 (60)	95% Sugar 4.5% T470 0.5% Unipeptine769S	Water + Citric acid pH : 3.121	4941 (Body) 8385 (Head)	2
72 (61)	95 % Sugar 4.5 % T470 0.5%Unipeptine769S	85%Water+10%EtOH+ 5%Glycerol+Citricacid pH:3.402	4558 (Body) 7894 (Head)	3
73 (62)	95 % Sugar 4 % T470 1 %Unipeptine769S	85%Water+10%EtOH+ 5%Glycerol+Citricacid pH:3.402	3557 (Body) 5463 (Head)	2
74 (63)	95% Sugar 4.5% T470 0.5%Unipeptine569S	Water + Citric acid pH : 3.121	4386 (Body) 7319 (Head)	3
75 (64)	95 % Sugar 4 % T470 1 %Unipeptine569S	85%Water+10%EtOH+ 5%Glycerol+Citricacid pH:3.402	5390 (Body) 6973 (Head)	3
76 (65)	95 % Sugar (Sieved) 4 % T470 1 %Unipeptine569S	85%Water+10%EtOH+ 5%Glycerol+Citricacid pH:3.402	4510 (Body) 3140 (Head)	1

\* Texture analysis were done on the body and head parts of the dumbbell shaped specimens.

\*\* Sample no in parenthesis show the corresponding no-humidity controlled runs.

As binder, different combinations of water, ethyl alcohol, glycerol, and specific pH values were employed and their effects on sugar, starch and unipeptine based powders were documented.

In almost all the samples at high RH (54.1%), the maximum force readings are higher than low humidity readings. As documented earlier at the RH given, cohesion of the matrices get stronger. An interesting observation is for samples 64,

65 where the texture can be called chewy at 30% RH, at higher RH (samples 75, 76) they are brittle. One can also notice the effect of using sieved powder on resolution where sample 65 has the highest resolution.

In the following series of experiments ammonium sulphate saturation at 77.5% RH was applied.

**Table 13.** Texture analysis results at 77.5% RH

Sample No	Powder	Binder	Maximum Force Average (g/cm)	Rating
79 (60)	95% Sugar 4.5% T470 0.5% Unipectine769S	Water + Citric acid pH : 3.121	2913 (Body) 4804 (Head)	2
80 (61)	95% Sugar 4.5% T470 0.5%Unipectine769S	85%Water+10%EtOH+ 5%Glycerol+Citricacid pH:3.402	1019 (Body) 1618 (Head)	3
81 (62)	95% Sugar 4% T470 1%Unipectine769S	85%Water+10%EtOH+ 5%Glycerol+Citricacid pH:3.402	946 (Body) 1324 (Head)	2
82 (63)	95% Sugar 4.5% T470 0.5% Unipectine569S	Water + Citric acid pH : 3.121	2796 (Body) 2776 (Head)	3
83 (64)	95 % Sugar 4% T470 1%Unipectine569S	85%Water+10%EtOH+ 5%Glycerol+Citricacid pH:3.402	2900 (Body) 2946 (Head)	3
84 (65)	95% Sugar (Sieved) 4% T470 1%Unipectine569S	85%Water+10%EtOH+ 5%Glycerol+Citricacid pH:3.402	2411 (Body) 1514 (Head)	1
85 (66)	94% Sugar 5% T470 1%Unipectine769S	85%Water+10%EtOH+ 5%Glycerol+Citricacid pH:3.463	1389 (Body) 1640 (Head)	3
86 (67)	93% Sugar 5% T470 2%Unipectine769S	85%Water+10%EtOH+ 5%Glycerol+Citricacid pH:3.463	1350 (Body) 1361 (Head)	2
87color (68)	94% Sugar 5% T470 3%Unipectine569S	85%Water+10%EtOH+ 5%Glycerol+Citricacid pH:3.463	1408 (Body) 1568 (Head)	3

**Table 13.** Continued...

88	94% Sugar 5% T470 1% Unipeptine569S	Water + Citric acid pH : 3.121	5155,Head, 30%RH 1199,Head, 77.5%RH	3
89	93% Sugar 5% T470 2% Unipeptine569S	Water + Citric acid pH : 3.121	7750,Head, 30%RH 1261,Head, 77.5%RH	2
90	92 % Sugar 5 % T470 3 % Unipeptine569S	Water + Citric acid pH : 3.121	8203,Head, 30%RH 2528,Head, 77.5%RH	2

\* Texture analysis were done on the body and head parts of the dumbbell shaped specimens.

\*\* Sample no in parenthesis show the corresponding no-humidity controlled runs.

Compared to 54.1% RH, the maximum force recorded is much smaller and the texture is chewy. One can conclude that at high humidity (or water activity) sugar matrices lose their brittle nature that is cohesive strength of sugar matrices in these formulations pass through a maximum around 50% RH. At even higher RH values with KNO<sub>3</sub> saturation, the samples look as if they are soaked in water with no holding strength. As it is well-known, over 60% RH, bacterial growth is also promoted, therefore, unless coated with a water vapour impermeable top-coat, one should not consider high RH preparations.

In summary, with Unipeptines at around 1% concentration in the powder and glycerol-ethyl alcohol-water containing binder texture considerable modification is possible and the resolution of the parts will be fine with sieved powders. The RH around 50-60% gives rise to stronger and more brittle structures.

### **3.4 FTIR analysis**

In FTIR analysis, pellets were produced as pure texturant material and with a sugar and calcium cation content. The peak assignments are almost the same with the alginate films as explained before in section 3.1.2. This is because; each texturant material has polysaccharide structure basically. Any additional information will be given in the relevant parts.

### 3.4.1 Alginate

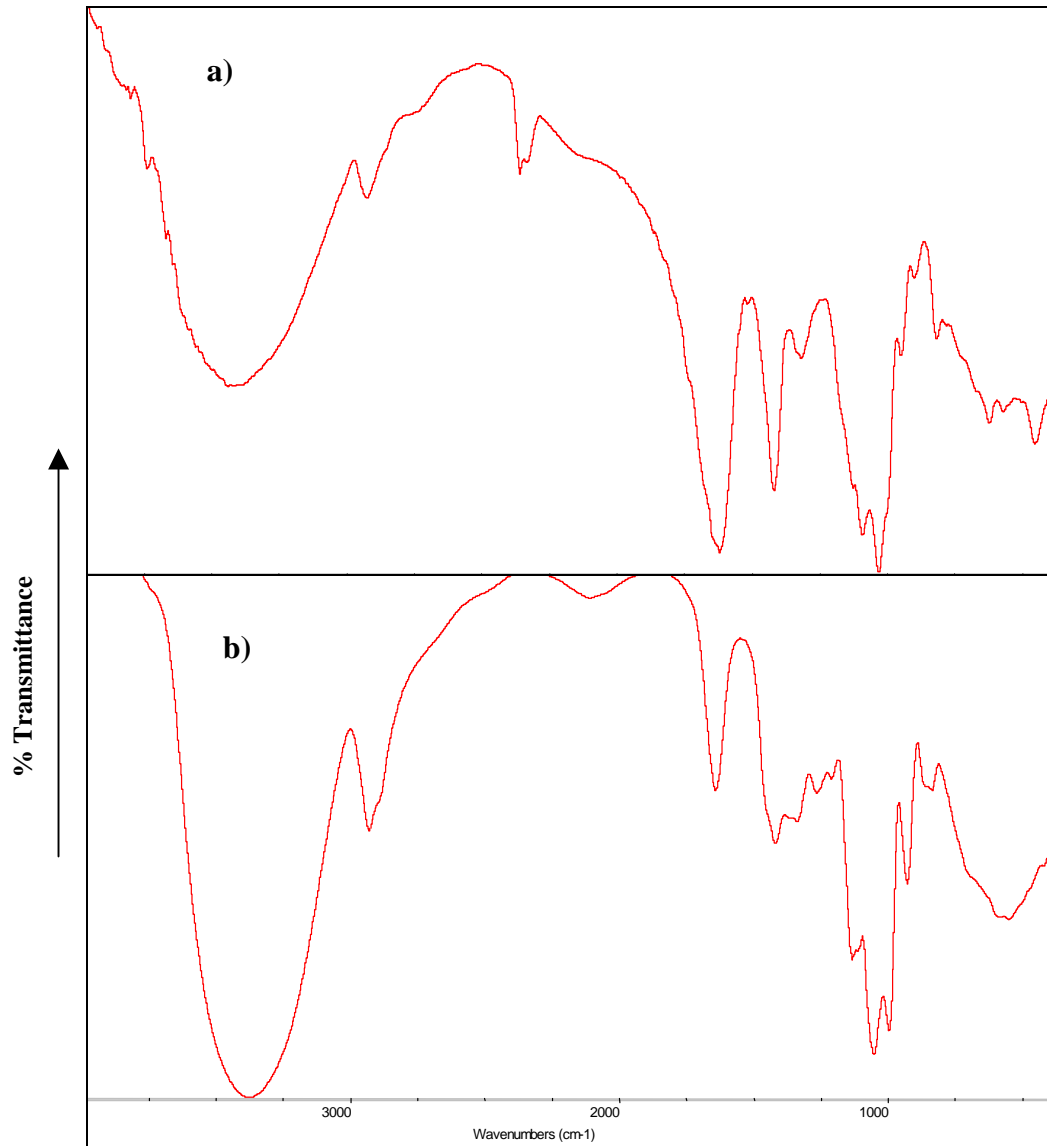


**Figure 26.** FTIR spectrum of **a)** Satalgine SG300, **b)** Satalgine SG300 in sugar solution with 0.01 M  $\text{Ca}^{2+}$

For alginate (Figure 26), increase in molecular bonding results in the O-H stretching peak to become narrower and higher in intensity at  $3350\text{ cm}^{-1}$ . At  $1610$  and  $1415\text{ cm}^{-1}$ , assigned for asymmetric and symmetric stretching for  $\text{COO}^-$ , the intensities decrease as a result of decrease in ionic bonding. With an addition of  $\text{Ca}^{2+}$ , peak at  $2360\text{ cm}^{-1}$  disappeared and new peak occurred at lower wavenumber

with very low intensity but no assignment could be done for that peak. Sugar content seemed not important for the IR spectrum.

### 3.4.2 Carrageenans

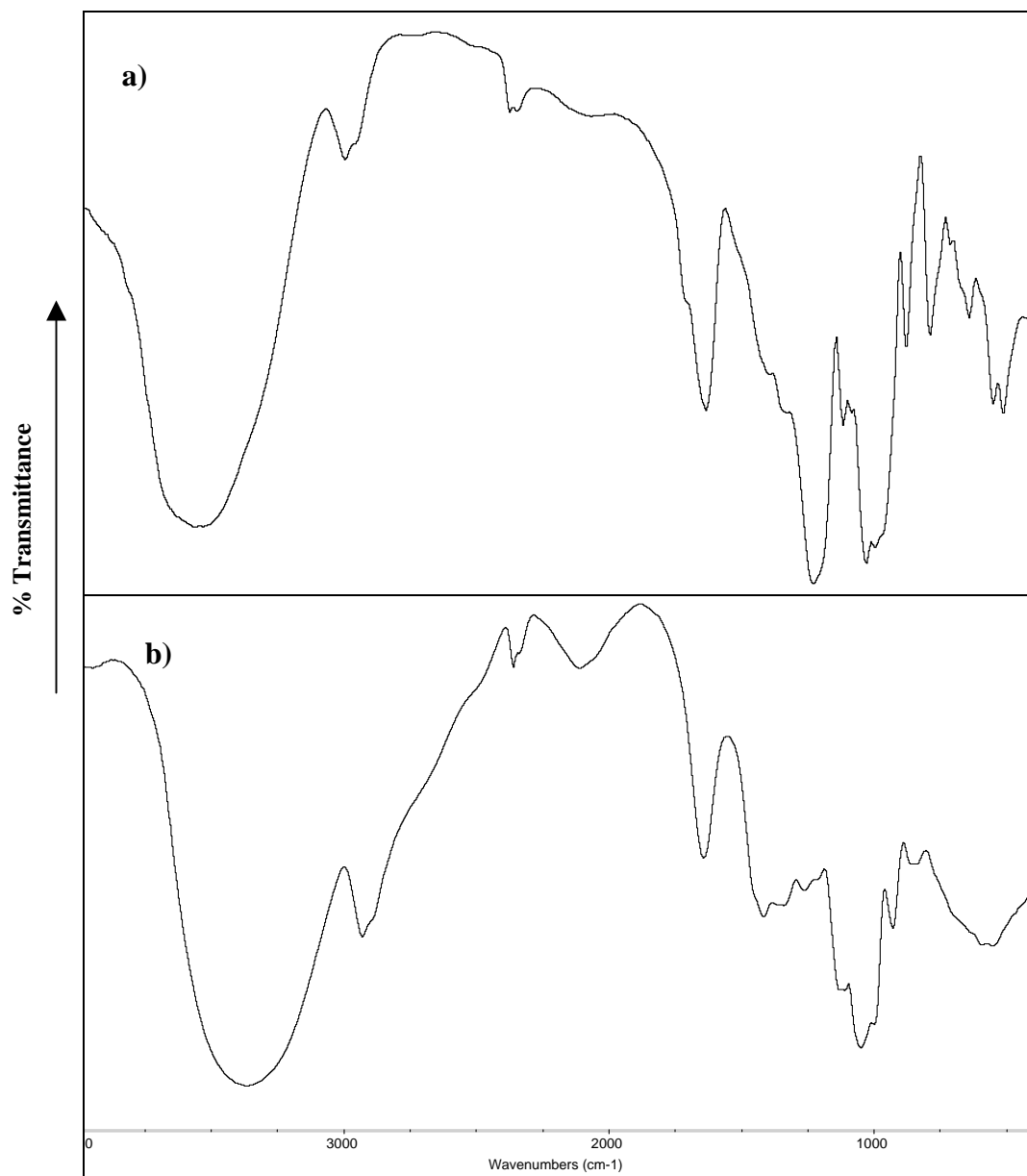


**Figure 27.** FTIR spectrum of **a)** Satiagum CD, **b)** Satiagum CD in sugar solution with 0.01 M  $\text{Ca}^{2+}$

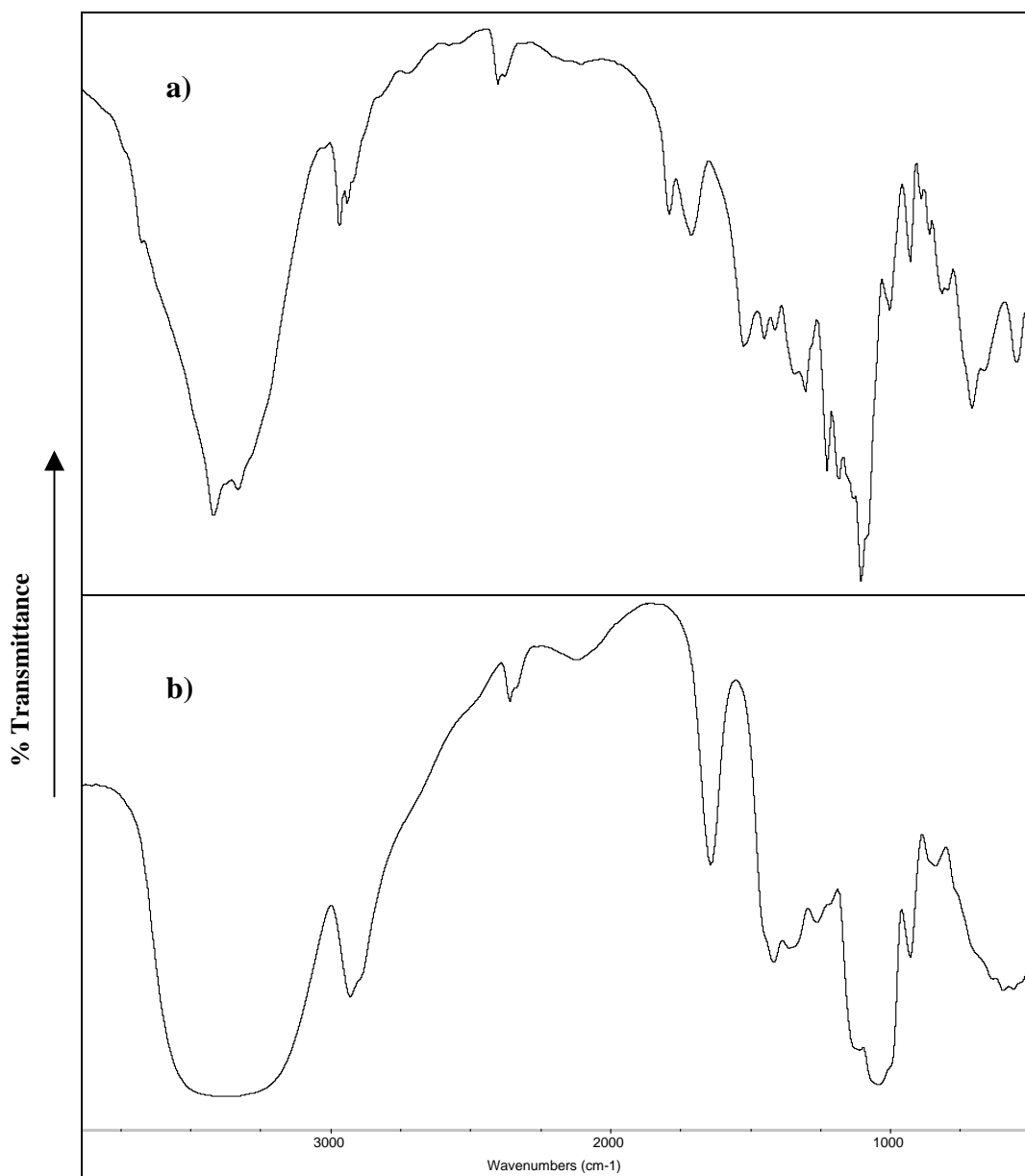


**Figure 28.** FTIR spectrum of **a)** Satiigel KHG30, **b)** Satiigel KHG30 in sugar solution with 0.01 M  $\text{Ca}^{2+}$

$\kappa$ -carrageenan is made up of  $\alpha$  (1 $\rightarrow$ 4) D-galactose-4-sulfate and  $\beta$  (1 $\rightarrow$ 3) 3,6-anhydro-D-galactose. In a  $\kappa$ -type seaweed extract some of the D-galactose contains 6-sulfate ester groups and some of the 3,6-anhydro-D-galactose contains 2-sulfate ester groups. As in the case of  $\kappa$ -carrageenan,  $\iota$ -carrageenan also shows irregularities in the form of 6-sulfate ester groups on some D-galactose residues. It follows that a lack of 2-sulfate ester groups on some 3,6-anhydro-D-galactose

residues makes ι-carrageenan more irregular. λ-carrageenan differs from κ- and ι-carrageenan by having a disulfated-D-galactose residue and no 4-sulfate in the -D-galactose residue. Instead of 4-sulfate ester groups, λ-carrageenan contains variable amounts of 2-sulfate ester groups.

**Table 14.** FTIR peak assignments for different types of carrageenans

Wavenumber (cm <sup>-1</sup> )	Functional group	Kappa	Iota	Lambda
1210 -1260	Ester sulfate	vs	vs	vs
1010 -1080	Glycosidic linkage	vs	vs	vs
928 - 933	3.6-anhydro-D-galactose	s	s	a-l
840 - 850	D-galactose-4-sulfate	m	m	a
820 - 830	D-galactose-2-sulfate	a	a	m
810 - 820	D-galactose-6-sulfate	a	a	m
800 - 805	3.6-anhydro-D-galactose-2-sulfate	a - l	m	a
vs = very strong    s = strong    m = medium    l = low    a = absent				

From the peak assignments, it can be concluded that our carrageenans basically made up of κ- and ι-carrageenans. For the satiagel, some λ-carrageenan may also be present which is responsible for the peaks at around 800 cm<sup>-1</sup>. With an addition of Ca<sup>2+</sup>, decrease in the peak intensities was seen again as a result of increase in molecular bonding and decrease in ionic bonding.

### 3.4.3 Pectins

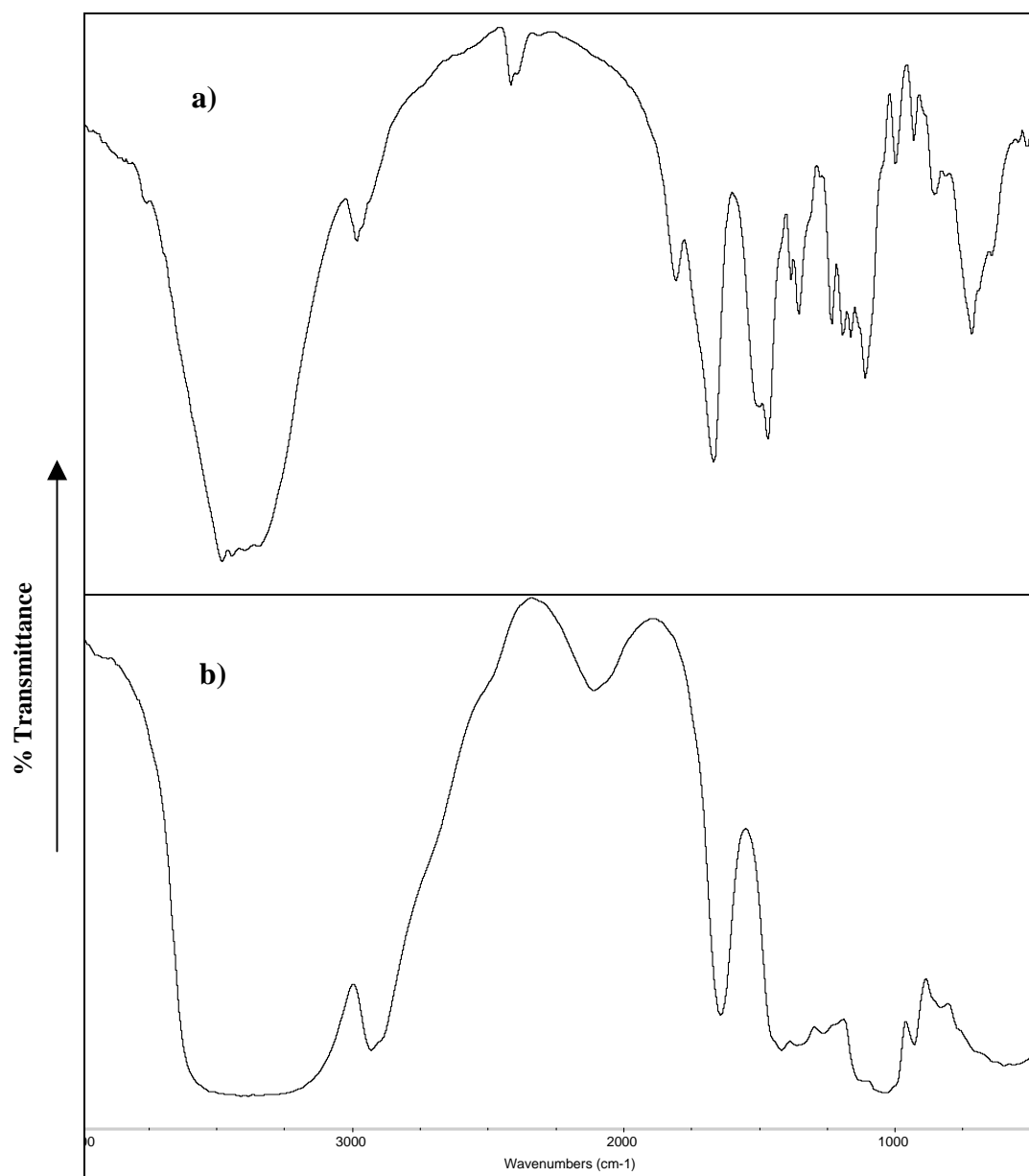


**Figure 29.** FTIR spectrum of **a)** Unipectine PG569S, **b)** Unipectine PG569S in sugar solution with 0.01 M Ca<sup>2+</sup>

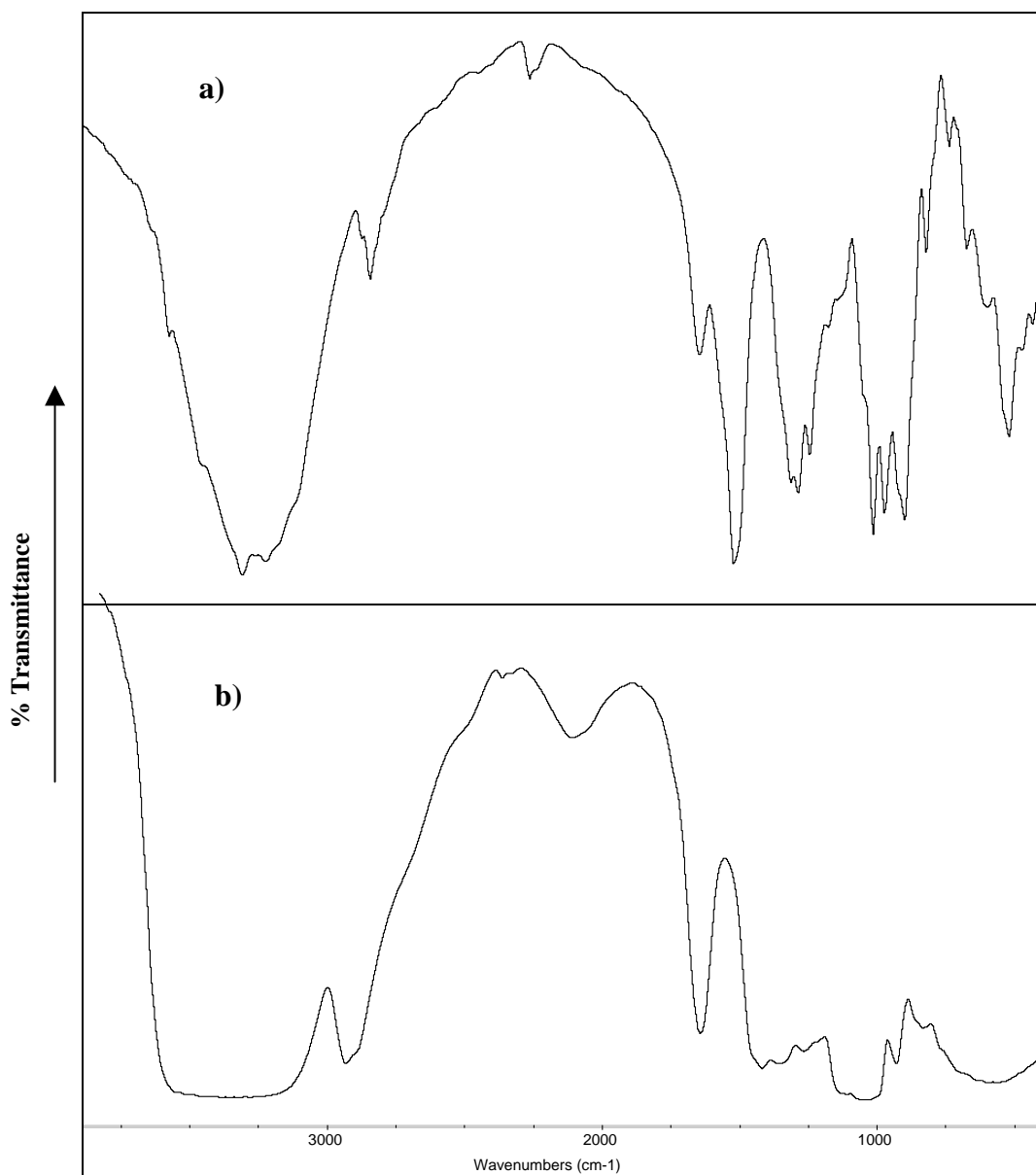


**Figure 30.** FTIR spectrum of **a)** Unipectine PG769S, **b)** Unipectine PG769S in sugar solution with 0.01 M  $\text{Ca}^{2+}$

In the case of pectins, the broad and intense O-H stretching band of hydroxyls and bound water is assigned at around  $3400\text{ cm}^{-1}$ . The  $2930\text{ cm}^{-1}$  band corresponds to the C-H stretching of  $\text{CH}_2$  groups and the two bands at  $1640$  and  $1420\text{ cm}^{-1}$  correspond to vibrations of the  $\text{O}=\text{C}-\text{O}$  structure. Both the  $\text{COOH}$  and  $\text{COOCH}_3$  groups of pectins absorb at the nearly same frequency around  $1740\text{ cm}^{-1}$ , but ionized carboxylate group ( $\text{COO}^-$ ) absorbs at around  $1640\text{ cm}^{-1}$ . The

carbohydrates show high absorbances between 1200 and 950  $\text{cm}^{-1}$  which constitutes the fingerprint region of polysaccharide based materials. Besides the other changes in the spectrum, introduction of the sugar and  $\text{Ca}^{2+}$  cation to the medium causes the peak around 1740  $\text{cm}^{-1}$  assigned for C=O stretching vibration of methyl esterified carboxylic group to be disappeared, while a new peak at 1640  $\text{cm}^{-1}$  to be appeared. That change is a result of the decrease in the methylation degree of the pectin molecules.

## CHAPTER 4

### CONCLUSIONS

Firstly, detailed study on the alginate solutions was performed and the behaviour of the texturant materials in water was understood. The rheological behaviour of alginate solutions with different multivalent cations was studied and it is concluded that:

- $Mg^{2+}$  cation was not big enough to fit the cavities of the alginate chains, therefore viscosity values were very low and change was limited between a small range. Temperature was also not so effective on the rheological property of solutions. Obtained temporary network could be destroyed easily between the chains and  $Mg^{2+}$  cations by applying a mechanical force.
- $Al^{3+}$  cation resulted in a higher viscosity values with increasing the alginate and cation concentrations and temperature. There was a critical cation concentration where the viscosity started to decrease. This value could be assigned for the formation of the gel beads. Less acidic medium caused an increase in viscosity up to the neutral region because less acidic medium enhanced the bonding between alginate segments at  $COO^-$  and  $Al^{3+}$ . Also,

it could be concluded that at low temperatures, H-bonding was favoured with alginate chains so decrease in viscosity was observed. In neutral and basic medium, viscosity stayed constant.

- $\text{Ca}^{2+}$  cation was the most effective among the others as far as viscosity concerned because it fits to the cavities of the alginate chains to form the egg-box structure. Increase in viscosity was much more higher with increasing cation concentration than alginate concentration. Viscosity decreased steadily with increasing temperature. Network formation could not be destroyed by thermally and mechanically. Different cation sources was not so effective on viscosity.
- Among the different cations,  $\text{Ca}^{2+}$  was found to be more effective on viscosity of alginate solutions which was more dramatic at higher cation concentrations. H-bonding and flow alignment were the basic reasons for the other cations studied had lower viscosity values at low temperatures. Size of the cation also was an important factor for determining viscosity.

For the sugar solutions with  $\text{Ca}^{2+}$  cations; effect of different texturants on viscosity was studied at different concentrations, temperatures, and rpms.

- Maximum viscosities were achieved with carrageenans and sodium alginate. Pectins showed relatively low viscosities with increasing  $\text{Ca}^{2+}$  concentration. Viscosity values increased up to the critical cation concentration and then started to decrease. At that critical value, gel-bead formation begun and polymer chain dissolution in the solution was decreased. Temperature affected viscosity inversely at all rpms and concentrations. The non-Newtonian behaviour of the solution gives higher viscosities at lower spindle speeds.

In 3DP studies, firstly, primitive formations were achieved with different powder and binder formulations to understand the applicability of the formulations on 3DP. The important results were as follows:

- Matrices that dissolve in the binder solution (dissolution type matrices) give large primitives which is detrimental to the resolution when extrapolated to 3DP operations. Sugar based matrices with aqueous based binders exhibit this type of behaviour.
- Low porosity powders create larger primitives since the binder engulfs more powder in the smaller pore volume available.
- Powders with radii less than  $\sim 50 \mu\text{m}$  or with a large percentage of small size powders have an initial slow impregnation due to small capillary dimensions, but form sharp holes at the surface because of increased surface area of the powder and its fast dissolution.
- Powders other than sugar exhibit slow impregnation (wetting problems), small primitives and larger lateral diffusion of the aqueous binder solutions giving rise to flat, dish like primitives.
- Another important finding is that the use of  $\text{Ca}^{2+}$  ions did not decrease the primitive size which suggests that its effect in obtaining good resolution in 3DP machine is negligible, therefore, we tried other approaches to increase resolution in machine trials.

Packing density of the powders in the build section of 3DP machine was not affected by the density of the powders in the feed section.

As a result of this study we have started to understand the capabilities of the 3DP machine, develop suitable powder and binder couples with good top, bottom and side resolution for candy formulations and to achieve textures other than hard and brittle which is the characteristic of all sugar matrices.

- The most important variable for good part resolution is found to be a narrow particle size distribution. We have shown that around  $100 \mu\text{m}$  mean diameter, resolution obtained is always satisfactory. The droplet radius is around  $50 \mu\text{m}$  in the ink-jet printing and the dissolution rate of sugar is

very high for finer powders, therefore, 100  $\mu\text{m}$  seem to be an optimum dimension.

- Starch and alginates reduce wicking of binder by gel formation. Too much water interferes with the spreading of the new layer. Optimum S and CS values are found to be around 1 and 0.43 respectively for sugar-based matrices.
- A variety of binder compositions can be used effectively with the Z-corporation machine - below are some formulations:

1. 85% sugar solution (45% sugar content)  
10% ethyl alcohol  
5% glycerol

*Advantage:* Gives good resolution, decreases the hardness.

*Disadvantage:* Ink-jet print head and reservoir require cleaning with water after use.

2. 85% water  
10% ethyl alcohol  
5% glycerol

*Advantage:* Easy to apply.

*Disadvantage:* More wicking compared to (1).

3. 60% glycerol  
40% water

*Advantage:* Less sugar fusing, better resolution.

*Disadvantage:* Longer time to dry.

4. 85% water that is 0.025 to 0.5% Ca-acetate  
10% ethyl alcohol  
5% glycerol

*Advantage:*  $\text{Ca}^{+2}$  ions enhance gelling, decrease wicking.

5. 85% water

10% ethyl alcohol

5% glycerol

pH adjusted to 3.0-3.5 with citric acid for pectins.

- No significant spreading problem was encountered with powders at RH values less than 40% with sugar, starch, additives and their combinations.
- The hardest objects with sugar based matrices were obtained around 50-55% RH. Below and above this region, the cohesive strength of the matrix decreases.
- Fondant and soft textures were not possible to obtain in the largely sugar based matrices investigated.
- More chewy textures were obtained in powder-binder combinations, which reduces the fusing of sugar during the 3D build stage. For this purpose starch and pectins are effective in reducing fusing also incorporation of as much glycerol and alcohol without exceeding the 10 cP viscosity restriction will help.

Some powder formulations are given below. Resolution will be better if sieved sugar of 0.1 mm average size is used.

1. 94-95% sugar

4-5% starch (T470)

0.5-1.5% Unipeptine 569S

*Characteristic:* chewy with binder 5 at RH ~30

2. 94-95% sugar

4-5% starch

0.5-1.5% alginate

*Characteristic:* hard and brittle, but, the texture can be changed with the binder used (1), (3) with Ca and (4) at varying RH.

In the FTIR analysis of the pure texturant material with sugar and  $\text{Ca}^{2+}$  ion, O-H stretching peaks at around  $3350\text{ cm}^{-1}$  became narrower and higher in intensity as a result of increase in molecular bonding. Preference of  $\text{Ca}^{2+}$  among the chains caused almost all of the peaks' intensity at the fingerprint region of polysaccharides ( $1750\text{-}950\text{ cm}^{-1}$ ) to decrease. No special effort was done to purify the texturant samples, therefore no further experiments were done on the molecular motions of the texturants with  $\text{Ca}^{2+}$  cation. Specific assignments were done at relevant parts in section 3.4.

## REFERENCES

- [1] E. Sachs, M. Cima, P. Williams, D. Brancazio and J. Cornie, “Three dimensional printing: rapid tooling and prototypes directly from a CAD model”, *Journal of Engineering for Industry*, 114, 481-488, 1992.
- [2] E. Sachs, M. Cima, J. Brecht, A. Curodeau, T. Fan and D. Brancazio, “CAD casting: direct fabrication of ceramic shells and cores by three dimensional printing”, *Manufacturing Review*, Vol.5, No.2, 117-126, 1992.
- [3] E. Sachs, J.S. Haggerty, M.J. Cima and P.A. Williams, “US Patent No, 5, 204, 055”, 1993.
- [4] Benjamin M. Wu and M.J. Cima, “Effect of solvent-particle interaction kinetics on microstructure formation during three-dimensional printing”, *Polymer Engineering and Science*, Vol.39, No.2, 249-260, February 1999.
- [5] L.G. Cima, J.P. Vacanti, C.A. Vacanti, D. Ingber, D. Mooney, R. Langer, “Tissue engineering by cell transplantation using biodegradable polymer substrates”, *Journal of Biomechanical Engineering*, 113, 143-151, 1991.

- [6] R.A. Giordano, B.M. Wu, S.W. Borland, L.G. Cima, E.M. Sachs, M.J. Cima, "Mechanical properties of dense polylactic acid structures fabricated by three dimensional printing", *Journal of Biomaterials Science, Polymer Edition*, Vol.8, No.1, 63-75, 1996.
- [7] W.E. Kastr, R.D. Palazzolo, C.W. Rowe, B. Giritlioglu, P. Teung, M.J. Cima, "Oral dosage forms fabricated by three dimensional printing", *Journal of Controlled Release*, 66, 1-9, 2000.
- [8] B.M. Wu, S.W. Borland, R.A. Giordano, L.G. Cima, E.M. Sachs, M.J. Cima, "Solid free-form fabrication of drug delivery devices", *Journal of Controlled Release*, 40, 77-87, 1996.
- [9] G.O. Aspinall, "Polsaccharides", Pergamon Press, Oxford, New York, USA, 1970.
- [10] D. Thom, I.C.M. Dea, E.R. Morris and D.A. Powell, "Interchain associations of alginate and pectins", *Progress in Food and Nutrition Science, Gums and Stabilizers for Food Industry, Interactions of Hydrocolloids*, Vol.6, 97-108, Pergamon Press, Great Britain, 1982.
- [11] J.M.V. Blanshard, "Hydrocolloid water interactions", *Progress in Food and Nutrition Science, Gums and Stabilizers for Food Industry, Interactions of Hydrocolloids*, Vol.6, 3-20, Pergamon Press, Great Britain, 1982.
- [12] P.W. Hales, M. Jefferies and G. Pass, "Some physical properties of hydrocolloids in aqueous solution", *Progress in Food and Nutrition Science, Gums and Stabilizers for Food Industry, Interactions of Hydrocolloids*, Vol.6, 33-43, Pergamon Press, Great Britain, 1982.

- [13] R.E. Schachat and L.Z. Raymond, "Some aspects of hydrocolloid gelation, Research Center, General Foods Corporation, Tarrytown, N.Y.", *Physical Functions of Hydrocolloids, Advances in Chemistry Series, American Chemical Society*, 25, 11-24, 1960.
- [14] A.B. Rodd, J. Cooper-White, D.E. Dunsten, D.V. Boger, "Gel point studies for chemically modified biopolymer networks using small amplitude rheometry", *Polymer*, 42 (1), 185-198, 2001.
- [15] J. Solms, "Some structural aspects of the gel formation of pectins and related polysaccharides, La Tour-de-Peilz, Vaud, Switzerland", *Physical Functions of Hydrocolloids, Advances in Chemistry Series, American Chemical Society*, 25, 37-44, 1960.
- [16] Degussa Texturant Systems Sales, LLC, Product Overview, 3582 McCall Place, NE, Atlanta, GA 30340 USA.
- [17] K.I. Draget, B. Strand, M. Hartmann, S. Valla, O. Smidsrod, G.S. Braek, "Ionic and acid gel formation of epimerised alginates; the effect of AlGE4", *International Journal of Biological Macromolecules*, 27, 117-122, 2000.
- [18] C. Sartori, D.S. Finch, B. Ralph and K. Gilding, "Determination of the cation content of alginate thin films by FTi.r. spectroscopy", *Polymer*, Vol.38, No.1, 43-51, 1997.
- [19] F. Llanes, D.H. Ryan, R.H. Marchessault, "Magnetic nanostructured composites using alginates of different M/G ratios as polymeric matrix", *International Journal of Biological Macromolecules*, 27, 35-40, 2000.

- [20] R. Falshaw, H.J. Bixler and K. Johndro, "Structure and performance of commercial kappa-2 carrageenan extracts I. Structure Analysis", *Food Hydrocolloids*, 15, 441-452, 2001.
- [21] S. Janswamy and R. Chandrasekaran, "Three-dimensional structure of the sodium salt of iota-carrageenan", *Carbohydrate Research*, 335, 181-194, 2001.
- [22] S. Janaswamy and R. Chandrasekaran, "Effect of calcium ions on the organization of iota-carrageenan helices: an X-ray investigation", *Carbohydrate Research*, 337, 523-535, 2002.
- [23] J.G. Lewis, N.F. Stanley, G.G. Guist, "Commercial production and application of algal hydrocolloids. In: Carole A. Lembi and J. Robert Walland, (eds.) *Algae and human affairs*", Cambridge University Press, Cambridge, 205-236, 1988.
- [24] V.J. Chapman and D.J. Chapman, "Seaweeds and their uses", Chapman and Hall, New York, 1980.
- [25] Y. Yuguchi, T.T.T. Thuy, H. Urakawa, K. Kajiwara, "Structural characteristics of carrageenan gels: temperature and concentration dependence", *Food Hydrocolloids*, Vol.16, Issue 6, 515-522, November 2002.
- [26] A-S. Michel, M.M. Mestdagh, M.A.V. Axelos, "Physico-chemical properties of carrageenan gels in presence of various cations", *International Journal of Biological Macromolecules*, 21, 195-200, 1997.

- [27] F. Kar, N. Arslan, "Effect of temperature on viscosity of orange peel pectin solutions and intrinsic viscosity-molecular weight relationship", *Carbohydrate Polymers*, 40, 277-284, 1999.
- [28] W.L. Kerr, L. Wicker, "NMR proton relaxation measurements of water associated with high methoxy and low methoxy pectins", *Carbohydrate Polymers*, 42, 133-141, 2000.
- [29] M.L. Fishman, D.R. Coffin, R.P. Konstance, C.I. Onwulata, "Extrusion of pectin/starch blends plasticized with glycerol", *Carbohydrate Polymers*, 41, 317-325, 2000.
- [30] S.-J.J. Lee, E. Sachs and M. Cima, "Layer position accuracy in powder-based rapid prototyping", *Rapid Prototyping Journal*, Vol.1, No.4, 24-37, 1995.
- [31] Three Dimensional Printing Laboratory Notes, Laboratory for Manufacturing and Productivity, Massachusetts Institute of Technology, Cambridge, MA 02139, USA, 2000.
- [32] Z-Corporation Z402<sup>TM</sup> User's Manual, 20 North Ave. 01803 Burlington, MA.
- [33] C. Ateş, "Synthesis and characterization of copolymers of ethyleneterephthalate oligomers and p-Acetoxy benzoic acid", M.S. Thesis, METU, September 2002.
- [34] H. Mark, "Physical chemistry of high polymeric systems", Vol.2, Wiley-Interscience, New York, 1940.

- [35] C.M. DeRamos, A.E. Irwin, J.L. Naus, B.E. Staut, “<sup>13</sup>C NMR and molecular modelling studies of alginic acid binding with alkaline earth and lanthanide metal ions”, *Inorganica Chimica Acta*, 256, 69-75, 1997.
- [36] A. Martinsen, G.S. Braek, O. Smidsrod, F. Zanetti and S. Paoletti, “Comparison of different methods for determination of molecular weight and molecular weight distribution of alginates”, *Carbohydrate Polymers*, Vol.15, Iss.2, 171-193, 1991.
- [37] O. Smidsrod, A. Haug, S.G. Whittington, “Molecular basis for some physical properties of polyuronides”, *Acta Chemica Scandinavica*, 26, 2063-2074, 1972.
- [38] B.E. Stout and C.M. DeRamos, in T. Murakami and R.C. Ewing (eds), “Int. Symp. Scientific Basis for Nuclear Waste Management, MRS Symposium Proc.”, Vol.353, Material Research Society, PA, 1995.
- [39] E.D.T Atkins, I.A. Niedoszynski, W. Mackie, K.D. Parker and E.E. Smolko, “Structural components of alginic acid II. The crystalline structure of poly- $\alpha$ -guluronic acid. Results of X-ray diffraction and polarized infrared studies”, *Biopolymers*, 12, 1879-1887, 1973.